Department of Socio-Cultural Environmental Studies

Graduate School of Frontier Sciences

The University of Tokyo

2016

Master's thesis

Study on spatial and temporal variation of anoxic water and sulfide in Tokyo Bay

Submitted July 19, 2016

Adviser: Professor Jun Sasaki

Co-Advisor: Associate Professor Jun Sato

Vu Tien Thanh

ABSTRACT

Tokyo Bay is located in central Japan and is considered to be a typical enclosed bay in the world. Because high nutrient loads have accelerated the accumulation of particulate organic matter around the head of bay that drives Tokyo Bay usually suffering from excess phytoplankton blooming and subsequently hypoxia and anoxia bottom occur from spring to autumn. Reclamation activities for foreshore or for navigation purposes along coast of the head of bay in the past that have created coastal trenches with a various spatial scales. Waters in these dredged pits are considerably stagnant and hypoxic or anoxic water appears with high frequency. Additionally, one of phenomena is blue tide originated when huge amount of hydrogen sulfide in the bottom sediment is produced during decomposition of organic matter under anoxic condition combined with upwelling of oxygen-depleted bottom water induced by northeast wind-driven circulation at the inner of Tokyo Bay, sometimes affects seriously to aquatic communities of animals across large zones. It is thus necessary to understand variation of anoxia and sulfide related to blue tide phenomenon to reduce hypoxia and anoxia in Tokyo Bay. This study aims to identify the characteristics of anoxic water and to estimate sulphide in dredged pits, navigation channels and flat bottom before proposing remedies for mitigating the impact of blue tide.

This study based on field observations and numerical simulation to examine variation of anoxic water and sulfide in Tokyo Bay. Four field surveys have carried out during summer in year 2015 to identify appearance of anoxia and sulfide in both flat bottom and dredged pit in Tokyo Bay. On the other hand, MIKE 3 model was used to reproduce water quality process in two years (2014 and 2015) to understand more comprehensively about development of anoxia and contribution of flat bottom and dredged pits to blue tide.

Result of research indicates that anoxia appears later and disappears sooner while hypoxia usually occurs sooner and vanishes later. Anoxic bottom waters normally develops from May to early November. From June to September anoxia on surface may develop frequently. Anoxia generally occurs seriously in July and August. From September onward, almost no anoxia is detected. Spatial variation of anoxia that can be exposed entire flat bottom from Kawasaki artificial island to head bay coastline beside anoxic waters have been found in dredged trenches. Dredged pits or navigation channel would be significant anoxic water sources. Anoxic waters appear frequently in both off-Urayasu dredged pit and off-Makuhari dredged pit. Release of sulfide is accompanied closely with development of anoxia. Although sulfide concentration of measurement in flat bottom was much lower than release of sulfide in dredged pits (observed sulfide concentration was the highest in off-Makuhari dredged pits) but flat bottom still showed its large contribution to blue tide phenomenon beside considerable contribution of dredged pit.

This study also proposes a solution to reduce appearance of hypoxia and anoxia by restoring initial topography including dredged pits in Tokyo Bay. This is hopefully a significant effort contributing to academic research.

ACKNOWLEDGMENT

First and foremost, I would like to express my hearty gratefulness to my supervisor, Prof. Jun Sasaki for his valuable and continuous support throughout my study in Japan. In my thought, he is truly a specialist on river estuary and coastal area and I feel so lucky when I could corporate with the kindest academic adviser ever. He has shown me how to carry out a research then took me in scientific research road, thank you for giving me input and ideas when there seemed to be no way out with my research. I strongly admire his working manner and his enthusiasm. Especially my limitation somehow would be broken by learning advanced knowledge from his vast insight. My research could not reach to final successful goals without his support.

I also want to send many thanks to my co-supervisor, Associate Prof. Jun Sato, Department of Socio-cultural Environmental Studies, the University of Tokyo. Thanks to his sincere advice and recommendations, I would correct my research contents of my thesis although we are not similar completely in major.

I would like to thank the former secretary Murozono for helping me so much since my first arrival in Japan. I greatly acknowledge Dr. Hae Chong O, a senior staff in Sasaki's Lab for supporting me. He guided me many things during field observations in Tokyo Bay and normal rules on Sasaki's Laboratory. Another special profound appreciation to my labmates for helping me to settle down my accommodation and sharing utilities in our laboratory.

My infinite gratitude to my parents, my sibling and other relatives who are my motivation. They always stood by me and my lonely and homesick feeling seemed to disappear even if we are thousands miles apart. Basing on their stimulation I might struggle

to stresses originated from research work. Specially, I would like to manifest my feeling to my lovely niece and nephew who are my inspiration due to their naivety always relieved my tension.

I'd like to say "thank you so much" to my colleagues who have been working for the Center for Oceanography in Hanoi, Vietnam. Although we are far way between two countries, however we still kept in touch during my stay in Japan and I felt stronger by their consultation.

I am so thankful to The Bureau of Waterworks, Tokyo Metropolitan Government for providing river discharge measured data. These data sources are very precious to enhance my research results. Furthermore, I am extremely grateful to ADB-Japan Scholarship Program for funding the full scholarship to pursue my master course in Graduate School of Frontier Science, the University of Tokyo. A special thanks goes to DHI Japan Branch (Danish Hydraulic Institute – Denmark) for granting license of MIKE 3 model to Sasaki's Laboratory, Department of Socio-cultural Environmental Studies, the University of Tokyo.

It is also fortunate when I met many Vietnamese kind friends who shared life experiences in Kashiwa Campus. Thank you for supporting and I really indebted you for all. Finally, I also enounce many thanks to other humans who might not be mentioned here though incited me only by small manners.

TABLE OF CONTENTS

LIST OF FIGURES

LIST OF TABLES

CHAPTER 1: INTRODUCTION

1.1. Background

Tokyo Bay locates in the central Japan along east coast of Honshu Island. It is well-known as typical semi-closed embayment in the world. Its size ranges from 20 kilometers wide to 50 kilometers long with average depth of 15 meters in inner bay while much deeper in outer bay. Tokyo Bay exchanges water with Pacific Ocean through its narrow bay mouth. Tokyo Bay represents a coastal ecological system normally bearing heavily eutrophication. Due to the very high density of population and industry in the catchment area surrounding Tokyo Bay, increase of nutrient loading from adjacent terrestrial areas have accelerated the accumulation of particulate organic matter around the head of bay (Wolanski, 2006). This is one of the causes to drive Tokyo Bay suffering from excess phytoplankton blooming and subsequent hypoxia and anoxia in the bottom from spring to autumn.

Hypoxia is a condition that occurs when dissolved oxygen (DO) falls below the necessary level for organism to survive. Many researchers consider hypoxia as DO $\leq$ 3 mg/L while others DO $\leq$ 4 mg/L. Hypoxia becomes anoxia when DO plummets to zero concentration. In principal, the causes of formation of hypoxia and anoxia are stratification of water column isolating oxygen from surface layer to bottom layer and oxygen consumption due to decomposition of organic matter in bottom layer. In Tokyo Bay, the stratification due to steep vertical gradients of temperature and salinity is intensified from June to October. On the other hand from November to March, it is characterized by uniform temperature and salinity in water column (Nakane et al., 2008). Hypoxia in summer in the bay has received considerable scientific and policy attention because of ecological and

economic impacts. Many studies have assessed effects of hypoxia on organism in the bay. For instance, development and persistence of hypoxia in Tokyo Bay from spring to autumn cause mortality of benthic organisms and failure of larval settlement (Kodama et al., 2011). Although many of the studies have focused on occurrence of hypoxia in Tokyo Bay, studies in revealing characteristics of anoxia, a more serious problem, are very limited.

In addition, there have been created dredged pits in which sediment materials were taken for reclamation of the foreshore and navigation channels at the head of the bay for several decades (**Figure 1.1**). Since waters in these pits are very stagnant, hypoxic and anoxic waters continuously appear from spring to autumn. Additionally, upwelling of oxygen-depleted bottom water induced by northeast wind-driven circulation in inner bay, especially waters in these pits with exhausted oxygen occasionally move up to upper layer affects seriously to aquatic communities of animals in tidal flat and shallow water areas along the coast at the head of the bay.

Moreover, a huge amount of hydrogen sulfide in bottom waters is produced during decomposition of organic matter under anoxic condition. One of phenomena associated with this problem is blue tide. In Japanese blue tide is called “Aoshio” phenomenon (“Ao” means blue while “shio” means tide). Blue tide is relevant simultaneously to depletion of oxygen and only endures in a short period. As a result of upwelling of bottom anoxic water with hydrogen sulfide and subsequent oxidation of the hydrogen sulfide ($H_2S + HS^-$) generating elemental sulfur (S^0) in upper layer containing dissolved oxygen (DO). When sunshine reflects off surface water containing these sulfur particles, the color of seawater turns to emerald green or milky blue.

Considerable efforts have been performed to improve hypoxia and anoxia in Tokyo

Bay by, for example, decreasing nitrogen and phosphorus loads from the catchment area and constructing artificial tidal flats and shallow water areas for reducing the effect of those waters along with providing habitats for benthic animals having a water purification function of absorbing organic materials in the shallow areas. To promote these environmental restoration activities, it is necessary to predict environmental restoration processes and evaluate these activities. For this purpose, numerical prediction model should be a useful tool. At the beginning of the environmental restoration may be detected by the reduction in anoxic waters and monitoring of anoxic waters are also very important. Thus it is significant to focus on anoxic water and consider its monitoring and numerical prediction for the purpose of proposing methods of improvement of the initial stage of environmental restoration. For this purpose the effect of each of anoxic waters on the magnitude of blue tide should be clarified along with the reduction potential of blue tides due to improving source areas of the anoxic waters.

This study presents an examination on variations of anoxic waters and sulfide related problem in Tokyo Bay recommended above. Hopefully, this is a considerable effort in mitigating the adverse impact of phenomenon.

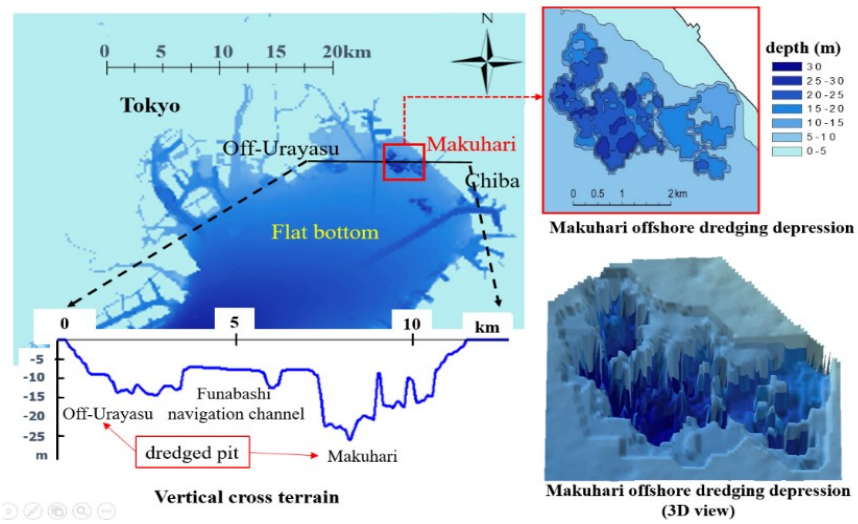

Figure 1.1. **Tokyo bay map and dredged pits**

1.2. Objectives of this study

This research will be accomplished by fulfilling the following objectives:

To identify the characteristics of anoxic water and to estimate total sulfide in dredged pits, navigation channels and flat bottom.

To reproduce temporal and spatial variation in anoxic waters and total sulfide by using numerical model.

To propose remedies for mitigating the impact of blue tide.

1.3. Literature review

Tokyo Bay hypoxic and anoxic waters assessment

Through field investigations during summer 1986 and 1987 (Han et al., 1992) revealed that *Skeletonema costatum* in plankton community was the major composition with seasonal variation of red tides in Tokyo Bay. Primary productivity of this diatom accounts for from 5.2 to 70.4% of total productivity in Tokyo Bay. Contribution of species-specific photosynthetic rate of *Skeletonema costatum* was determined by the micromanipulation of C-labeled cells and has been normalized with cell volume. They found that volume of species-specific photosynthetic rate stood at high level during initial phase of bloom before falling down with cell division, and went down to bottom level when the bloom peaked.

Temporal and spatial abundance of plankton community depends strongly on variety of physical, chemical and biological processes (Pennock, 1985). (Nakane et al., 2008) pointed out several short-term bloom of plankton in Tokyo Bay by inspecting water temperature, salinity, nutrient concentrations and composition of plankton community at three stations in inner Tokyo Bay from June in 1995 to April in 1996. The result showed that period of June to October was the development of stratification of temperature and salinity whereas temperature and salinity were almost uniform from November to March. Significant

fluctuation of plankton as responses to temporal changes in water quality from June to November. Primary production remained low when water temperature and solar radiation decreased during mixing period (from November to February). The study denoted evidence of phosphorus depletion on the surface when supply of nutrient loads was high due to inland fresh water inflow. This suggested that phosphorus is the limiting factor for growth of phytoplankton in Tokyo Bay.

During the same time of phytoplankton blooming, oxygen-depleted water mass forms in the bottom layer. (Sato et al., 2012) proved contribution of wind and river effect on DO concentration in Tokyo Bay. They showed the example that in summer wind changed from northeast direction to southwest direction leading to enhancement of bay circulation which is related to intrusion of water from bay mouth. That would provide high DO concentration in water from Pacific Ocean into Tokyo bay during summer. They developed a conceptual DO model to evaluate contribution of wind and river discharge with occurrence of hypoxic water in Tokyo Bay. Beside with using this DO conceptual model, they also simulated 3D hydrostatic ecological model ELCOM&CAEDYM (Hoges, 2000) to reproduced DO concentration averaged at lower layer around head bay from May to August in 2003. Environmental variables are phytoplankton, ammonium, nitrate, filterable reactive phosphorus, particulate organic phosphorus, silica and DO. Dissolved oxygen is contributed by sediment, photosynthesis, phytoplankton respiration and nitrification process. They pointed out that wind contributes to 58±20% (average±standard deviation) to lower DO bottom whereas 11±11% is from river discharge. When flood or strong winds over 10 m/s, these effect of both factor was 50% or more and these extreme events recover DO bottom from hypoxia at DO bottom. However it is difficult when they only used a DO measured station to estimate appearance of hypoxic water.

(Komada et al., 2006) elucidated that hypoxia (DO ≤ 2 mg/L) presented continually at bottom in Tokyo Bay from April to October but it tended to decline in late June and early September in 2004. They also indicated proportion of hypoxic area where hypoxic area in the bay developed from May onwards and might expand from 5% to 67% entire of the bay in July and August. They showed that hypoxia reduced since August and there was no hypoxia observed after November since hypoxia reduced after August. Their group just encountered hypoxia in the central area of the bay and they said expansion of hypoxia is from northern to southern part from late July to August.

(Fujiwara et al., 2002) investigated the displacement of hypoxic water mass driven by inflow and outflow into Tokyo Bay through data collection in summer 1998. He considered hypoxic water in which DO ≤ 4 mg/L. He found that hypoxic water mass existed in two patterns: bottom hypoxic water mass and subsurface hypoxic water mass. He explained that when dense water from bay mouth intrudes into lower layer of inner bay, it would push bottom hypoxic water moving to head bay and transform into hypoxic subsurface water mass at intermediate depth by lifting it up. Hypoxic subsurface water mass afterward enlarges pycnocline and flows out to bay mouth. When salty oceanic stream withdraws from the bay, bottom hypoxic water mass is substituted to bay mouth by bottom outflow. Finally, he pointed out that subsurface hypoxia occurs frequently in southern half of the bay while bottom hypoxia usually locates in northern bay.

(Ishii et al., 2010) have possessed a long term data set from 1955 to 2009 provided by Chiba Prefectural Fisheries Research Center to examine variation in water quality and hypoxic water mass (DO ≤ 2.5 mg/L). He showed that terrestrial nitrogen and phosphorus discharged into bay from inland peaked in the 1980's but have declined to same level in the

1960's in recent years. Moreover, dissolved inorganic nitrogen and phosphorus just tended to fall down after 1990. He indicated that hypoxic water mass spread across a wide range at bottom layer in inner bay from May before going down in September. In a comparison between years, hypoxia developed in the 1960's and remained the same size in recent years.

(Kuramoto et al., 1991) executed numerical model to simulate the formation and displacement of an oxygen deficient water mass in Tokyo Bay. With hydrodynamic results, he found that tidal residual current (M2 constituent is dominant wave) inside the bay are weak except bay mouth area and mean current are strongly driven by winds and buoyancy. There is a flow with direction from the middle to the head bay and this flow is characterized as considerable factor contributing to formation of oxygen deficient water mass at bottom layer. They used four environmental factors (N, P, COD, DO) to calculate water quality in the bay. The outcomes depicted formation of oxygen deficient water mass with $DO \leq 2$ mg/L at the lowest layer in the head bay in case of no wind. If northeast wind is blowing for two days then hypoxic water mass with $DO \leq 3$mg/L can be seen at the first layer (0-2m). His group continued experiment with case of 2-day-southwest wind blows, movement of an oxygen deficient water mass may be tracked from the head to the middle of the bay.

(Sasaki et al., 2009) has suggested a countermeasure to solve hypoxic and anoxic problems in an estuary trench through application of a mechanical circulator. He and his partners have performed numerical experiment on the required flow rate and direction with the physical mechanism of its effectiveness. They developed a circulator prototype to generate downward flow. An impeller is attached to the main floating body of the circulator to transport surface water to bottom through flexible draft tube connected to the floating body. The effectiveness was verified by field tests in a dredged pit in Tokyo Bay. The

mechanical circulator has demonstrated its advantage, including reduction in hypoxia and improvement of water quality in the trench.

(Yoshimoto et al., 2009) used numerical model to study measures for hypoxia reduction in a dredged trench in coastal area of Tokyo Bay. The proposal related to installation of duct to supply oxygen to bottom layer. The result showed that less dense surface water is transported effectively and more practically. Especially, this research constructed a water quality model to simulate well dissolved oxygen while result of sulfide reached at certain degree.

Sulfide

(Sasaki et al., 2007) estimated total amount of released sulfide in flat bottom and dredged pits based on relationship with pH and DO (**Figure 1.2**). According this graph total sulfide usually began released from spring before ending in autumn. The result also shows a significant contribution of flat bottom compared to dredged trench in case of large scale blue tide.

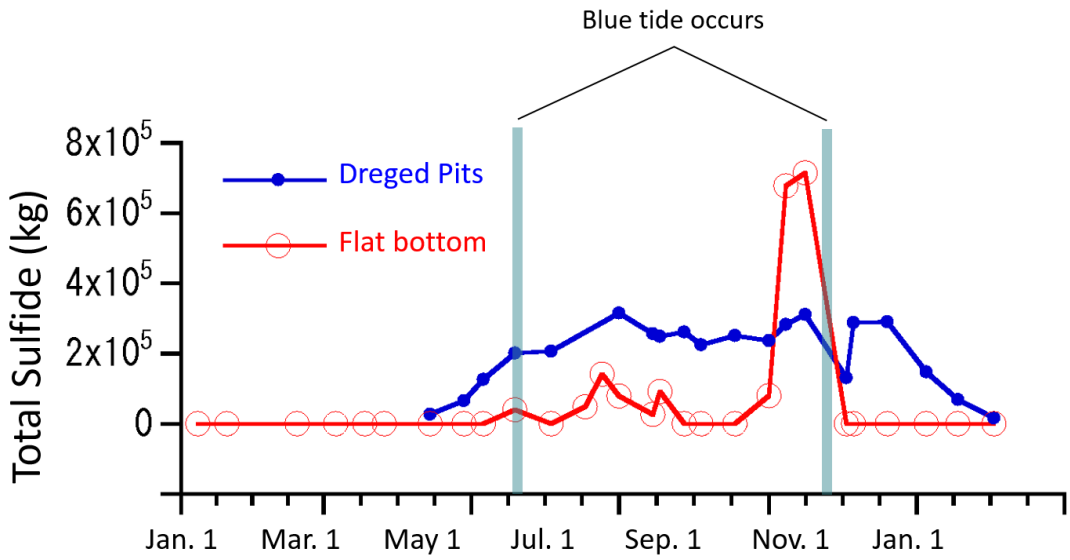

Figure 1.2. Estimation of total sulfide in year 2003 by Sasaki (2007)

(Ichioka et al., 2009) evaluated anoxic water sources in navigation channels and dredged trenches in Tokyo Bay. They conducted field surveys to measure vertical profile of pH, oxygen reduction potential (ORP) and sulfide at the bottom then estimated the amount of sulfide released in these areas. They also reproduced sulfide by numerical model to examine contribution of each area to magnitude of blue tide. Result of reproduction shown that sulfide concentration is relatively high in off-Urayasu dredged pit and off-Makuhari dredged pit while off-Makuhari dredged pit is much more than off-Urayasu dredged pit. However result of reproduction was still below with measured data.

(Sato et al., 2015) considered enhancing the numerical model to reproducing sulfide in head Tokyo Bay. They also monitored anoxic water, sulfide and sediment quality in summer 2014. Through analysis for reproduction of sulfide in 2010, they realized that contribution in success of sulfide reproducibility is governed by organic matters production and resultant flux to sediment. The study showed the difference in sulfide concentration between a large and a small dredged pits.

Blue tide

(Kakino et al., 1987) examined the relationship between blue tide (Aoshio), blue turbidity water and wind driven current. They collected a data set of meteorology (wind) and water quality (bottom current, temperature, salinity, density, sulfide and dissolved oxygen), then analyzed these data to demonstrate when prevailing wind changes its direction from onshore to offshore (or northeast wind appears) and remains at least two or three days, at the entrance of Funabashi area usually appeared Aoshio firstly due to bottom water containing sulfide moving upwards at this area.

(Otsubo et al., 1991) conducted field survey and hydraulic research on blue tide in

summer 1988. They divided into three groups for investigation: group I took images from helicopter, group II collected sea data (temperature, salinity, dissolved oxygen, transparency, Chl-a, etc.) and group III harvested bacteria to determine the numbers of particular species. They have witnessed blue tide on September 8th, 1998. Northeast and eat northeast blew at the speed of 5-6 m/s on blue tide day occurred. According to field results, blue tide happened in a small-scale at the end of Funabashi channel and harbor and in the Honda wharf. More specifically, transparency in blue tide areas was lower than non-blue tide zones and Chl-a value was also high in non-blue sites. Surveys revealed that total sulfur concentration in blue tide zones were 10-20 times higher than in non-blue tide zones. The highest observed value of sulfur might reach to 0.417 mg/L. They proposed new hypothesis of this phenomenon that elemental sulfur could not transformed from hydrogen sulfide within a short upwelling process. If it is possible, concentration of hydrogen sulfide is not high enough to make milky blue color of the sea. They thought that most of sulfur particulates have been formed and accumulated at the interface between oxic and anoxic layer. This means that middle layer is major reason caused blue tide especially when northeast wind blows.

(Matsuyama et al., 1990) carried out both numerical experiments and field observation on upwelling in Tokyo Bay in relation to Aoshio. The field results realized that upwelling of anoxic water mass originates from lower layer when northeast wind blows. Additionally, two-layer numerical model indicates generation of upwelling near the head bay and he proved that upwelling will be strengthened if northeast wind blows continually in two days. Through numerical model, they found that the coastal upwelling in the head bay normally appears in early autumn rather than in summer because northeast wind prevails and stratification is weaker.

(Zhu and Isobe, 2012) preliminarily proposed criteria to predict for the occurrence of wind driven upwelling associated with blue tide on the southeast shore of Tokyo Bay. Using two analytical solutions based on some specific assumption to apply a two-layered fluid. Criteria shown valid by comparing with observation data. (Zhu and Yu, 2014) then derived some analytical solutions to make a simple model for estimation of occurrence of Aoshio phenomenon on the northeast area in Tokyo Bay. The model has achieved at some certainties.

Literature review can be concluded as follows:

1. Tokyo Bay usually occurs phytoplankton bloom coupled hypoxia and anoxia phenomenon in summer. There were many researchers pointed out characteristics of hypoxic waters in Tokyo Bay with considerable efforts to reduce this problems. However, it is necessary more studies to specify more specifically on temporal and spatial variations of anoxia in which dissolved oxygen concentration is almost zero.

2. There were several researches reproducing total sulfide processes when anoxic waters appear and evaluated preliminarily contribution of total sulfide released in flat bottom and dredged trenches. Nevertheless, improvement of sulfide reproduction is required to estimate more accurately these contributions.

3. Upwelling of anoxic waters leads to appearance of blue tide (Aoshio) phenomenon which contains sulfur particulates. It is seem to lack works considering fate of this element. Sulfur formation is actually a product of sulfide oxidation. Beside reproducing of sulfide, numerical results may provide information of sulfur in this study.

1.4. Organization of the thesis

The thesis is organized into five chapters. Contents of each chapter are described

briefly as below:

Chapter 1 introduces general issue of topic and states objectives of the study.

Chapter 2 explains methodology to carry out this study.

Chapter 3 reveals results obtained from field surveys and simulation.

Chapter 4 points out the findings of the study and sensitivity analysis of model for reproducibility of water quality.

Chapter 5 concludes the work of the thesis and proposes the recommendations for mitigating this issue.

CHAPTER 2: METHODS

2.1. Field survey

2.1.1. Study site

A schematic plan was created to survey water quality as shown by **Figure 2.1** and **Table 2.1**. Observation areas focused on inner bay (mainly from Kawasaki artificial island to head of the bay). This scheme covered almost important places such flat bottom, navigation channel, off-Urayasu dredged pit and off-Makuhari dredged pit. Period for field surveys spread in summer months when anoxia and hypoxia is identified highly to emerge, especially when Northeast blows. Namely, there were four investigation trips on July 2, August 24, September 1 and September 16 in 2015 carried out to measure water environmental factors.

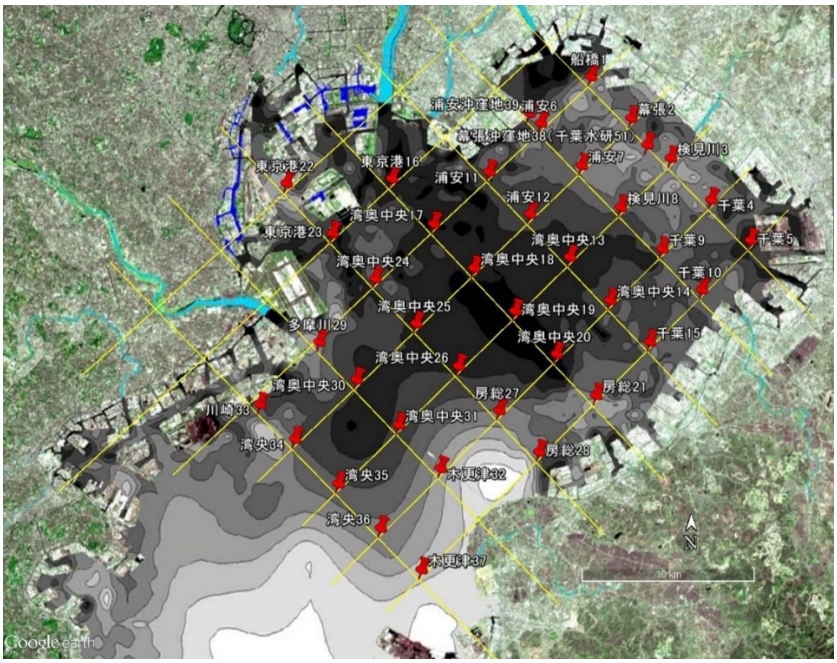

Figure 2.1. Stations of field observation in Tokyo Bay (Google Earth)

Table 2.1. Coordination of stations in field survey

Station name	Latitude	Longitude
Funabashi1	35°39’19.67”	139°58’32.77”
Makuhari2	35°38’02.10”	140°00’06.03”
Kemigawa3	35°36’45.64”	140°01’35.13”
Chiba4	35°35’26.96”	140°03’10.68”
Chiba5	35°34’11.77”	140°04’41.76”
Urayasu6	35°37’51.97”	139°56’36.00”
Urayasu7	35°36’31.79”	139°58’10.84”
Kemigawa8	35°35’16.51”	139°59’43.30”
Chiba9	35°33’56.92”	140°01’19.88”
Chiba10	35°32’40.19”	140°02’48.78”
Urayasu11	35°36’20.75”	139°54’36.31”
Urayasu12	35°35’01.96”	139°56’13.33”
Head of the Bay13	35°33’41.91”	139°57’42.85”
Head of the Bay 14	35°31’11.46”	139°59’19.16”
Chiba15	35°31’03.14”	140°00’46.97”
Tokyo Bay16	35°36’08.87”	139°50’57.47”
Head of the Bay 17	35°34’45.44”	139°52’36.73”
Head of the Bay 18	35°33’22.89”	139°54’03.08”
Head of the Bay 19	35°31’59.70”	139°55’37.65”
Head of the Bay 20	35°30’40.37”	139°57’13.01”
Bo-so21	35°29’23.30”	139°58’40.97”
Tokyo Bay22	35°36’00.34”	139°46’52.58”
Tokyo Bay23	35°34’27.56”	139°48’38.55”
Head of the Bay 24	35°33’01.98”	139°50’17.59”
Head of the Bay 25	35°31’38.58”	139°51’53.39”
Head of the Bay 26	35°30’16.81”	139°53”29.92”
Bo-so27	35°28’53.70”	139°55’01.33”
Bo-so28	35°27’36.01”	139°56’34.22”
Tamagawa29	35°31’03.27”	139°48’11.34”
Head of the Bay 30	35°29’51.93”	139°49’32.60”
Head of the Bay 31	35°18’18.31”	139°51’09.42”
Kisarazu32	35°27’05.98”	139°52’47.32”

Table 2.1. Coordination of stations in field survey (continue)

Station name	Latitude	Longitude
Kawasaki33	35°29’05.41”	139°45’53.45”
Inner part of Bay34	35°28’01.96”	139°47’10.17”
Inner part of Bay35	35°26’37.17”	139°48’53.19”
Inner part of Bay36	35°25’15.85”	139°50’29.55”
Kisarazu 37	35°23’56.82”	139°52’03.89”
Makuhari pit 38	35°38’04.19”	140°00’21.26”
Urayasu pit39	35°38’18.04”	139°56’17.15”
Chiba channel C2	35°35’65.00”	140°04’13.00”
Chiba channel C4	35°34’43.00”	140°01’73.00”
Chiba channel C6	35°32’78.00”	139°58’52.00”

2.1.2. Measurement of water quality

Field observations performed with corporation between Sasaki’s laboratory project and the Sanyo Techno Marine company. To quickly identify appearance of anoxia (when DO $\leq$ 0.05 mg/L), AAQ-Rinko water quality profiler (**Figure 2.2**) was firstly used to measure dissolved oxygen concentration. This equipment measures not only dissolved oxygen profile but also temperature, salinity, turbidity and chlorophyll *a*. AAQ-Rinko is able to measure DO profile with high speed thereby significantly reducing observation time.

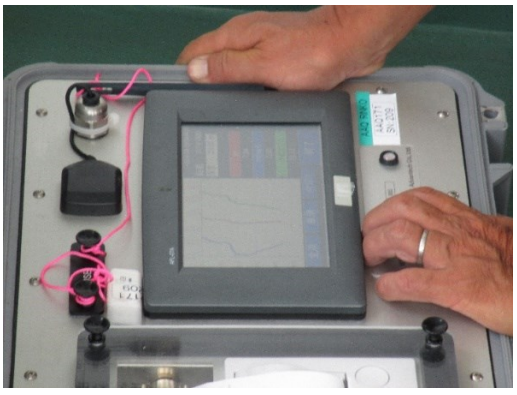

Figure 2.2. AAQ-RINKO water quality profiler

Whenever anoxic water was detect at observation points by AAQ-Rinko, water was also collected by water sampler (**Figure 2.3**). Water sample are taken only for measuring sulfide concentration.

Figure 2.3. Water sampler and anoxic water sample

Taking bed sediment was executed at anoxic points. The grab would dredge sediment on seabed 30 centimeters in thick (**Figure 2.4**).

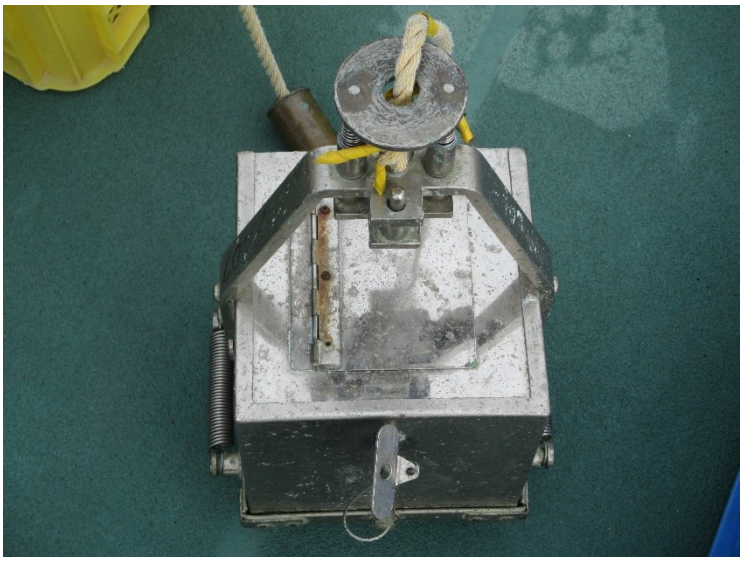

Figure 2.4. Sediment grab

Bed sediment samples (**Figure 2.5**) after that were brought to the laboratory of Sanyo

Techno Marine to analyze total sulfide concentration in bed sediment. Results of total sulfides in sediment will be used to refer to outcomes of total sulfide concentration in water which analyzed by Sanyo Techno Marine company.

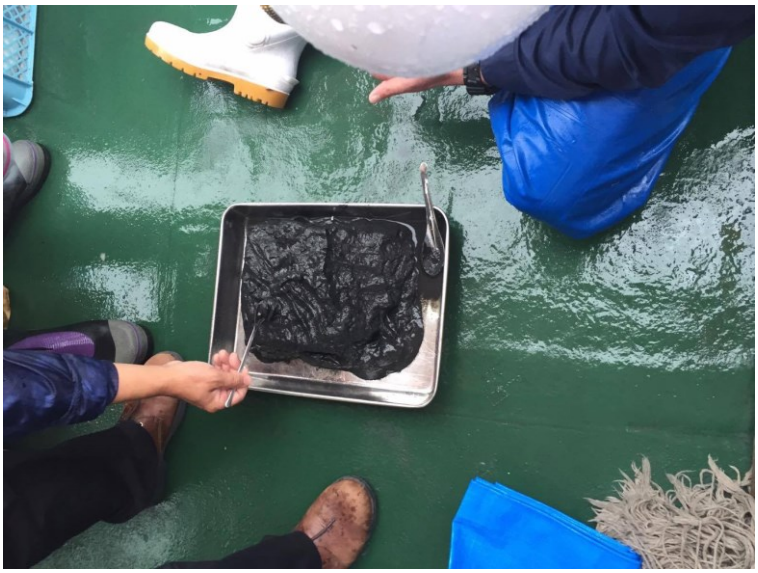

Figure 2.5. Bed sediment sample

2.2. Numerical model

2.2.1. DHI MIKE 3 model

MIKE 3 Model is one of modellings in MIKE family powered by DHI (Denmark Hydraulic Institute). The three dimensional, baroclinic (changes in density), non-hydrostatic model is especially suitable for wide range of application such as oceans, coastal regions, estuaries. There are three modules inside MIKE 3 model. They are hydrodynamic module, advection and convection module and ecological module. Hydrodynamic module simulates unsteady three-dimensional flows to supply for another module. Advection and Dispersion module simulates the spreading of substances when provided the flow field from hydrodynamic module. ECO Lab module simulates the resulting concentrations of water quality variables. Advection and dispersion module is coupled to ECO Lab module to

simulate the simultaneous of transport and dispersion processes. Mechanism of MIKE 3 Model operation is described as **Figure 2.6** below.

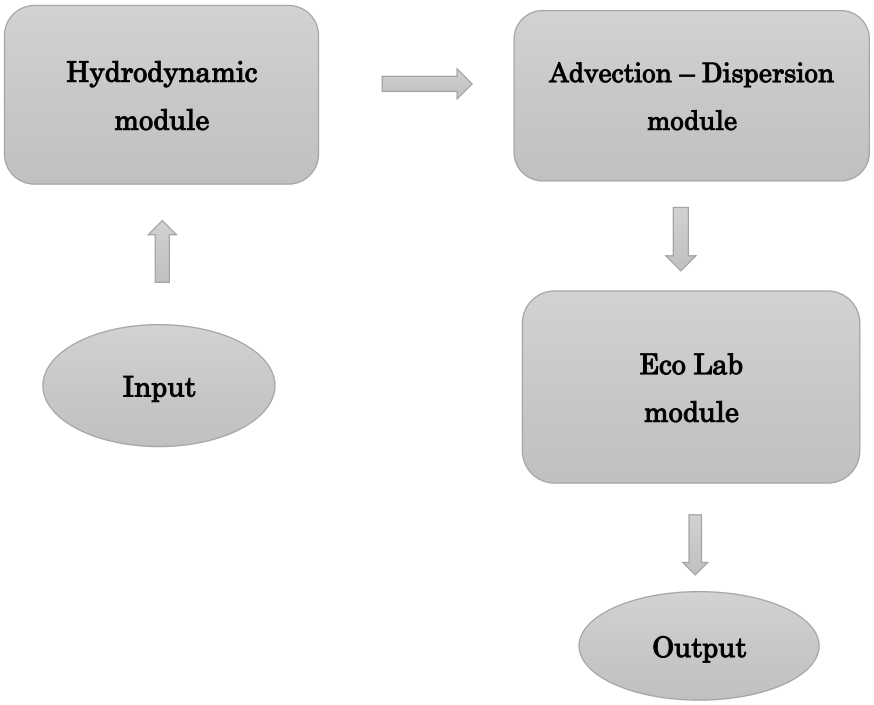

Figure 2.6. Operation flow of MIKE 3 Model.

2.2.2. Hydrodynamic module

Hydrodynamic module is the basic component in MIKE 3 model. To simulate unsteady flows field, it takes in to accounts of bathymetry and external forcings such as meteorological conditions, tidal elevation, current and other hydrographic conditions. This module solves the equations of mass conservation, the Reynolds-averaged Navier-Stokes including the effects of turbulence and variable density, together with conservation equations for salinity and temperature.

(2.1)

$$\frac{1}{\rho c_s^2}\frac{\partial P}{\partial t}+\frac{\partial u_j}{\partial x_j}=SS$$

$$\frac{\partial u_i}{\partial t}+\frac{\partial(u_i u_j)}{\partial x_j}+2\Omega_{ij}u_j=-\frac{1}{\rho}\frac{\partial P}{\partial x_i}+g_i+\frac{\partial}{\partial x_j}\left(\nu_T\left\{\frac{\partial u_i}{\partial x_i}+\frac{\partial u_j}{\partial x_j}\right\}-\frac{2}{3}\delta_{ij}k\right)+u_i SS \qquad (2.2)$$

$$\frac{\partial S}{\partial t}+\frac{\partial}{\partial x_j}(Su_j)=\frac{\partial}{\partial x_j}\left(D_S\frac{\partial S}{\partial x_j}\right)+SS \qquad (2.3)$$

$$\frac{\partial T}{\partial t}+\frac{\partial}{\partial x_j}(Tu_j)=\frac{\partial}{\partial x_j}\left(D_T\frac{\partial T}{\partial x_j}\right)+SS \qquad (2.4)$$

Where:

ρ : the local density of fluid

c_s : the speed of sound in seawater

u_i : the velocity in the x_i - direction

Ω_{ij} : the Coriolis tensor

P: the fluid pressure

g_i : the gravity vector

ν_T : the turbulent eddy viscosity

δ : Kronecker's delta

k: the turbulent kinetic energy

S and T: the salinity and temperature

D_S and D_T : the associated dispersion coefficient

t: denotes the time.

2.2.3. ECO Lab module

2.2.3.1. Framework of water quality model

An ecological model was developed by Sasaki (1998) and Yoshimoto (2009) then to

describe ecological cycle in Tokyo bay (**Figure 2.7**). Seven state variables are dominant these processes, they are: phytoplankton carbon (PPL), suspended organic matter (detritus carbon DET), dissolved oxygen (DO), sediment (SED), nutrient (phosphorus PO4), sulfide (H2S) and sulfur. These state variables associated closely to each other and reflect clearly variation of water quality in Tokyo bay.

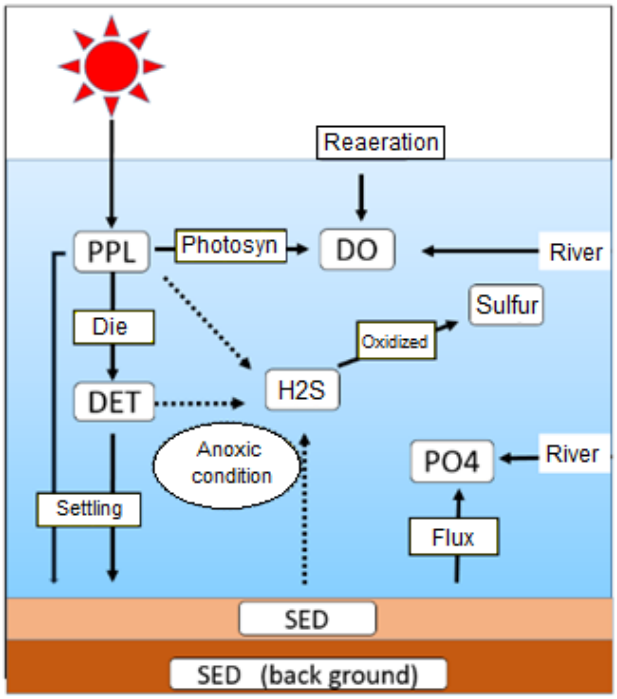

Figure 2.7. Ecological cycle in ECO Lab for Tokyo bay

The transport equation for a component concentration is formulated as:

$$\frac{DC}{Dt} = \frac{\partial}{\partial x_j}\left(\delta_j \frac{\partial C}{\partial x_j}\right) + S(C) \qquad (2.5)$$

where C is concentration of any dependent variable, δ_j is dispersion coefficient in the j-direction, S(C) is source/sink term

In MIKE 3, dispersion coefficients may proportionally vary to the local effective eddy viscosity or to the local velocity components in each direction or to the local current vector.

2.2.3.2. Kinetic differential equations for each state variables

The kinetic equation of state variables in ECO Lab are adopted from Matsunashi Junzaburo (1993).

Phytoplankton carbon

$$\frac{\partial C_{PC}}{\partial t} = phtsyn - death - breath - pcsettling$$

Where:

phytsyn: photosynthesis

death: death of phytoplankton carbon

breath: breath of phytoplankton carbon

pcsettling: phytoplankton carbon settling

$$phtsyn = G \times C_{PC}$$

$$G = G_{max} \times \frac{I}{I_{opt}} exp\left(1 - \frac{I}{I_{opt}}\right) \times \frac{C_{PO_4}}{K_{PO_4} + C_{PO_4}}$$

$$G_{max} = \alpha \times exp(\beta T)$$

$$I = I_{opt}(-kz)$$

$$k = \frac{K_2}{Z_T}$$

$$Z_T = -1.0085ln(C_{chl-a}) + 5.461$$

$$C_{chl-a} = 0.021 \times C_{PC} \times 1000$$

$$death = m_{PC} \times exp(a_1 T) \times C_{PC}$$

$$breath = R_{PC} \times exp(a_2 T) \times C_{PC} \times \frac{C_{DO}}{C_{DO} + K_{DO}}$$

$$pcsettling = w_{PC} \frac{\partial C_{PC}}{\partial z}$$

Therefore:

$$\frac{\partial C_{PC}}{\partial t} = \left\{G_{max} \times \frac{I}{I_{opt}} \exp\left(1 - \frac{I}{I_{opt}}\right) \times \frac{C_{PO_4}}{K_{PO_4}} \times C_{PC}\right\} - \{m_{PC} \times \exp(a_1 T) \times C_{PC}\}$$
$$- \left\{R_{PC} \times exp(a_2 T) \times C_{PC} \times \frac{C_{DO}}{K_{DO} + C_{DO}}\right\} - \left\{w_{PC} \times \frac{\partial C_{PC}}{\partial z}\right\}$$

Detritus carbon

$$\frac{\partial C_{detC}}{\partial t} = \left(detprc - detdecomp1 \; - \; detdecomp2 - detsettling\right)$$

Where:

detprc: detritus carbon production

detdecomp1: decomposition of detritus carbon due to bacteria

detdecomp2: decomposition of detritus carbon due to bacteria under anoxic condition to release hydrogen sulfide

detsettling: detritus carbon settling

$$detprc = m_{PC} \times exp(a_1 T) \times C_{PC}$$

$$detdecomp1 = m_{om} \times b_1 \times exp(a_1 T) \times \frac{C_{DO}}{C_{DO} + K_{DO}} \times C_{detC}$$

$$detdecomp2 = \left\{ v_{poc}^{anb}(T, DO) \times C_{detC} \times 2.7 \right\}$$

$$v_{poc}^{anb} = \alpha_{poc}^{anb} exp\left(\beta_{poc}^{anb} \times T\right)\left(1 - \frac{C_{DO}}{C_{DO} + K_{DO}}\right)$$

$$\frac{\partial C_{detC}}{\partial t} = w_{detC} \frac{\partial C_{detC}}{\partial z}$$

Therefore:

$$\frac{\partial C_{detC}}{\partial t} = \{m_{PC} \times exp(a_1 T) \times C_{PC}\} - \left\{m_{om} \times b_1 \times exp(a_1 T) \times \frac{C_{DO}}{C_{DO} + K_{DO}} \times C_{detC}\right\}$$

$$- \left\{ v_{poc}^{anb}(T, DO) \times C_{detC} \times 2.7 \right\} - \left\{ w_{detC} \frac{\partial C_{detC}}{\partial z} \right\}$$

Dissolved oxygen

$$\frac{\partial C_{DO}}{\partial t} = oprc - odpc - oddet + reaer - odsed - odh2s$$

Where:

oprc: oxygen production by photosynthesis

odpc: oxygen consumption by breath of phytoplankton carbon

oddet: oxygen consumption due to decomposition of detritus carbon

reaer: reaeration

odsed: oxygen sediment demand

odh2s: oxidation of hydrogen sulfide

$$oprc = R_1 \times G \times C_{PC}$$

$$odpc = R_1 \times R_{PC} \times exp(a_2 T) \times C_{PC}$$

$$oddet = R_1 \times b_1 \times m_{om} \times exp(a_1 T) \times \frac{C_{DO}}{K_{DO} + C_{DO}} \times C_{detC}$$

$$reaer|_{surface} = K_{reaer}(C_{sat} - C_{DO})$$

$$K_{reaer} = \left\{3.93 \times vsp^{\frac{1}{2}} \times dz^{-\frac{3}{2}}\right\} + \left\{\frac{\left(0.728 \times wsp^{\frac{1}{2}}\right) - (0.371 \times wsp) + (0.0372 \times wsp^2)}{dz}\right\}$$

Where:

vsp: horizontal current speed

wsp: wind speed

$C_{sat} = 14.65 - 0.0841 \times S + T\{0.00256 \times S - 0.41022 + T \times (0.007991 - 0.0000374 \times S - 0.000077774 \times T)\}$

$$odsed = dR_1 \times m_{omsed} \times exp\left(\beta_{poc}^{anb} \times T\right) \times \frac{C_{DO}}{K_{DO} + C_{DO}} \times C_{sed}$$

$$odh2s = 2v_{H_2S}^{oxc}(T, DO) \times C_{H_2S}$$

$$v_{H_2S}^{oxc} = \alpha_{H_2S}^{oxc} \times exp\left(\beta_{H_2S}^{oxc} \times T\right) \times \frac{DO}{DO + K_{DO}^{oxc}}$$

Therefore:

$$\frac{\partial C_{DO}}{\partial t} = \{R_1 \times G \times C_{PC}\} - \{R_1 \times R_{PC} \times exp(a_2 T) \times C_{PC}\} - \left\{R_1 \times m_{om} \times exp(a_1 T) \times \frac{C_{DO}}{K_{DO} + C_{DO}} \times C_{detC}\right\} + \{K_{reaer}(C_{sat} - C_{DO})\} - \left\{dR_1 \times m_{omsed} \times exp\left(\beta_{poc}^{anb} \times T\right) \times \frac{C_{DO}}{K_{DO} + C_{DO}} \times C_{sed}\right\} - \left\{2 \times \alpha_{H_2S}^{oxc} \times exp\left(\beta_{H_2S}^{oxc} \times T\right) \times \frac{DO}{DO + K_{DO}^{oxc}} \times C_{H_2S}\right\}$$

Sediment

$$\frac{\partial C_{sed}}{\partial t} = (\text{sed1} + \text{sed2} - \text{sed3} - \text{sed4})$$

Where:

sed1: deposition of phytoplankton carbon

sed2: deposition of detritus carbon

sed3: decomposition of sediment

sed4: decomposition of sediment under anoxic condition to release hydrogen sulfide

$$sed1 = w_{PC} \frac{\partial C_{PC}}{\partial z}$$

$$sed2 = w_{detC}\frac{\partial C_{detC}}{\partial z}$$

$$sed3 = m_{omsed} \times b_1 \times exp\left(\beta_{poc}^{anb} \times T\right) \times \frac{C_{DO}}{C_{DO} + K_{DO}} \times C_{sed}$$

$$sed4 = v_{poc}^{anb}(T, DO) \times C_{sed} \times \left(1 - \frac{C_{H_2S}}{K_{H_2S} + C_{H_2S}}\right)$$

Therefore:

$$\frac{\partial C_{sed}}{\partial t} = \left\{w_{PC}\frac{\partial C_{PC}}{\partial z} + w_{detC}\frac{\partial C_{detC}}{\partial z}\right\} - \left\{m_{omsed} \times b_1 \times exp\left(\beta_{poc}^{anb} \times T\right) \times \frac{C_{DO}}{C_{DO} + K_{DO}} \times C_{sed}\right\} - \left\{\alpha_{poc}^{anb} exp\left(\beta_{poc}^{anb} \times T\right)\left(1 - \frac{C_{DO}}{C_{DO} + K_{DO}}\right) \times C_{sed} \times \left(1 - \frac{C_{H_2S}}{K_{H_2S} + C_{H_2S}}\right)\right\}$$

Hydrogen sulfide

$$\frac{\partial C_{H_2S}}{\partial t} = sul1 + sul2 - sul3$$

Where:

sul1: Hydrogen sulfide released from decomposition of sediment under anoxic condition

sul2: Hydrogen sulfide released from decomposition of detritus carbon due to bacteria under anoxic condition

sul3: oxidation of hydrogen sulfide

$$sul1 = v_{poc}^{anb}(T, DO) \times C_{sed} \times 2.7$$

$$sul2 = v_{poc}^{anb}(T, DO) \times C_{detC} \times 2.7$$

$$v_{poc}^{anb} = \alpha_{poc}^{anb} exp\left(\beta_{poc}^{anb} \times T\right)\left(1 - \frac{C_{DO}}{C_{DO} + K_{DO}}\right)$$

$$sul3 = v_{H_2S}^{oxc}(T, DO) \times C_{H_2S}$$

$$v_{H_2S}^{oxc} = \alpha_{H_2S}^{oxc} \times exp\left(\beta_{H_2S}^{oxc} \times T\right) \times \frac{DO}{DO + K_{DO}^{oxc}}$$

Therefore:

$$\frac{\partial C_{H_2S}}{\partial t} = \left\{v_{poc}^{anb}(T, DO) \times C_{sed} \times 2.7\right\} + \left\{v_{poc}^{anb}(T, DO) \times C_{detC} \times 2.7\right\} - \left\{\alpha_{H_2S}^{oxc} \times exp\left(\beta_{H_2S}^{oxc} \times T\right) \times \frac{DO}{DO + K_{DO}^{oxc}} \times C_{H_2S}\right\}$$

Phosphorus

$$\frac{\partial C_{PO_4}}{\partial t} = -Dp1 + Dp2 + Dp3 + Dp4 + Dp5$$

Where:

Dp1: phosphorus ingested by phytoplankton carbon

Dp2: transformation of phosphorus from organic matters to inorganic matters

Dp3: phosphorus released from sediment

Dp4: phosphorus released from phytoplankton carbon breath

Dp5: phosphorus released from decomposition of detritus carbon

$Dp1 = R_2 \times G \times C_{PC}$

$R_2 : C = \frac{31}{12m}$

$Dp2 = dR_2 \times m_{om} \times exp(a_1 T) \times \frac{C_{DO}}{C_{DO} + K_{DO}} \times C_{detC}$

$Dp3 = k_p \times exp(pt \times T - 0.35 \times C_{DO})$

$Dp4 = R_2 \times R_{PC} \times exp(a_2 T) \times \frac{C_{DO}}{C_{DO} + K_{DO}} \times C_{PC}$

$Dp5 = dR_2 \times m_{omsed} \times \exp(\beta_{poc}^{anb} \times T) \times \frac{C_{DO}}{C_{DO} + K_{DO}} \times b1 \times p1$

Therefore:

$$\begin{aligned}\frac{\partial C_{PO_4}}{\partial t} = &-\{R_2 \times G \times C_{PC}\} + \left\{dR_2 \times m_{om} \times exp(a_1 T) \times \frac{C_{DO}}{C_{DO} + K_{DO}} \times C_{detC}\right\} \\ &+ \{k_p \times exp(pt \times T - 0.35 \times C_{DO})\} \\ &+ \left\{R_2 \times m_{PC} \times exp(a_2 T) \times \frac{C_{DO}}{C_{DO} + K_{DO}} \times C_{PC}\right\} \\ &+ \left\{dR_2 \times m_{omsed} \times \exp(\beta_{poc}^{anb} \times T) \times \frac{C_{DO}}{C_{DO} + K_{DO}} \times b1 \times p1\right\}\end{aligned}$$

Sulfur

$$\frac{\partial C_{S0}}{\partial t} = S1 - S2$$

S1: formation of sulfur from oxidation of hydrogen sulfide

S2: sulfur settling

$S1 = 0.5 \times \nu_{H_2S}^{oxc}(T, DO) \times C_{H_2S}$

$S2 = w_{S0} \times \frac{\partial C_{S0}}{\partial z}$

Therefore:

$$\frac{\partial C_{S0}}{\partial t} = \{0.5 \times \nu_{H_2S}^{oxc}(T, DO) \times C_{H_2S}\} - \left\{w_{S0} \times \frac{\partial C_{S0}}{\partial z}\right\}$$

2.2.3.3. Construction of ECO Lab module

An advanced application of MIKE 3 is that engineers may design their own ECO Lab templates. Basing on kinetic differential equations of environmental variables listed above, there is a template of an ECO Lab module constructed. General information of template are shown in **Table 2.2** below.

Table 2.2. General overview of ECO Lab for Tokyo bay

State variables	7
Constants	32
Forcings	6
Auxilary variables	16
Processes	31

State variables

In ECO Lab, state variables describe the state of the ecosystem that user want to predict. State variables represent the target variables. Value of state variables vary over time. State variables are constituted by processes. There are six state variables used to simulate water quality in Tokyo bay and each state variable is characterized as **Table 2.3** shown below.

Table 2.3. List of state variables in ECO Lab

No.	Symbol	Description	Expression	Type
1	PC	Phytoplankton Carbon	*phtsyn – death – breath - pcsettling*	Concentration
2	detC	Detritus Carbon	*detprc-detdecomp1 - detdecomp2-detsettling*	Concentration
3	DO	Dissolved oxygen	*oprc-odpc-oddet+reaer-odsed-odh2s*	Concentration

Table 2.3. List of state variables in ECO Lab (continue)

No.	Symbol	Description	Expression	Type
4	sed	Sediment	$sed1 + sed2 - sed3 - sed4$	Mass per Area
5	H2S	Hydrogen sulfide	$sul1 + sul2 - sul3$	Concentration
6	PO4	Dissolved phosphorus	$-Dp1 + Dp2 + Dp3 + Dp4 + Dp5$	Concentration
7	S0	Sulfur	$S1 - S2$	Concentration

Constants

Constants influence to internal calculations and are used as arguments in the mathematical expressions of process in ECO Lab model. Value of constants are always stable in time but can vary in space. Attributes of constants are listed as in **Table 2.4** below**.**

Table 2.4. List of constants in ECO Lab

No.	Symbol	Default value	Spartial variation	Unit	Description
1	gmax	0.693	NONE	1/day	Maximum growth speed coefficent of phytoplankton
2	Lopt	50	NONE	Eintein/m^2/day	Optimal light
3	mppl	0.05	NONE	Per day	Dead speed of phytoplankton
4	R1	3.47	NONE	Dimensionless	Ratio of oxygen production by phytoplankton
5	R2	0.0243	NONE	Dimensionless	Ratio of phosphorus production by phytoplankton
6	dR1	3.47	NONE	Dimensionless	Ratio of oxygen production by detritus
7	dR2	0.0243	NONE	Dimensionless	Ratio of phosphorus production by detritus

Table 2.4. List of constants in ECO Lab (continue)

No.	Symbol	Default value	Spartial variation	Unit	Description
8	Rppl	0.02	NONE	Per day	Phytoplankton breath speed
9	Mom	0.14238	NONE	Per day	Transformation speed from organic matters to inorganic matters
10	Momsed	0.14238	H&V	Per day	Decomposition speed of sediment
11	gt	0.0693	H&V	Dimensionless	Temperature coefficient for maximum growth speed of phytoplankton
12	a1	0.0693	NONE	Dimensionless	Temperature coefficient 1
13	a2	0.0523	NONE	Dimensionless	Temperature coefficient 2
14	bsed	0.0693	NONE	Dimensionless	Temperature coefficient for decomposition of sediment
15	b1	0.6	NONE	Dimensionless	Decomposition due to bacteria
16	Kdo	0.3	NONE	mg/L	Anoxic dissolved oxygen concentration coefficient
17	Kp	0.0002	NONE	mg/L	Phosphorus sediment coefficient
18	wppl	0.022	NONE	m/day	Phytoplankton settling speed
19	wdet	1.7	NONE	m/day	Detritus settling speed
20	o2	0.5	NONE	mg/L	Sulfide dissolution oxygen limit
21	K2	1.93	NONE	Dimensionless	Constant number
22	asul	12	NONE	1/day	Sulfide oxidation coefficient 1
23	fsul	2.8	NONE	Dimensionless	ratio sulfide/C
24	ased	0.05	H	1/day	sediment coefficient

Table 2.4. List of constants in ECO Lab (continue)

No.	Symbol	Default value	Spartial variation	Unit	Description
25	bsul	0.0693	NONE	Dimensionless	sulfide oxidation coefficient 2
26	kp	0.00015	NONE	Dimensionless	Sediment P coefficient
27	pt	0.115	NONE	Dimensionless	Sediment-P temperature coefficient
28	p1	1	NONE	Dimensionless	Phosphorus coefficient
29	ksul	40	NONE	mg/L	Anoxic decomposition coeffient of background sediment
30	sed_bg	0.8	H	g/m²	Background sediment concentration
31	ws	0.5	NONE	m/day	Sulfur settling speed
32	wsa	0	H	mg/l	surface air

H&V: Horizontal and vertical

Forcings

Forcings are representatives for external factors that affects to ecosystem. They are used as arguments in the mathematical expressions of processes in ECO Lab model also. They change over time and space. All forcings which specified in **Table 2.5** below, are built availably in MIKE model except forcing L0.

Table 2.5. List of forcings in ECO Lab

No.	Symbol	Scope	Spartial variation	Unit	Description
1	T	WC	H&V	Degree C	Temperature
2	L0	Not specified	NONE	Dimensionless	Surface light
3	dz	WC	H&V	m	Water layer height
4	S	WC	H&V	psu	Salinity

Table 2.5. List of forcings in ECO Lab (continue)

No.	Symbol	Scope	Spartial variation	Unit	Description
5	vsp	WC	H&V	m/s	Horizontal current speed
6	wsp	WS	H	m/s	Wind speed

WC: water column

WS: water surface

H&V: Horizontal and vertical

Auxiliaries

Auxiliary variables are defined as intermediate calculations. They are arguments in processes' formula and are also expressed by mathematical expressions. Auxiliaries may be optional outcomes if user want to specify additional results. Details of auxiliaries are depicted as **Table 2.6** below.

Table 2.6. List of auxiliaries in ECO Lab

No.	Symbol	Expression	Description
1	Gmax	gmax*EXP(gt*T)	Growth max speed
2	Ccha	0.021*PPL*1000	Ratio of Chl-a
3	Zt	IF(Ccha<0.002) THEN 12 ELSE - 1.0085*LN(Ccha)+5.461	Underwater visibility
4	K	K2/Zt	Evaporation coefficient
5	L	(LAMBERT_BEER_1(L0,dz,K) + LAMBERT_BEER_2(L0,dz,K))/2	Light
6	Lightonly	(L/Lopt)*EXP(1-(L/Lopt))	Light only
7	Ponly	MAX(0,DP)/(Kp+MAX(0,DP))	Phosphorus only
8	DOonly	MAX(DO,0)/(Kdo+MAX(DO,0))	DO only
9	G	Gmax*Lightonly*Ponly	Growth rate

Table 2.6. List of auxiliaries in ECO Lab (continue)

No.	Symbol	Expression	Description
10	ppldead	mppl*EXP(a1*T)	Phytoplankton death
11	pplbreath	Rppl*EXP(a2*T)*Doonly	Phytoplankton breath
12	detbunkai	Mom*EXP(a1*T)*Doonly	Detritus decomposition
13	sed3_bg	*IF* (DO<o2) *THEN* ased*EXP(bsed*T)*(1-(max(DO,0)/(max(DO,0)+Kdo)))*sed_bg*(1-(sul/(sul+ksul))) *ELSE* 0	Background sediment anoxic decomposition rate
14	Kreaer	3.93*POW(vsp,0.5)*POW(dz,-1.5)+(0.728*POW(wsp,0.5)-0.371*wsp+0.0372*POW(wsp,2))/dz	Reaeration rate
15	csair	OXYGENSATURATION(S,T)	Oxygen saturation concentration
16	CSAT	csair-DO	Mediate auxiliary

Processes

Processes are components to contribute the variation of state variables. Each process vary in time and space and is expressed by a formula. **Table 2.7** below reveals information of processes used in ECO Lab for Tokyo bay.

Table 2.7. List of processes in ECO Lab

No.	Symbol	Expression	Scope
1	phtsyn	$G \times PC$	WC
2	death	$ppldead \times PC$	WC
3	breath	$pplbreath \times PC$	WC
4	pcsettling	$(wppl \times PC)/dz$	WC
5	detprc	$death$	WC

Table 2.7. List of processes in ECO Lab (continue)

No.	Symbol	Expression	Scope
6	decomp1	$detbunkai \times b1 \times detC$	WC
7	decomp2	$IF\ (DO < o2)\ THEN\ ased \times exp(bsed \times T) \times \left(1 - \frac{DO}{DO - Kdo}\right) \times detC\ ELSE\ 0$	WC
8	detsettling	$(wdet \times detC)/dz$	WC
9	oprc	$R1 \times G \times PC$	WC
10	odpc	$R1 \times pplbreath \times PC$	WC
11	oddet	$R1 \times detbunkai \times b1 \times detC$	WC
12	reaer	$IF\ (DO > 0.0)\ THEN\ Kreaer \times \left(max(wsa, CSAT)\right)\ ELSE\ Kreaer \times csair$	WS
13	odsed	$odsed1/dz$	WB
14	odsed1	$dR1 \times Momsed \times exp(bsed \times T) \times DOonly \times b1 \times (sed + sed\_bg\ )$	WB
15	odh2s	$2 \times sul3$	WC
16	sed1	$SEPC \times dz$	WC
17	SEPC	$(wppl/dz) \times PC$	WC
18	sed2	$SEDC \times dz$	WC
19	SEDC	$(wdet/dz) \times detC$	WC
20	sed3	$Momsed \times exp(bsed \times T) \times DOonly \times b1 \times sed$	SED
21	sed4	$IF\ (DO < o2)\ THEN\ ased \times \exp(bsed \times T) \times (1 - DO/(DO - Kdo)) \times sed \times (1 - H2S/(H2S - ksul))\ \ ELSE\ 0$	SED
22	sul1	$(sed4 + sed4\_bg) \times fsul$	WB
23	sul2	$detdecomp2 \times fsul$	WC
24	sul3	$IF\ (DO > 0.1)\ THEN\ asul \times exp(bsul \times T) \times \left(1 - \frac{DO}{DO - Kdo}\right) \times H2S\ ELSE\ 0$	WC
25	Dp1	$R2 \times G \times PC$	WC
26	Dp2	$dR2 \times detbunkai \times b1 \times detC$	WC
27	Dp3	$kp \times exp(pt \times T - 0.35DO)$	WB
28	Dp4	$pplbreath \times PC \times R2$	WC

Table 2.7. List of processes in ECO Lab (continue)

No.	Symbol	Expression	Scope
29	Dp5	$dR2 \times Momsed \times exp(bsed \times T) \times DOonly \times b1 \times p1$	WB
30	S1	$IF\ (DO > 0.1)\ THEN\ asul \times exp(bsul \times T) \times \left(1 - \frac{DO}{DO - Kdo}\right) \times H2S\ ELSE\ 0$	WC
31	S2	$(ws \times S0)/dz$	WC

WC: water column
WS: water surface
WB: water bed
SED: sediment

2.2.4. Simulation method

2.2.4.1. Grids

To reproduce environmental processes in Tokyo bay for simulation period from 2014 and 2015, two meshes with proportional size were chose for simulation. The resolution of meshes are considered to fit suitably with the scale of Tokyo bay, computational time and accuracy. A coarse rectangular mesh with the resolution of 450 meter is applied for parallel calculation of fine structure grid of 150 meter enclosed with major domain (**Figure 2.8**) and 30 layers with 1 meter thickness for both meshes. Fine grid is to focus more on off-Urayasu dredged pits and off-Makuhari dredged pits. The larger domain contains total 104×143 points (including both land points and water points) along *x* and *y* horizontal directions respectively whereas small domain consists of 97×85 points (including both land points and wet points) along *x* and *y* horizontal directions. Total computational points are 130,611 points (77,154 points in large area whereas 53,457 points in small area). Origin point (0,0) for fine grid is equivalent to point (60,93) in coarse grid.

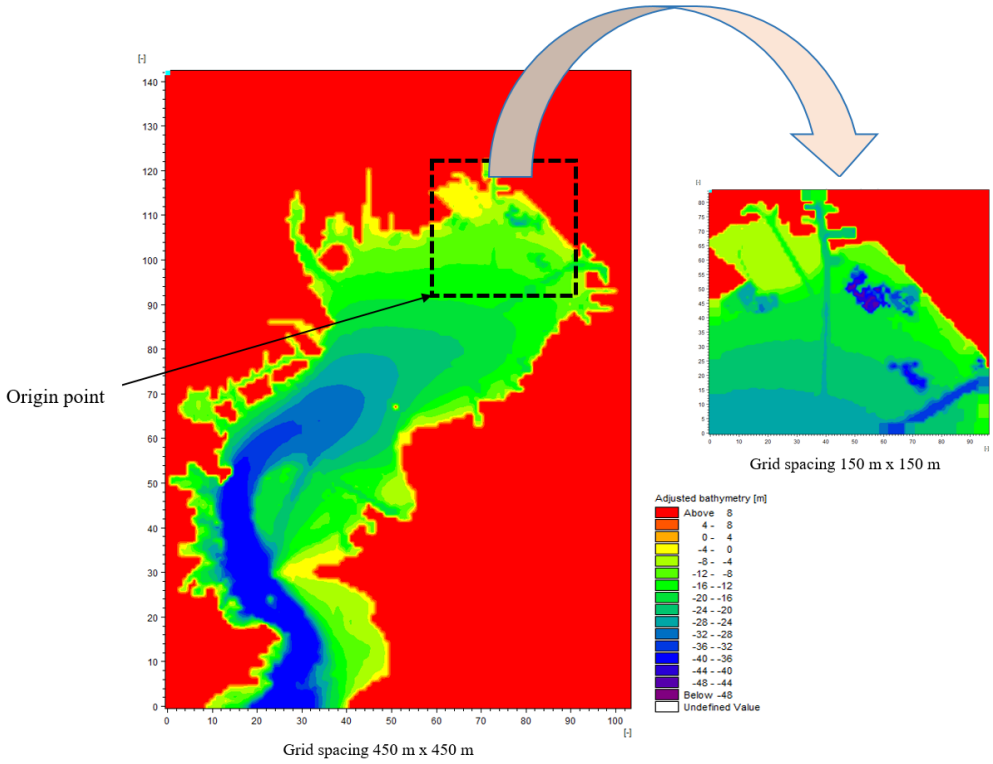

Figure 2.8. Coarse grid coupled with fine grid for reproduction

2.2.4.2. Boundary conditions

Boundary of the domain is only identified at the bay mouth (**Figure 2.9**). Boundary positions in the grid coordinates are identified along x, y, z axes as 9-40, 0-0, 0-30 respectively. A data set of tide, salinity and sea water temperature at the bay mouth for hydrodynamic simulation have been collected to provide for simulation. Tide at Yokosuka station which is the nearest station to bay mouth is chose to supply surface elevation for the model. Salinity and water temperature at boundary are downloaded from website https://hycom.org/dataserver. Sources of salinity and water temperature are assimilative and reanalyzed data with 40 layers and resolution up to $1/12^0$. List of figures below show salinity and sea water temperature at boundary. Because there are no measured data providing ECO Lab module at boundary, values are set as constant and presented in next subsection. **List of figure 2.10, 2.11, 2.12, 2.13** show water temperature and salinity at boundary taken into

model for simulation.

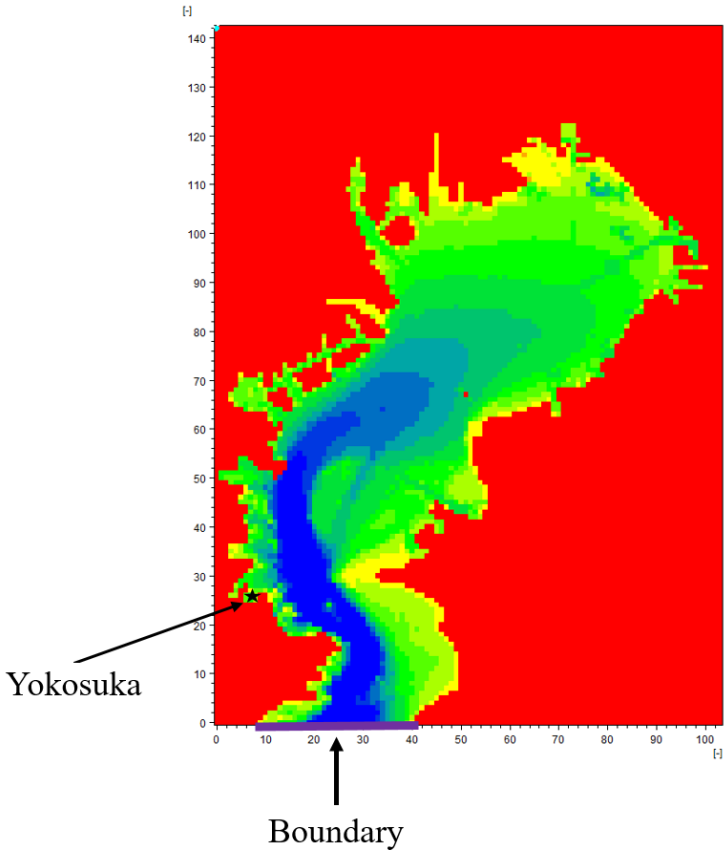

Figure 2.9. Boundary in simulation

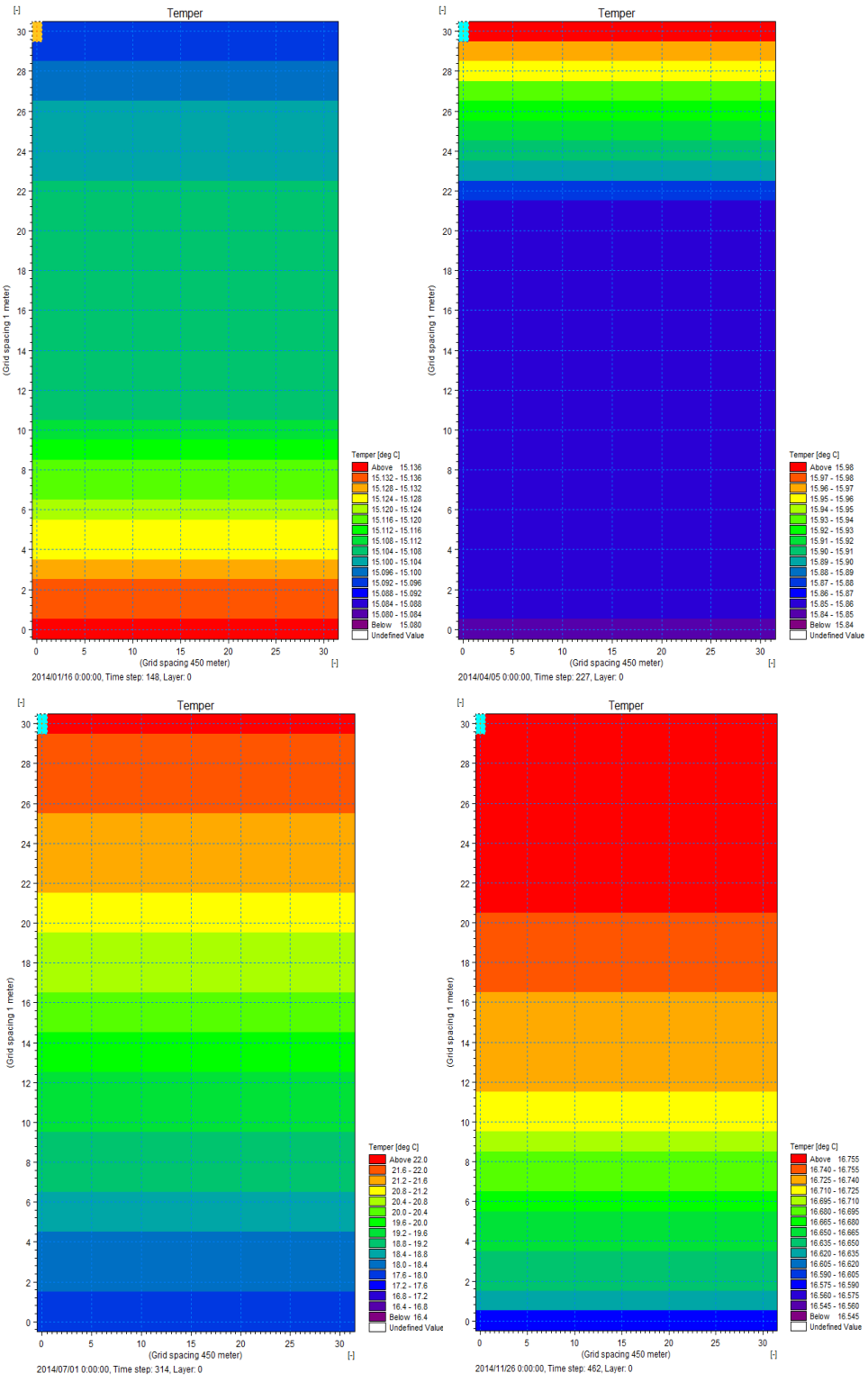

Figure 2.10. Water temperature at boundary in year 2014

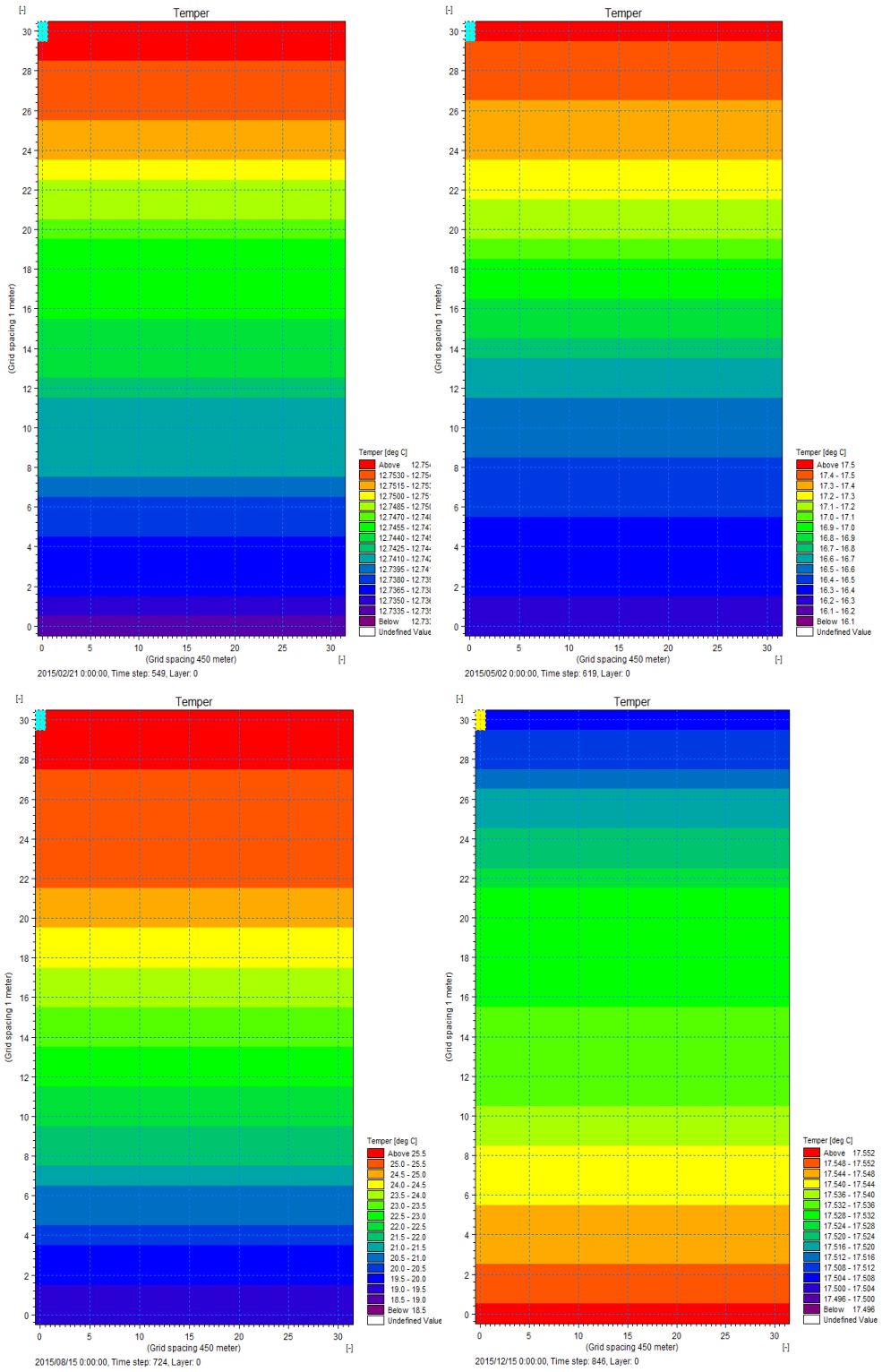

Figure 2.11. Water temperature at boundary in year 2015

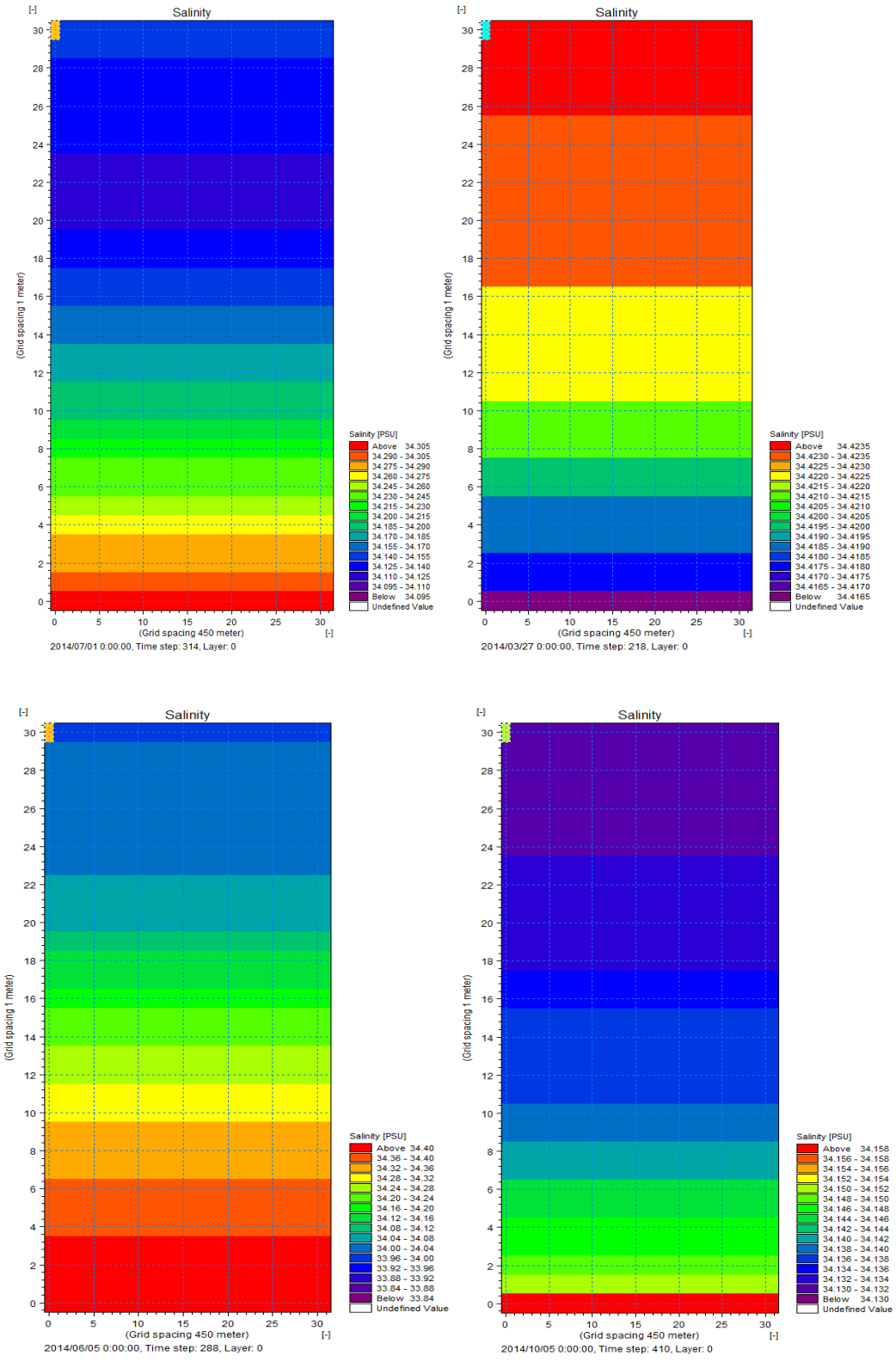

Figure 2.12. Salinity at boundary in year 2014

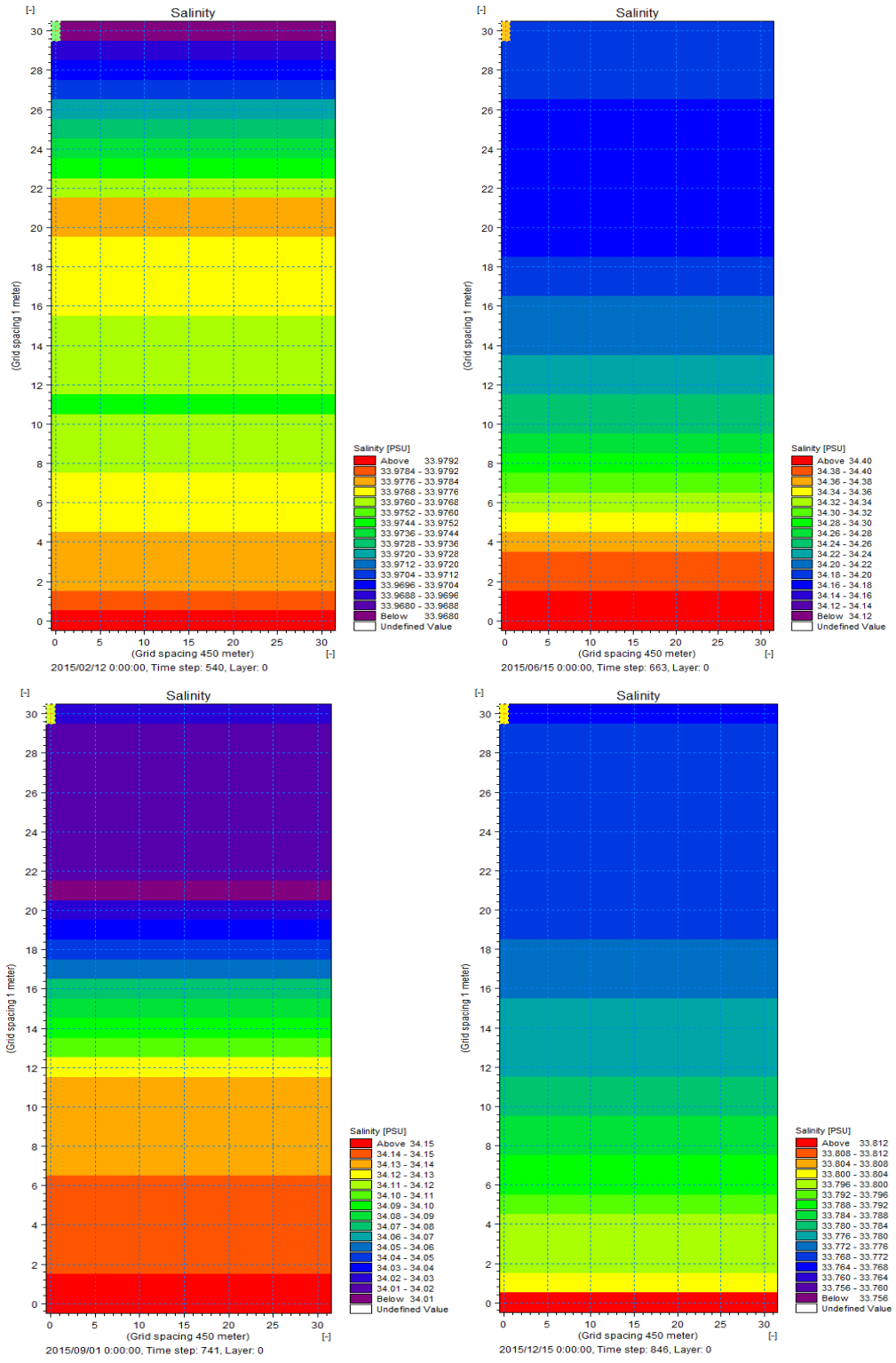

Figure 2.13. Salinity at boundary in year 2015

2.2.4.3. External forcings

Variation of environmental processes is governed by meteorological conditions. These external forcings need to be taken into model to simulate interaction of hydrodynamic and water quality processes. Hourly data of air temperature, precipitation, wind (speed and direction), relative humidity, cloud cover in Chiba station (35˚36'06''N, 140˚06'12''E) are dowloaded from Japan Meteorological Agency website whereas solar radiation in Tokyo station (35˚41'30''N, 139˚45'00''E) is provided by government. Variations of meteorology are shown in **Figure 2.14** below.

All external forcing may insert directly MIKE 3 model except solar radiation data. Because observed hourly solar radiation unit is in MJ/m² while MIKE 3 only accepts unit of Einstein/m²/day. Thus there need be a conversion from MJ/m² to Einstein/m²/day.

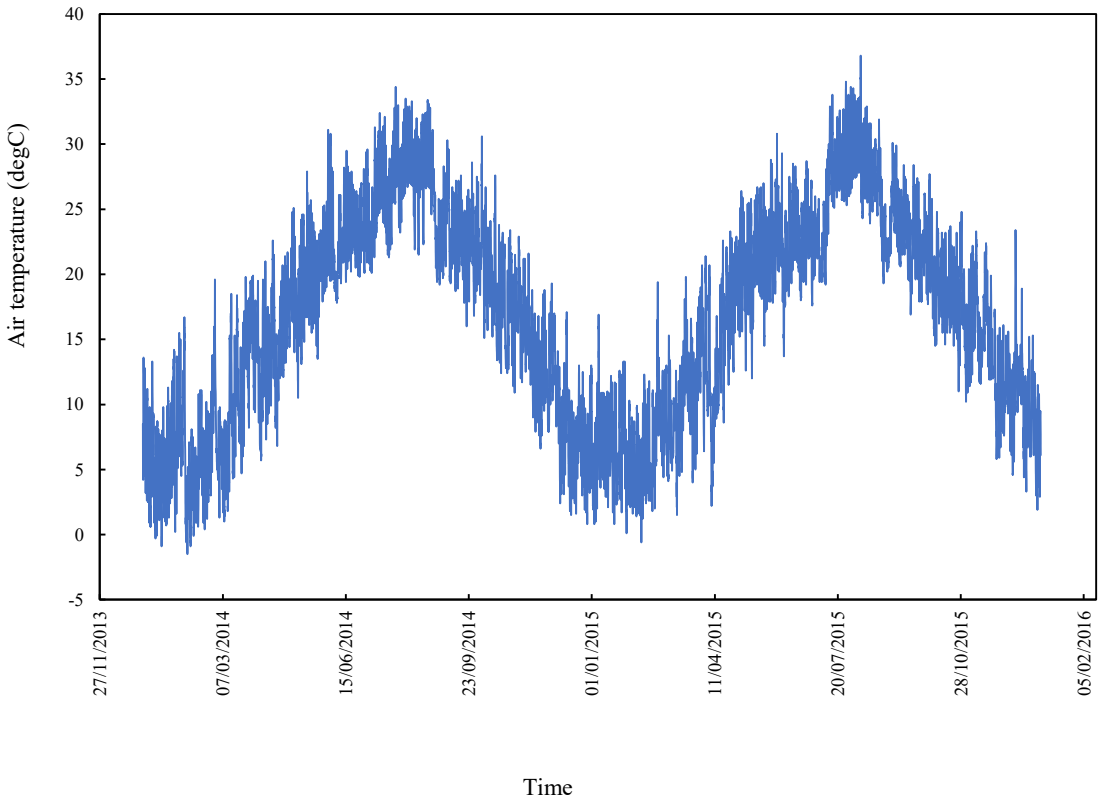

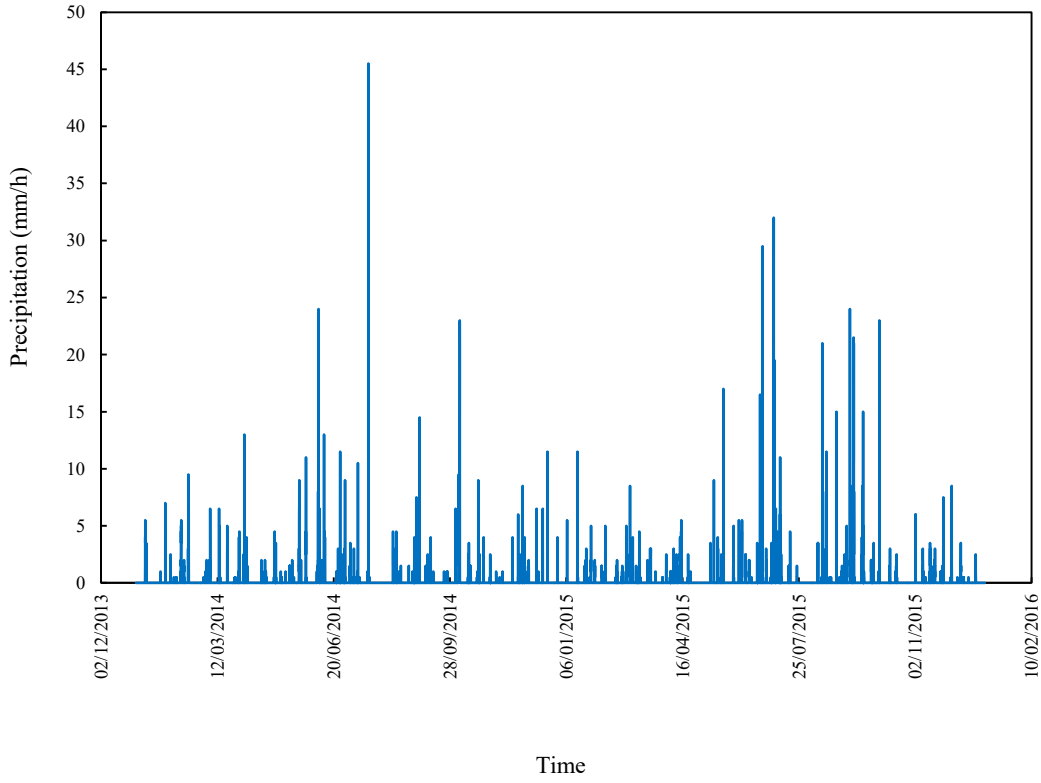
Precipitation (mm/h)
50
45
40
35
30
25
20
15
10
5
0
02/12/2013
12/03/2014
20/06/2014
28/09/2014
06/01/2015
16/04/2015
25/07/2015
02/11/2015
10/02/2016
Time

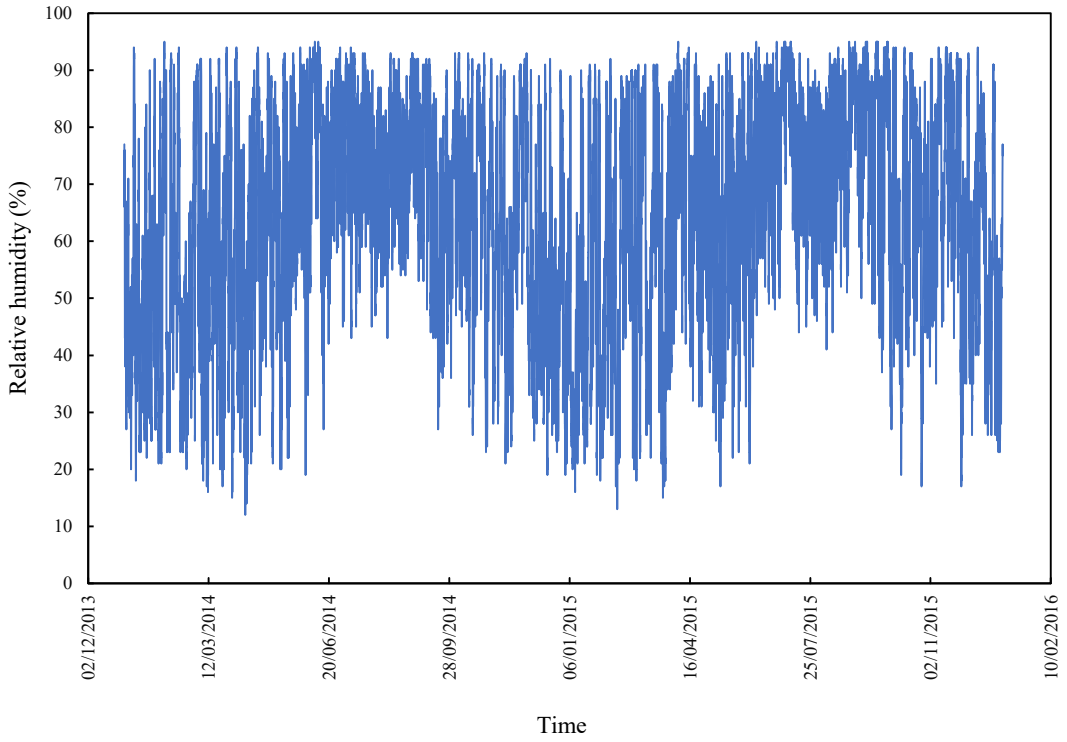
Relative humidity (%)
100
90
80
70
60
50
40
30
20
10
0
02/12/2013
12/03/2014
20/06/2014
28/09/2014
06/01/2015
16/04/2015
25/07/2015
02/11/2015
10/02/2016
Time

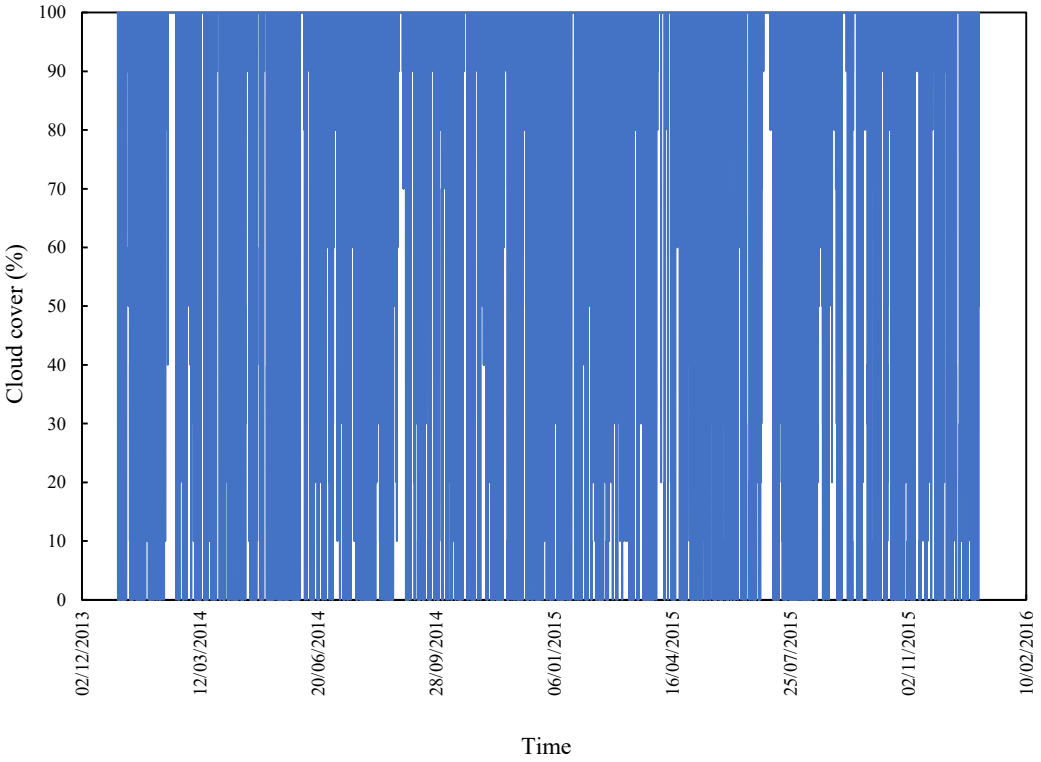
Cloud cover (%)
100
90
80
70
60
50
40
30
20
10
0
02/12/2013
12/03/2014
20/06/2014
28/09/2014
06/01/2015
16/04/2015
25/07/2015
02/11/2015
10/02/2016
Time

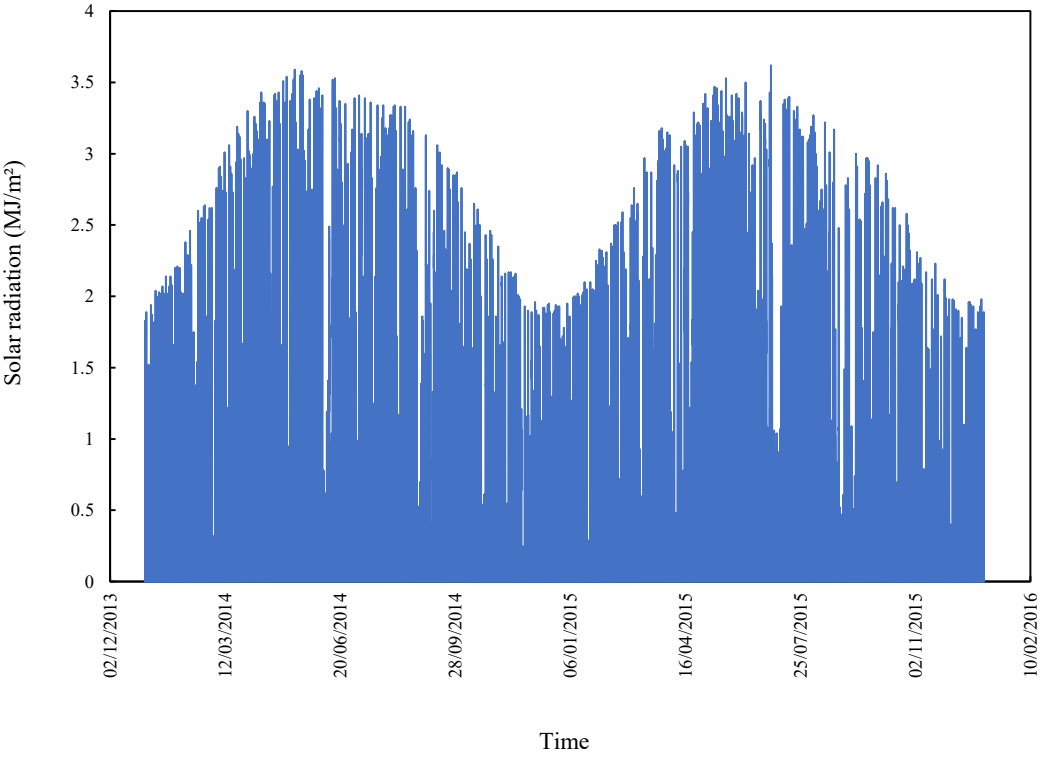
Solar radiation (MJ/m²)
4
3.5
3
2.5
2
1.5
1
0.5
0
02/12/2013
12/03/2014
20/06/2014
28/09/2014
06/01/2015
16/04/2015
25/07/2015
02/11/2015
10/02/2016
Time

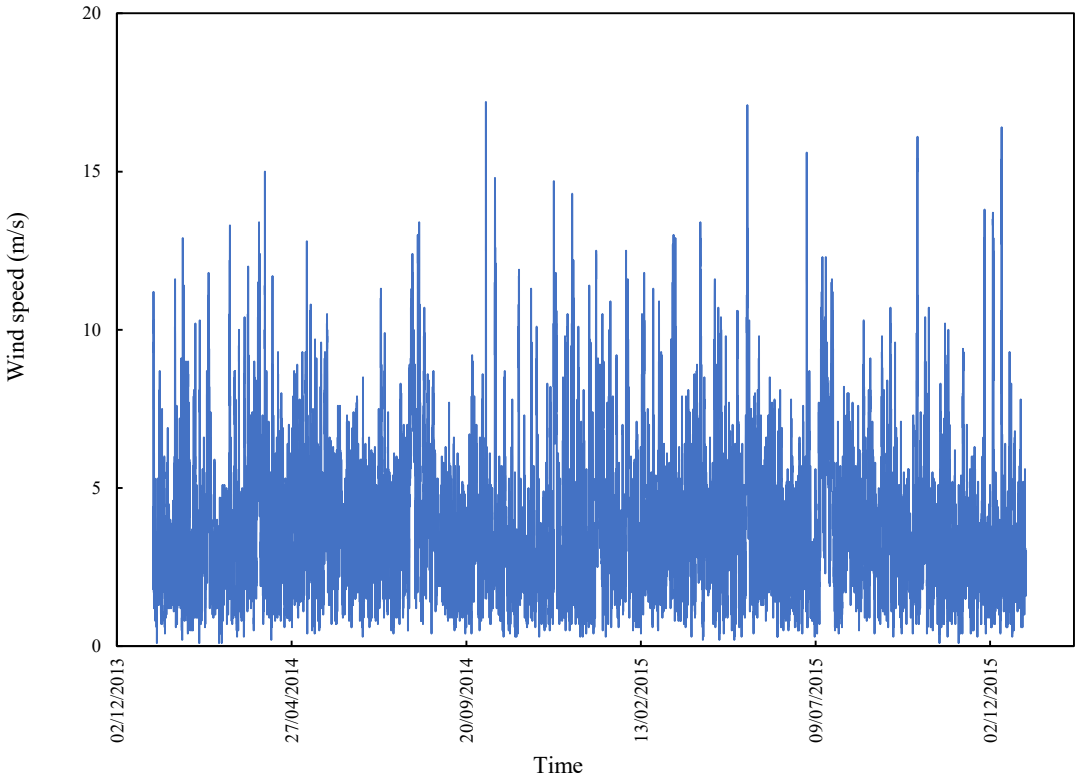

Figure 2.14. Meteorological conditions in year 2014 and year 2015

2.2.4.4. Sources and sinks

Sources and sinks in this simulation are considered as four main rivers discharging into Tokyo Bay. They are Arakawa river, Edogawa river, Tamagawa river and Tsurumigawa river. Locations of these rivers in coarse grid coordinates are shown in **Table 2.8** and **Figure 2.15** below. These points must be placed at a computational point (a wet point, not on land) and fitted to actual position.

Table 2.8. Sources and sinks points to Tokyo bay

River name	Grid point
Arakawa	45,120,30
Edogawa	50,110,30
Tamagawa	23,86,30
Tsurumigawa	14,73,30

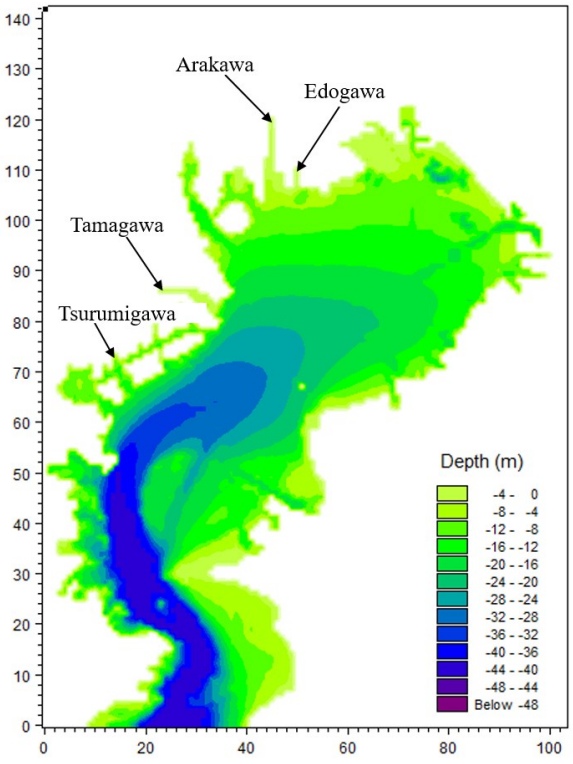

Figure 2.15. Locations of rivers discharging Tokyo bay in model grid coordinates

Daily measured discharge data of Edogawa and Tamagawa rivers in year 2014 and 2015 are provided by The Bureau of Waterworks, Tokyo Metropolitan Government. Basing on discharge data in year 2010 dowloaded from the Ministry of Land, Infrastructure, Transport and Tourism website (http://www1.river.go.jp) to estimate discharge data for two other rivers (Arakawa and Tsurumigawa). To increase the accuracies, these discharge data have been tuned during model simulation process.

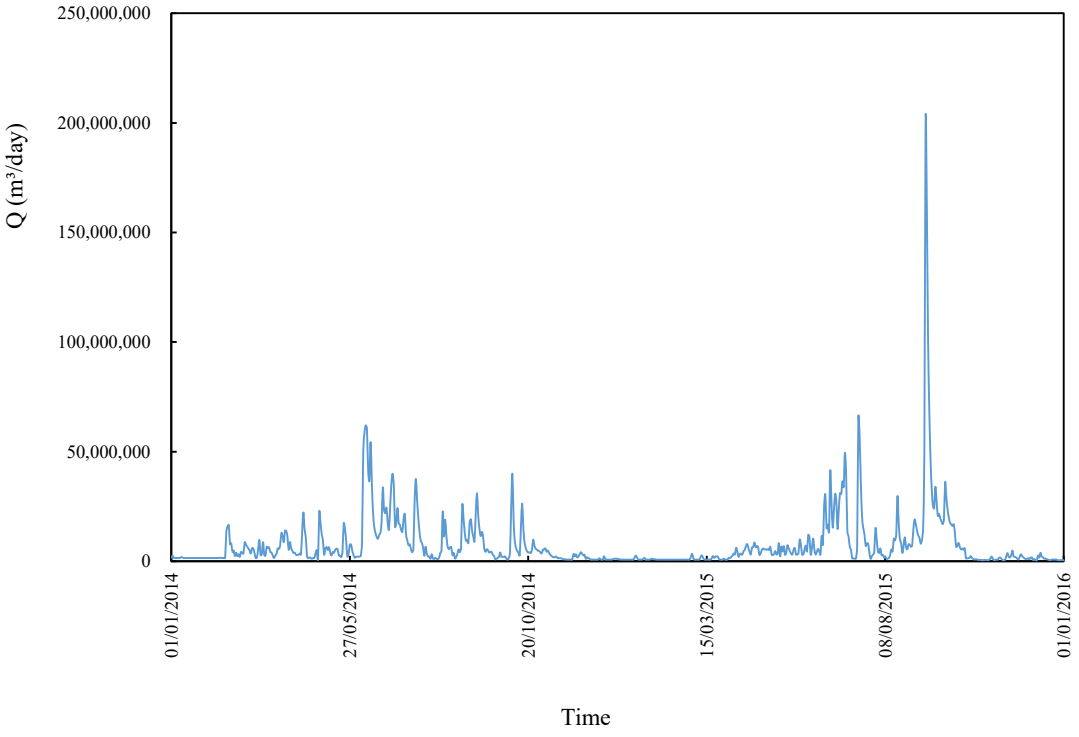

Figure 2.16. Arakawa river discharge

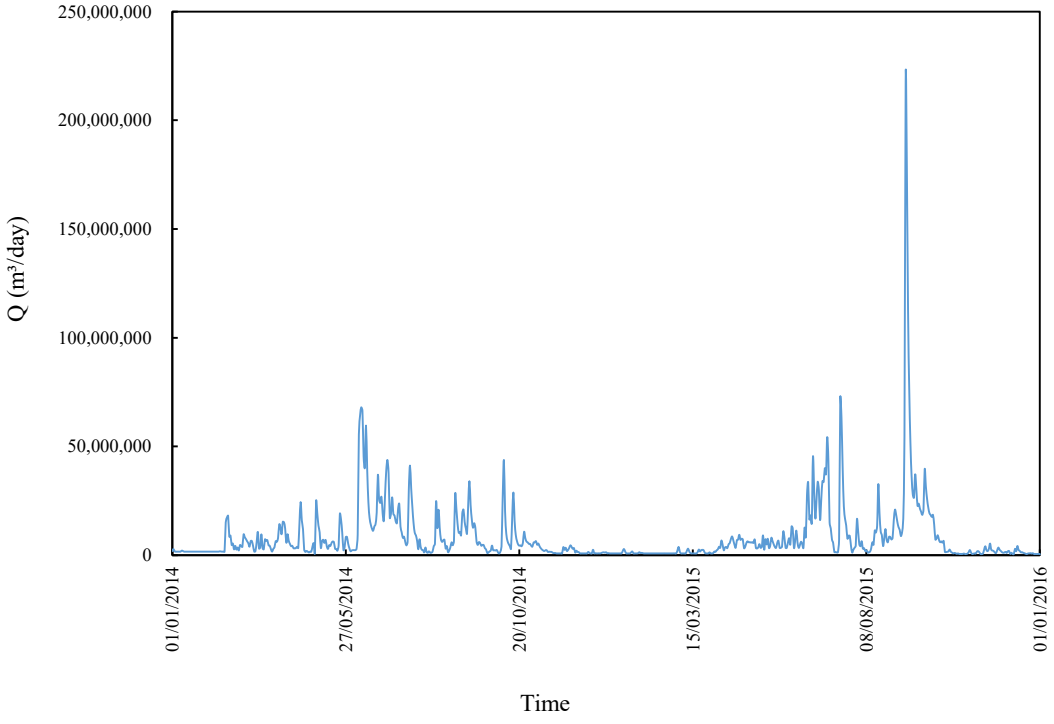

Figure 2.17. Edogawa river discharge

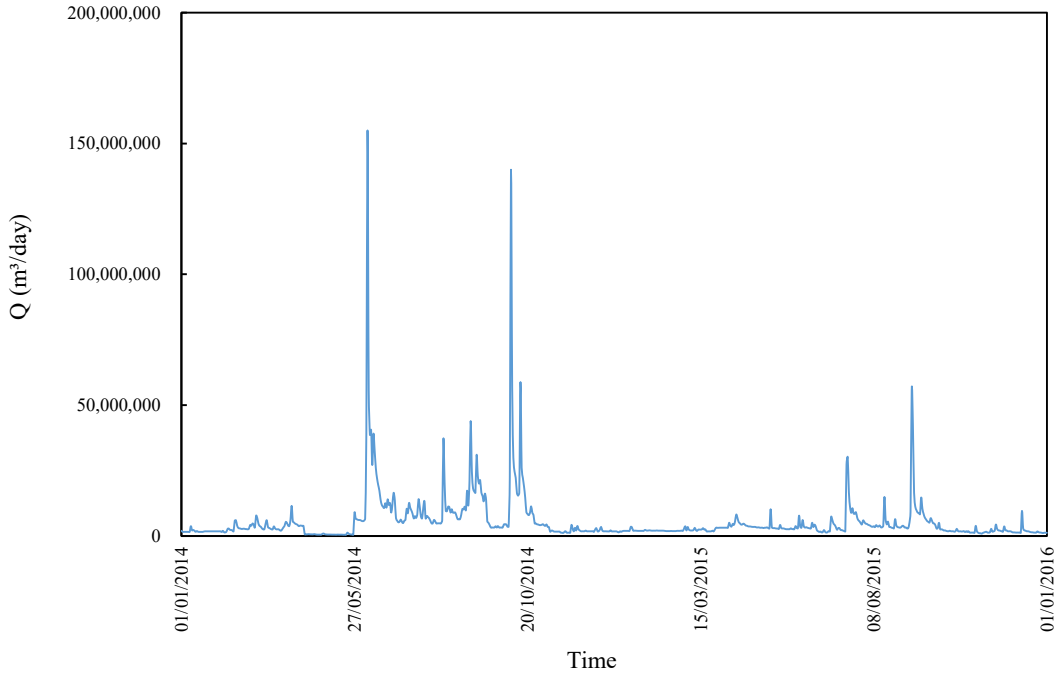

Figure 2.18. Tamagawa river discharge

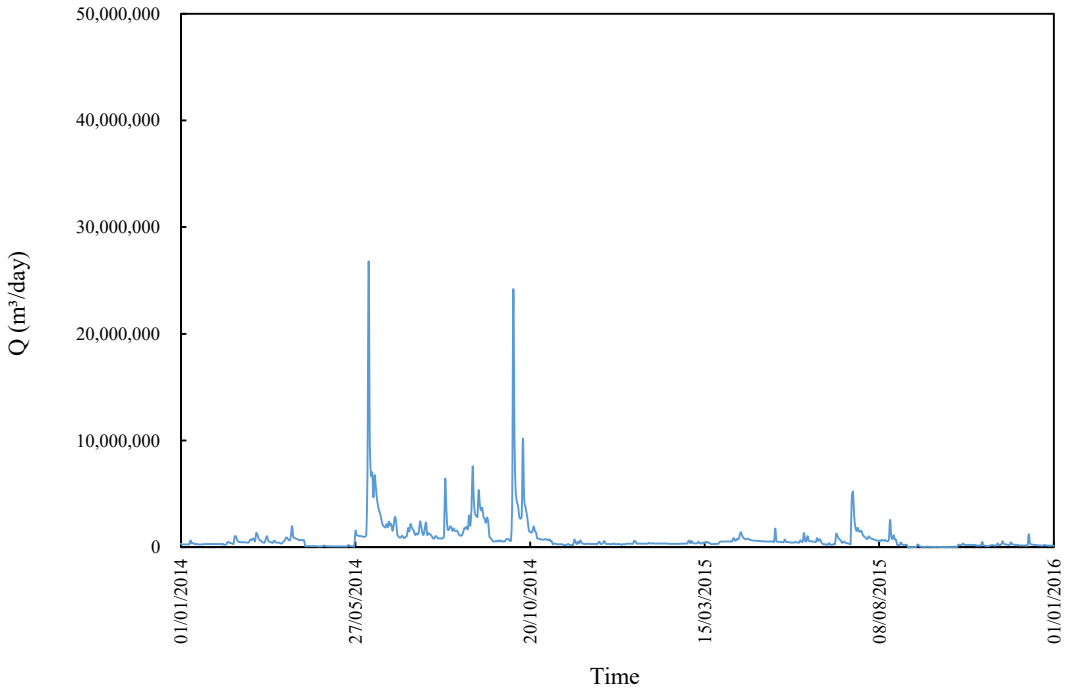

Figure 2.19. Tsurumigawa river discharge

2.2.4.5. Setting up model

Time step

MIKE 3 model is designed to achieve maximum Courant number up to 5 for stability, time step of computation therefore is set at 30s which satisfies Courant number. The criterion form is as follows:

$$C_{R=}\sqrt{gh}\frac{\Delta t}{\Delta s} \leq 5$$

where Δt is time step, Δs the grid spacing, g is the gravitational acceleration, h is depth. Courant number maximizes with fine mesh of 150m grid size and maximum water depth 40m, Δt should be:

$$\Delta t \leq \frac{150 \times 5}{\sqrt{10 \times 40}} = 37.5s$$

Turbulence model

Turbulence model selection is the mean of the mixed k-ε/Smagorinsky formulation with a standard k-ε model in the vertical and a Smagorinsky formulation in the horizontal.

Initial conditions for hydrodynamic module

To avoid generation of shock waves, initial surface elevation is set to match roughly with the start of simulation. Value of initial elevation is fixed at 0.1 meter for both areas.

Initial temperature is set 14 degree Celcious while initial salinity values at 33 psu. Beside that background temperature and background salinity which is used to minimize numerical inaccuracies, are set 20 degree Celcious and 33 psu respectively.

Boundary conditions and bounda for ECO Lab module

Boundary conditions

Because of not having observed data at boundary, values of environmental variables are nominated constants over time and vertical layer. They are set in **Table 2.9** as follows:

Table 2.9. Boundary parameters of state variables

Phytoplankton carbon	0.01 mg/L
Detritus carbon	0.01 mg/L
Dissolved oxygen	8 mg/L
sulfide	0 mg/L
Dissolved phosphorus	0.001 mg/L
Sulfur	0 mg/L

Initial conditions and background concentration for state variables

Set of values of state variable in **Table 2.10** as follows:

Table 2.10. Initial parameters of state variables

Phytoplankton carbon	0.1 mg/L
Detritus carbon	0.1 mg/L
Dissolved oxygen	8 mg/L
sulfide	0 mg/L
Dissolved phosphorus	0.04 mg/L
Sulfur	0 mg/L

Concentration of environment variables in sources and sinks

Due to Tokyo Bay is an estuary therefore values of these variables also need to be assigned to examine effects of river to ecosystem in bay. They are set in **Table 2.11** as follows:

Table 2.11. Parameters of state variables in sources and sinks

Phytoplankton carbon	0 mg/L
Detritus carbon	0 mg/L
Dissolved oxygen	10.9 mg/L
sulfide	0 mg/L
Dissolved phosphorus	0.05 mg/L
Sulfur	0 mg/L

2.2.4.6. Model verification

2.2.4.6.1. Elevation

Tidal data of three tidal stations around Tokyo Bay shoreline (**Figure 2.20**) are used to compare between model and measurement. The results show high compatibility of measured and simulated elevation. Correlation indexes at all stations are very impressed with the highest value of 0.941 at Yokosuka station. Simulated and observed tides are suitable highly in both phase and magnitude. Results of three stations are shown as **Figure 2.21, 2.22, 2.23** below.

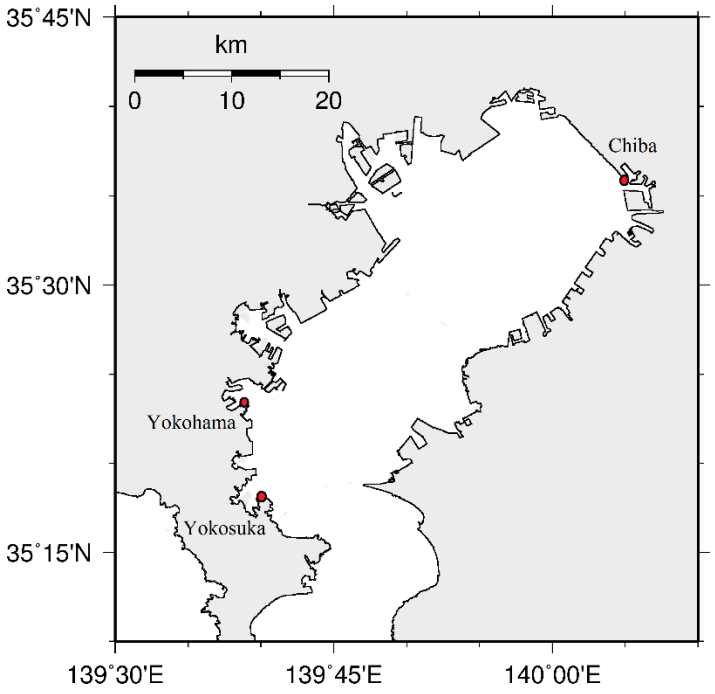

Figure 2.20. Locations of tidal stations

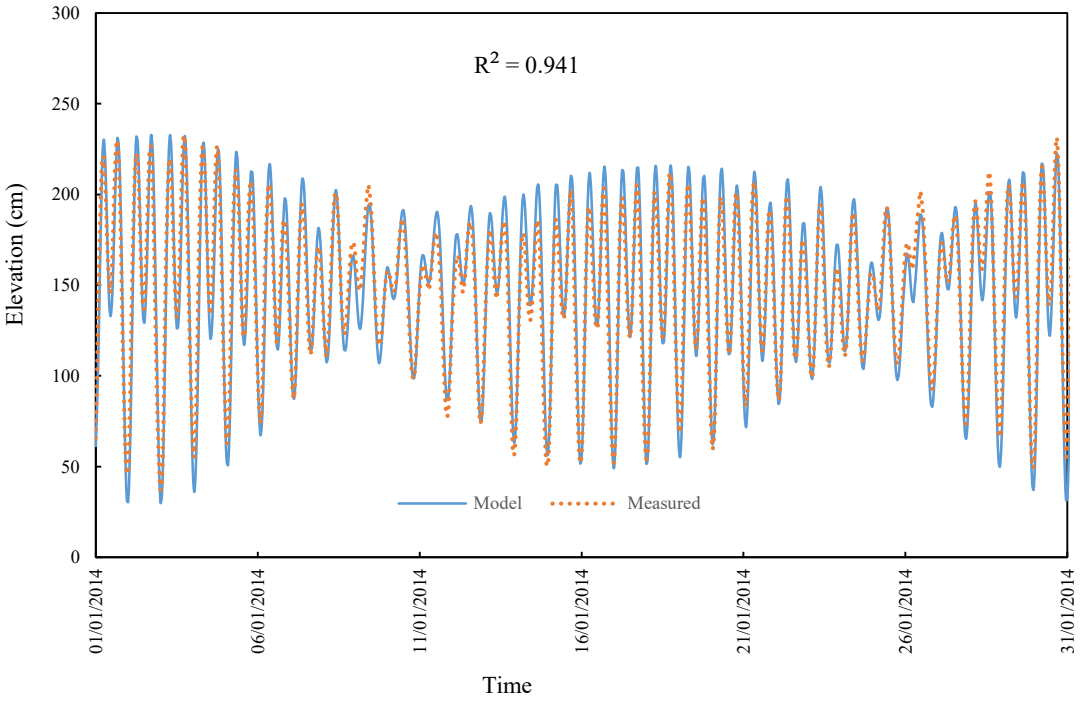

Figure 2.21. Elevation comparison between model and measured data at Yokosuka in January, 2014

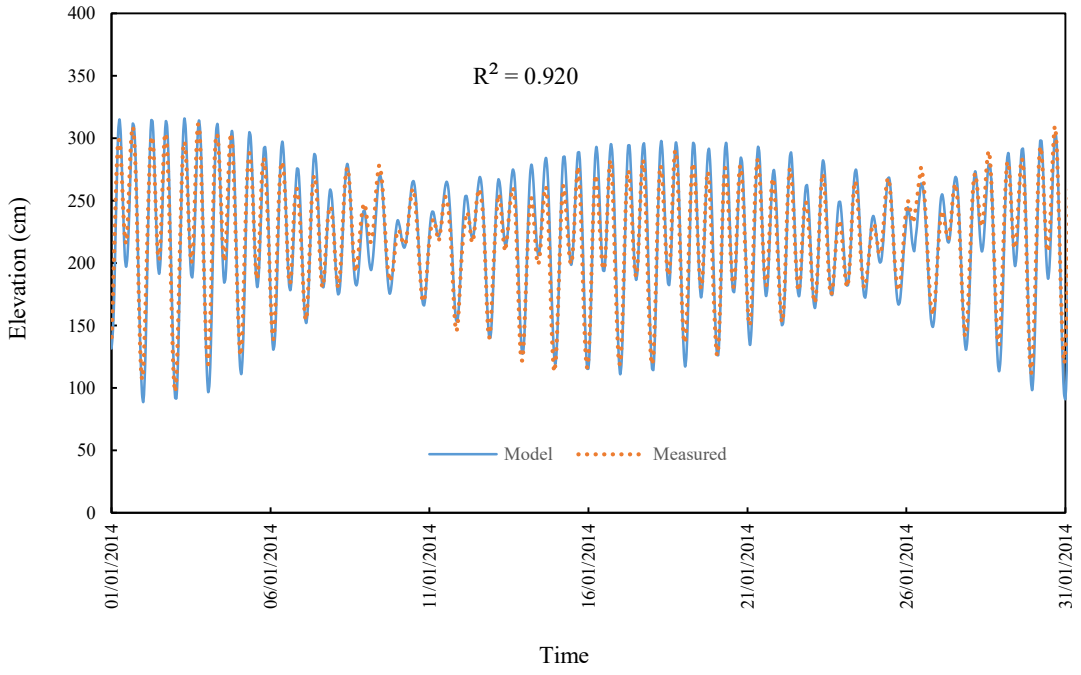

Figure 2.22. Elevation comparison between model and measured data at Yokohama in January, 2014

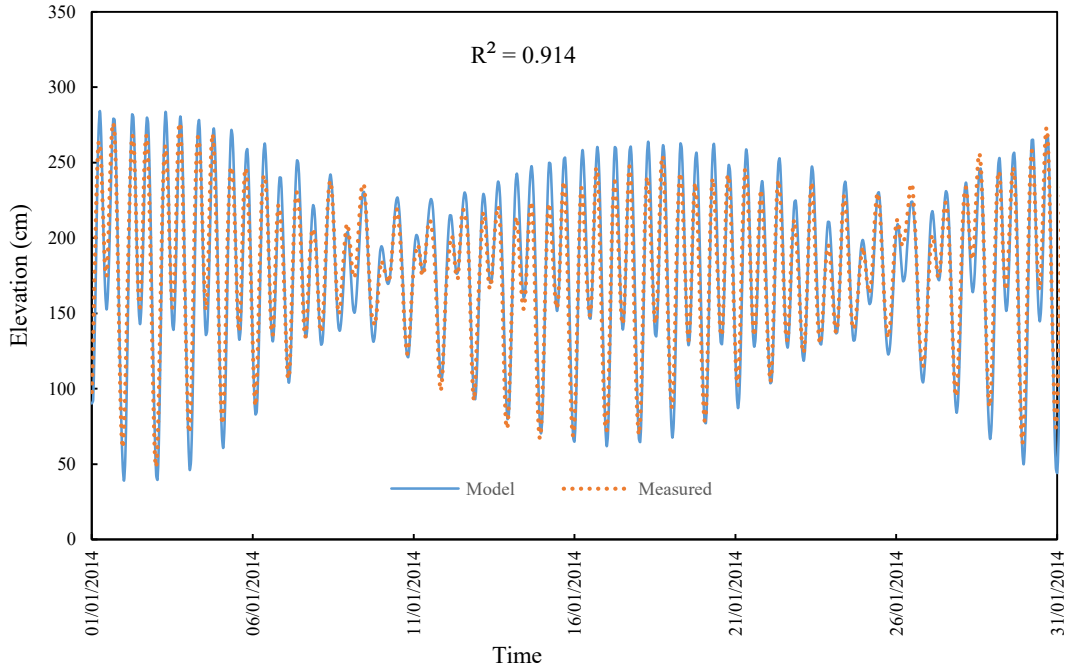

Figure 2.23. Elevation comparison between model and measured data at Chiba in January, 2014

2.2.4.6.2. Temperature

There are four water quality stations are used to verify water temperature and salinity between simulation and measurement **(Figure 2.24)**. Depths of Kawasaki, Chiba Light Beacon, Chiba Port and Urayasu are 29 meter, 19.1 meter, 8.4 meter and 5.4 meter respectively. It is clearly seen that model simulated well variation of water temperature in Tokyo bay. Correlation factors of four stations are all over 0.9. Seasonal variation of water temperature is similar to changing of air temperature. Water temperature often is down in winter before rising up in summer. The water temperature in summer 2015 seems to be little higher in summer 2014. Depending on depth of each station that related to disturbance, difference of seasonal variation between surface layer and bottom layer. Kawasaki station and Chiba Light Beacon station shown larger ranges than shallow stations (Chiba Port and Urayasu).

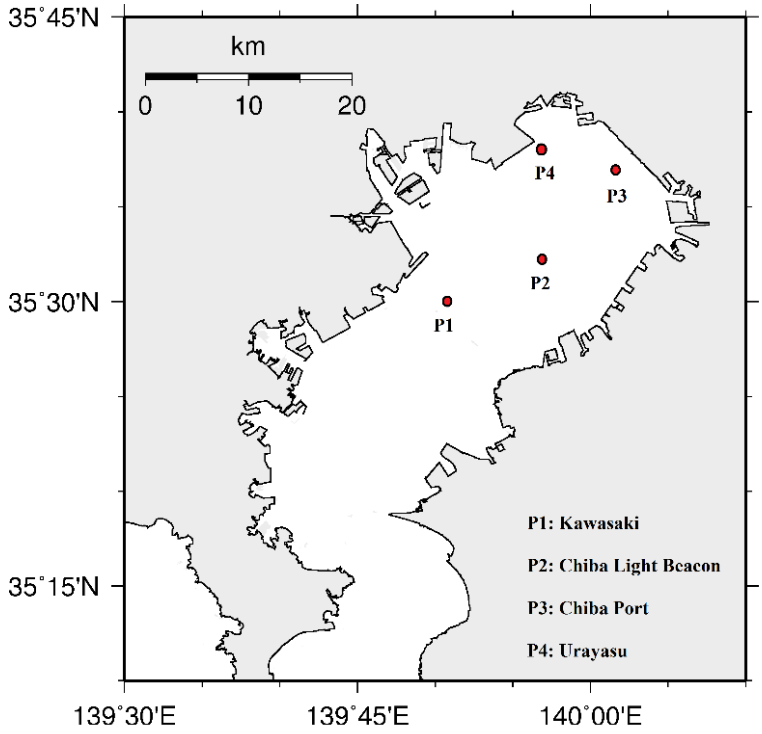

Figure 2.24. Locations of water monitoring stations

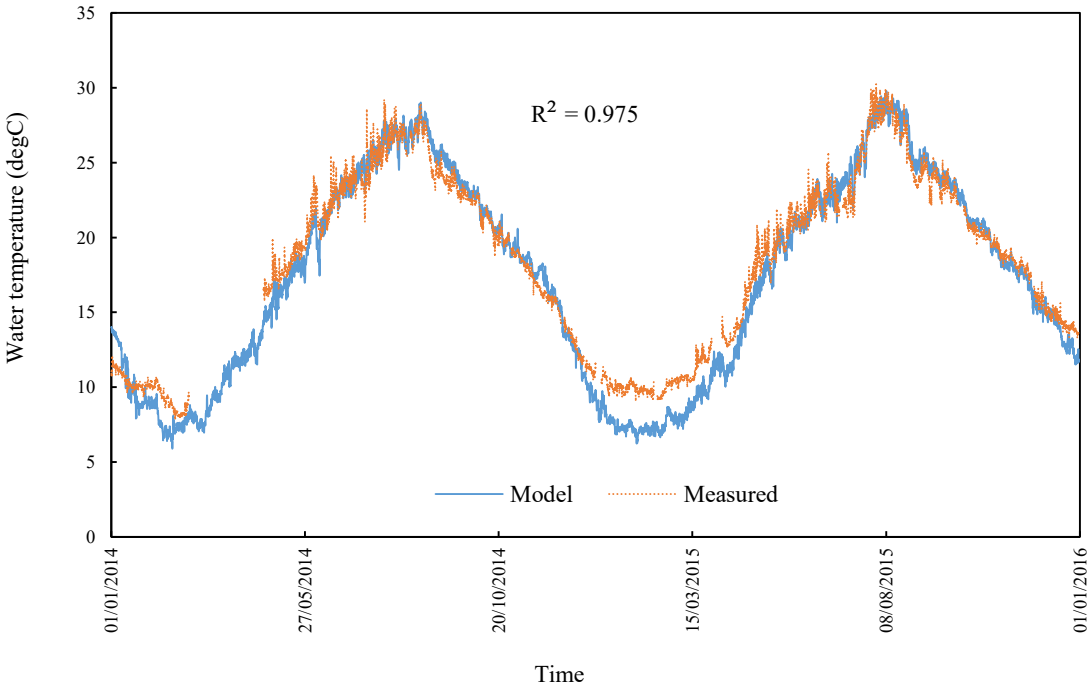

Figure 2.25. Comparison of water temperature between model and measurement at surface layer in Kawasaki station

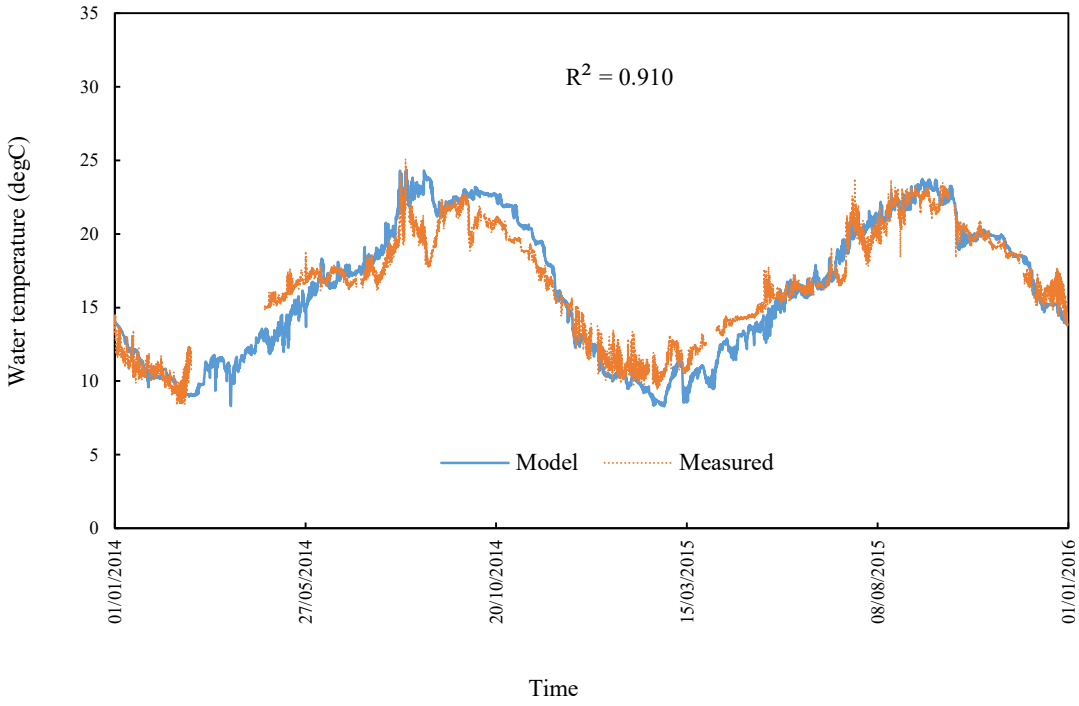

Figure 2.26. Comparison of water temperature between model and measurement at bottom layer in Kawasaki station

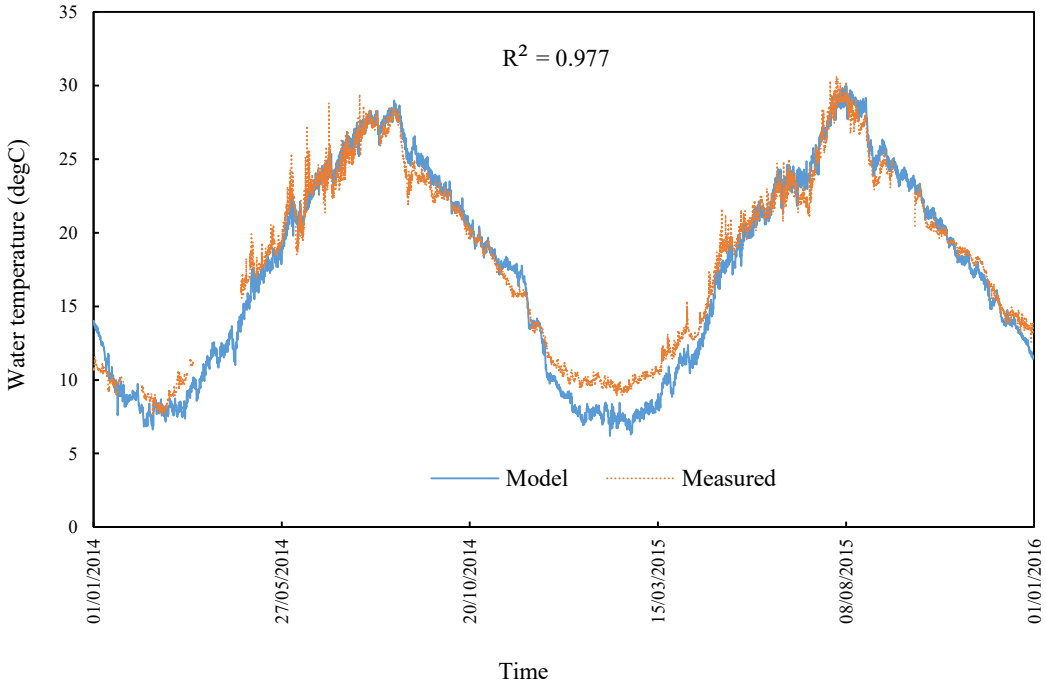

Figure 2.27. Comparison of water temperature between model and measurement at surface layer in Chiba Light Beacon station

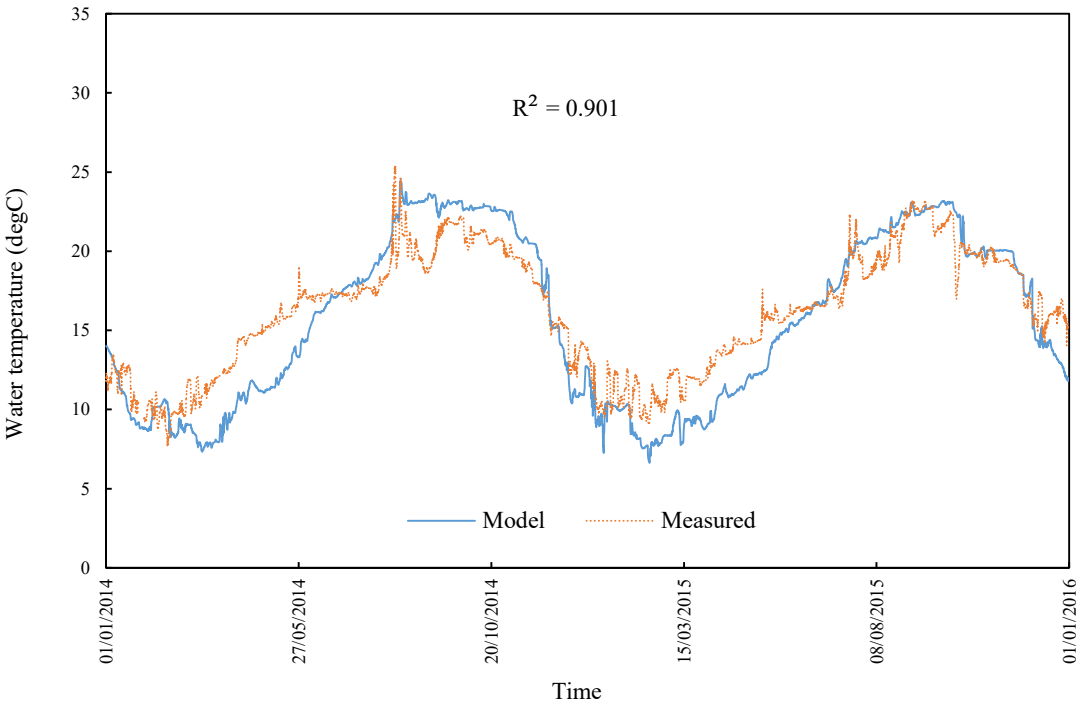

Figure 2.28. Comparison of water temperature between model and measurement at bottom layer in Chiba Light Beacon station

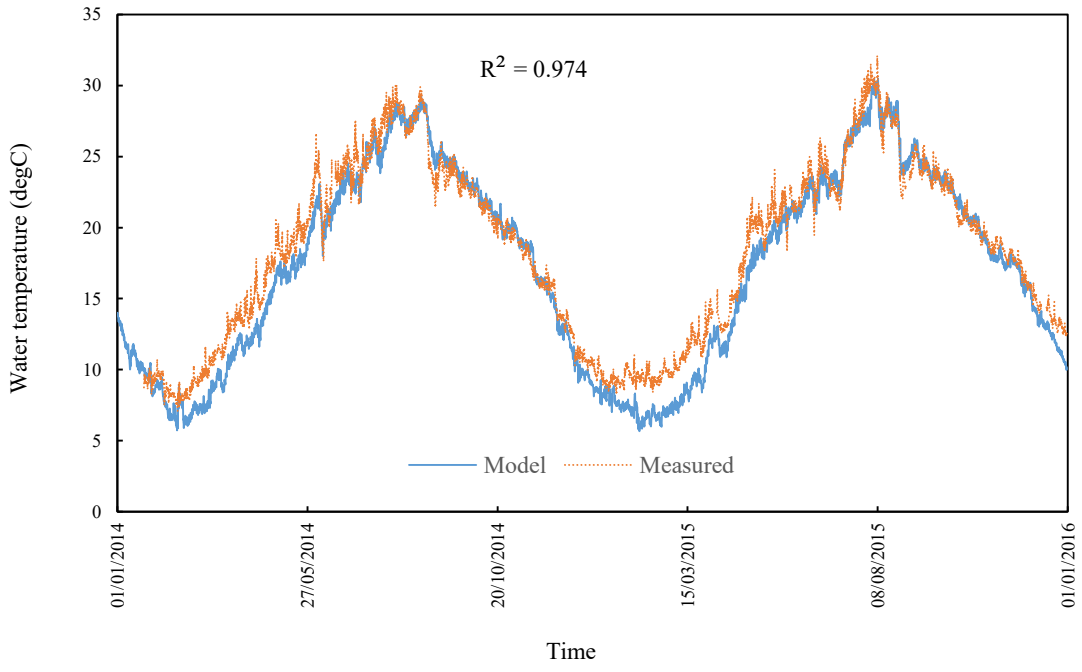

Figure 2.29. Comparison of water temperature between model and measurement at surface layer in Chiba Port station

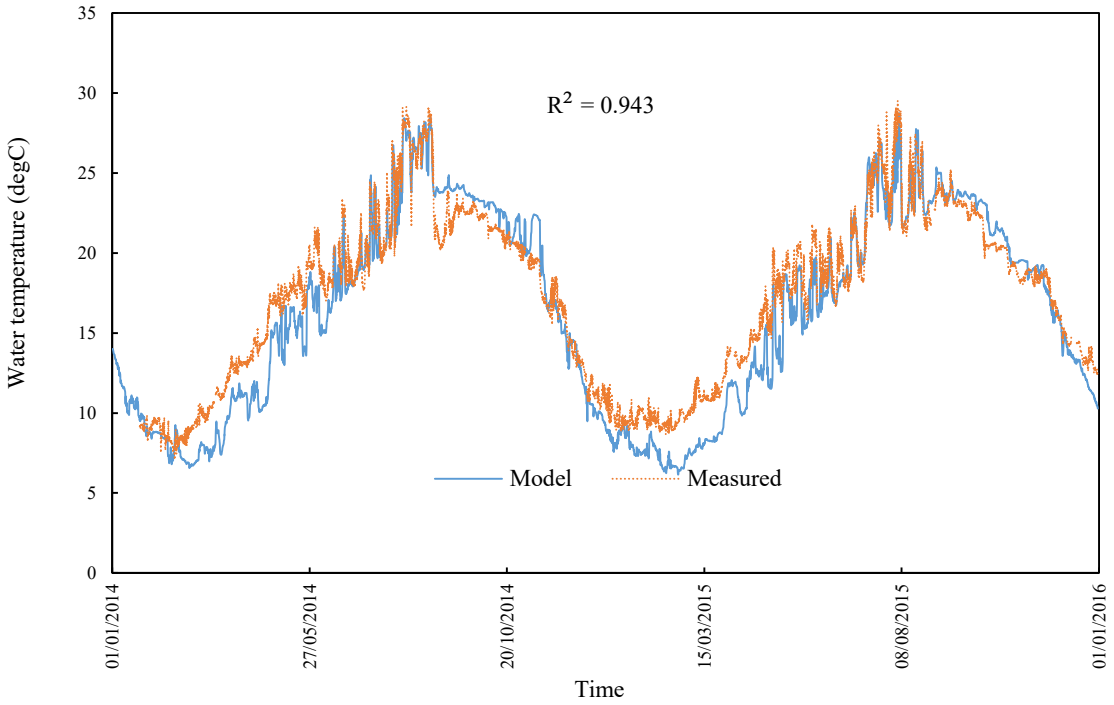

Figure 2.30. Comparison of water temperature between model and measurement at bottom layer in Chiba Port station

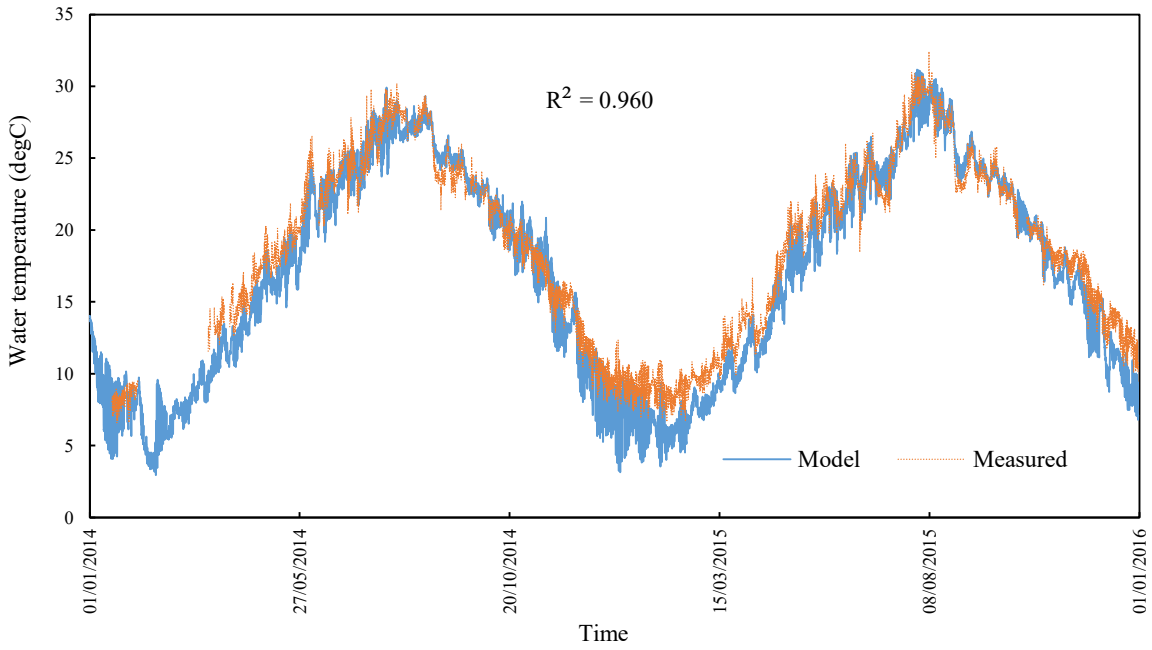

Figure 2.31. Comparison of water temperature between model and measurement at surface layer in Urayasu station

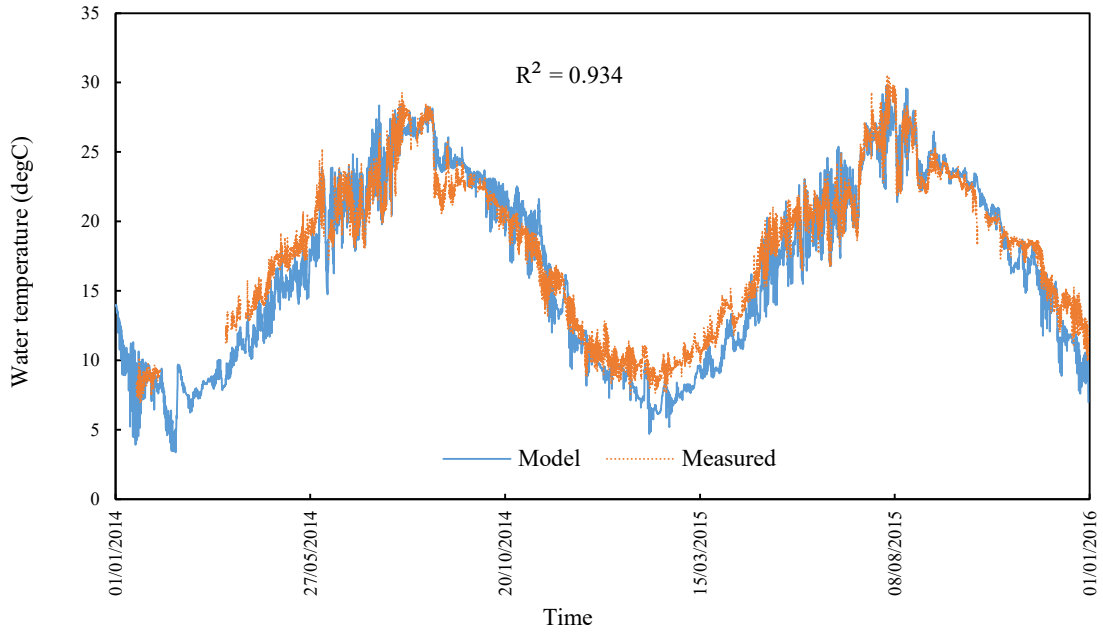

Figure 2.32. Comparison of water temperature between model and measurement at bottom layer in Urayasu station

2.2.4.6.3. Salinity

Similarly, model computed well seasonal variation of salinity in Tokyo Bay. It can be seen that surface salinity is affected strongly due to river discharge. For instance, at Kawaski station bottom salinity rarely reduced below 30 psu while surface salinity could alter from 15 psu to 34 psu. Result also indicates difference on surface salinity in flood period and dry period. Both surface salinity and bottom salinity are steady in winter. Because of strong disturbance at shallow stations (Chiba Port or Urayasu), salinity stratification between upper layers and lower layers would be weaker than deep stations (Kawasaki and Chiba Light Beacon) during wet season. Although correlation indexes of bottom salinity in deep stations are not impressive but model results reflect stable trend of salinity at bottom layer at these stations.

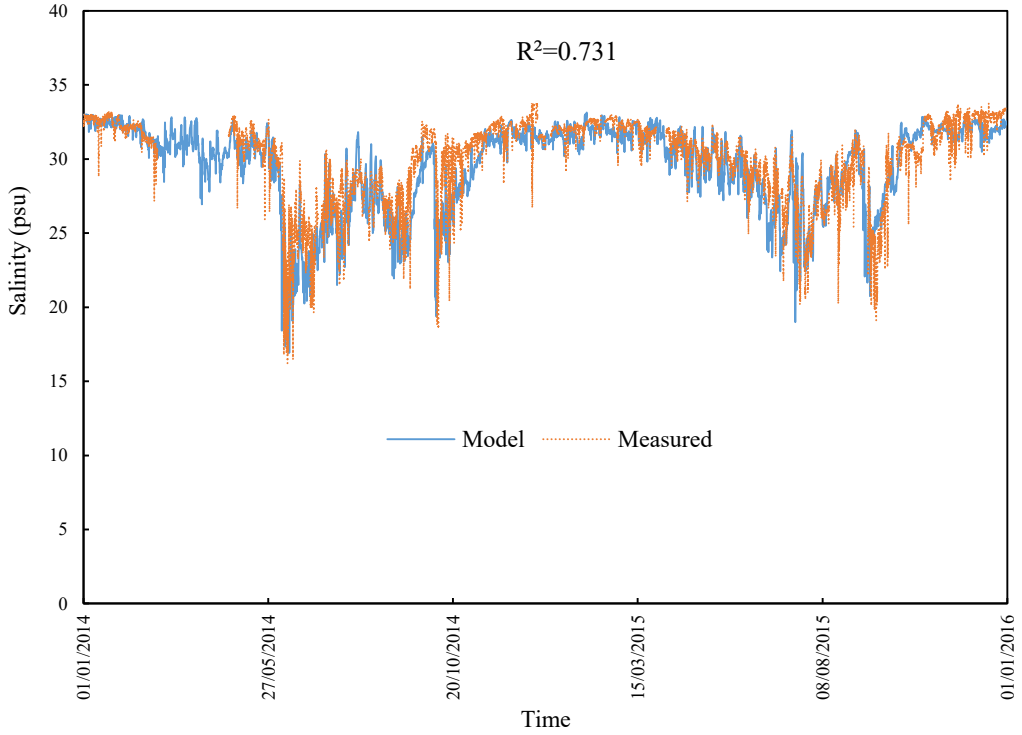

Figure 2.33. Comparison of salinity between model and measurement at surface layer in Kawasaki station

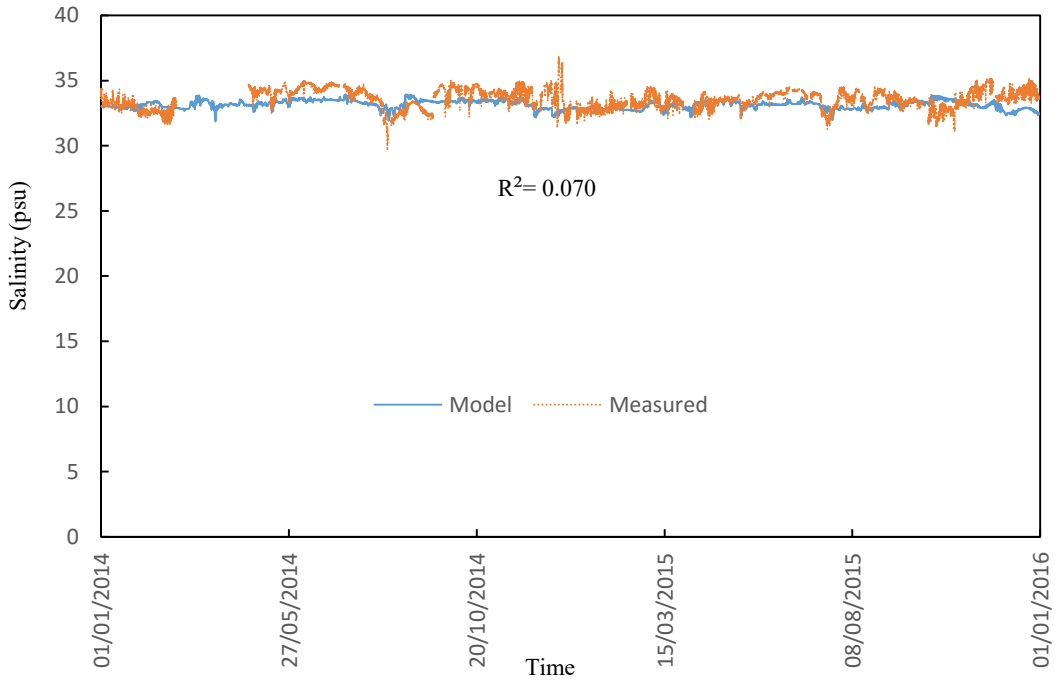

Figure 2.34. Comparison of salinity between model and measurement at bottom layer in Kawasaki station

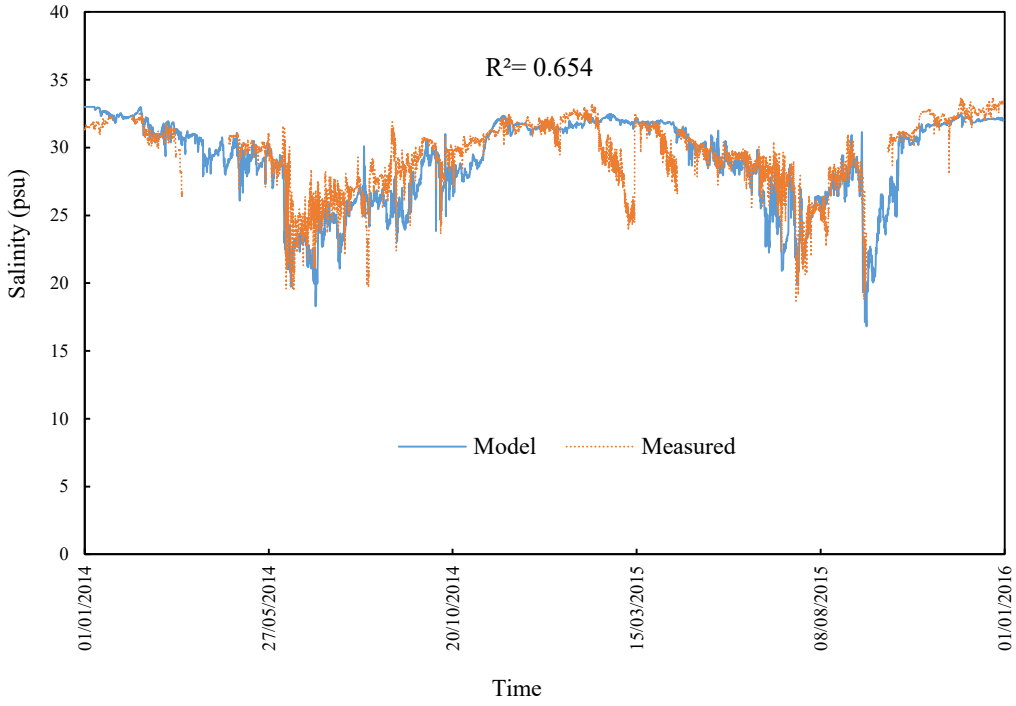

Figure 2.35. Comparison of salinity between model and measurement at surface layer in Chiba Light Beacon station

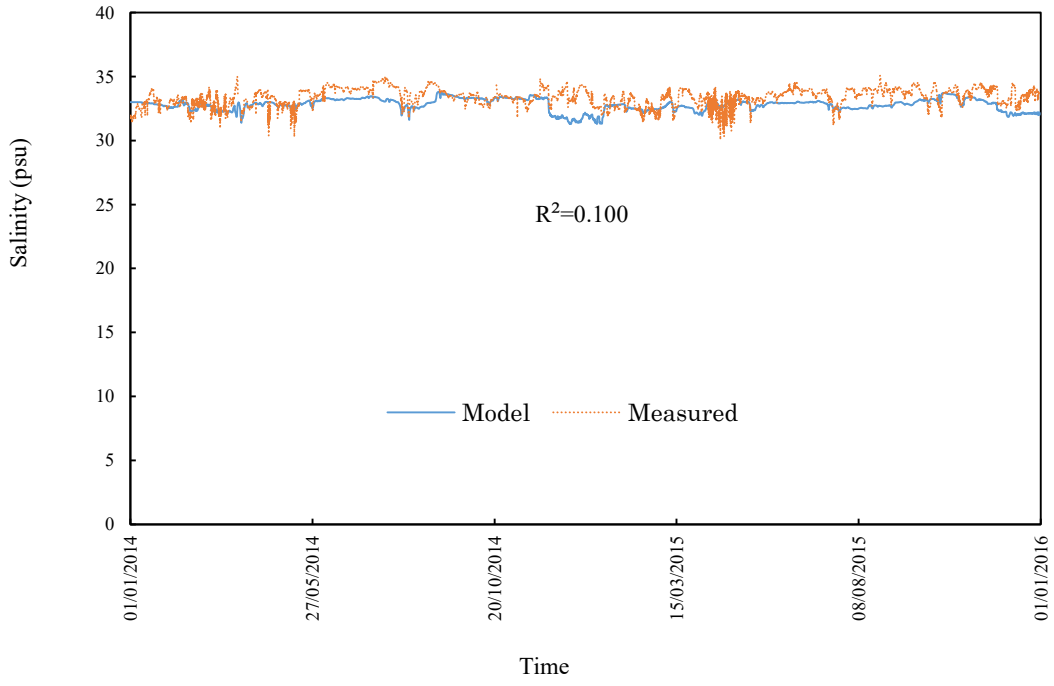

Figure 2.36. Comparison of salinity between model and measurement at bottom layer in

Chiba Light Beacon station

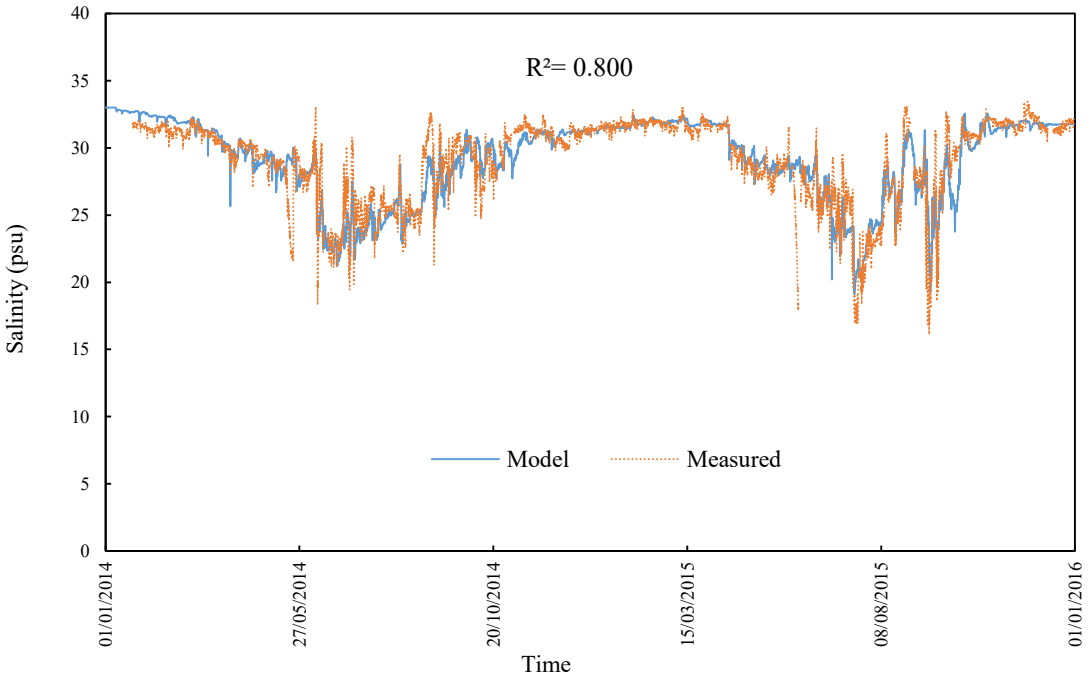

Figure 2.37. Comparison of salinity between model and measurement at surface layer in Chiba Port station

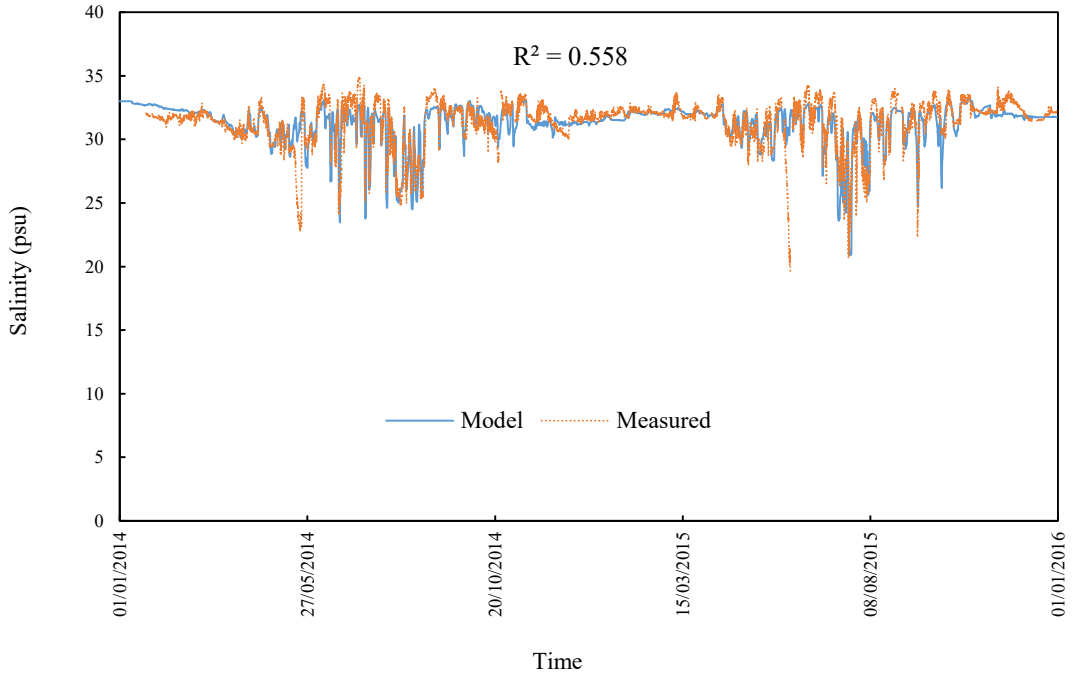

Figure 2.38. Comparison of salinity between model and measurement at bottom layer in Chiba Port station

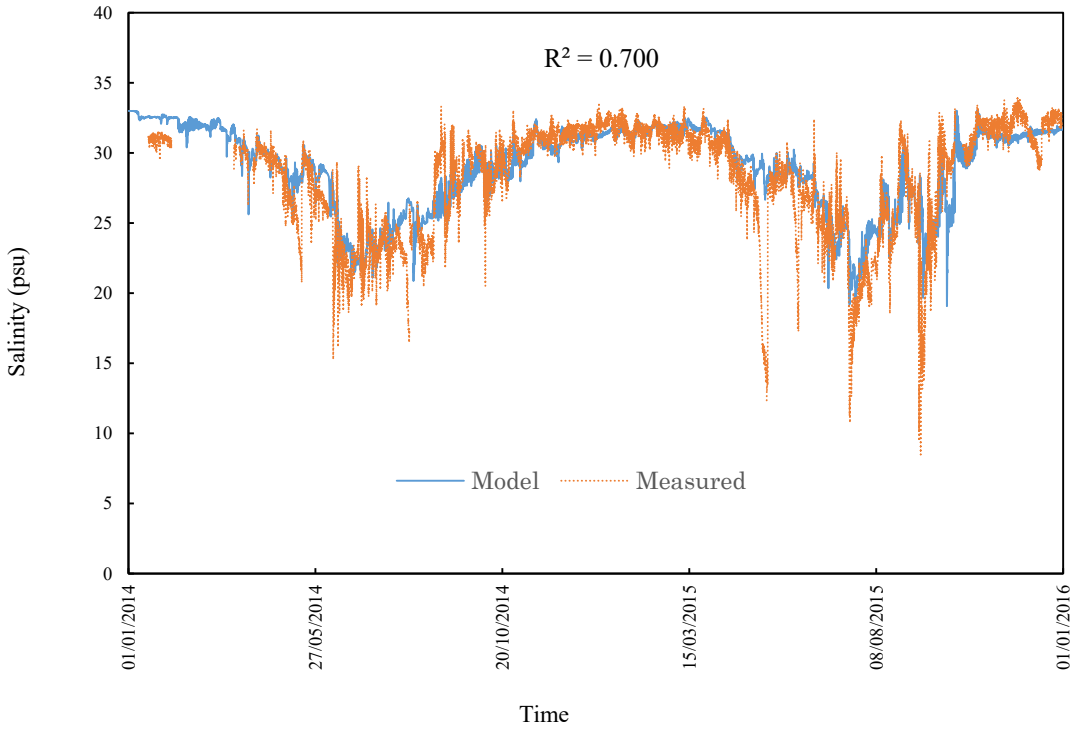

Figure 2.39. Comparison of salinity between model and measurement at surface layer in Urayasu station

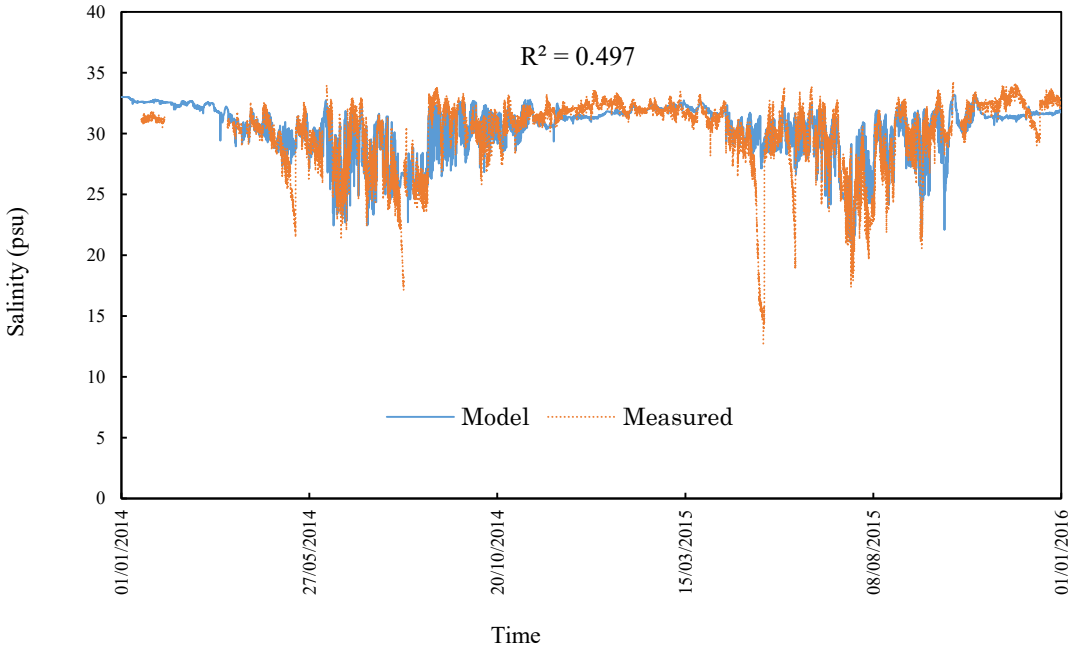

Figure 2.40. Comparison of salinity between model and measurement at bottom layer in Urayasu station

CHAPTER 3: RESULTS

3.1. Results of field surveys

3.1.1. Weather conditions

Four field surveys conducted during day time from 8.00 to 17.00 on July 24, August 24, September 1 and September 16 in 2015. Generally, meteorological conditions were appropriate for carrying out these observations. It almost didn't rain during the whole four days except a little bit rain in the afternoon on day September 1. Because of a sunny day, air temperature on day July 24 was the highest with range of 27-32 degree celsius while other days were quite cool during day time. Breeze blew on July 24, September 1, September 16 whereas wind speed was moderately strong on August 24 with average wind speed of 5.72 m/s and North-northeast and Northeast directions dominated on that day. **Table 3.1** below describes more details on weather conditions based on experiences in field surveys and data in Chiba meteorological station.

Table 3.1. Weather conditions during field observations

Day	Wind			Air temperature	Sky condition	Rain
	Average speed (m/s)	Maximum speed (m/s)	Direction			
24/7	3.41	5.8	WSW, SE, SW	27 - 32˚C	Sunny	No
24/8	5.72	6.6	NNE, NE	23 – 28˚C	Interval of clouds and sunshine	No
1/9	2.82	4.9	SE	23 - 27˚C	Cloudy	Light rain in the afternoon
16/9	4.18	5.1	ENE, NE	21 – 25˚C	Cloudy	No

3.1.2. Water quality in flat bottom

Results of water quality from four field surveys in 2015 are shown by list of figure below. Namely:

On July 24, (**Figure 3.1**) anoxia just happened in small areas, hypoxia governed mainly in Kawasaki flat bottom. Total sulfide concentration released across Kawasaki flat bottom was low, highest concentration was below 0.2 mg/L. Highest tubidity was 6 FPU.

On August 24, (**Figure 3.2**) anoxia broaden thought out flat bottom included navigation channel while hypoxia was in flat bottom in Kawasaki. Total sulfide concentration in navigation channel flat bottom was low, highest value of total sulfide was 0.4 mg/L. Highest turbidy was 6 FPU.

On September 1, (**Figure 3.3**) entire flat bottom of inner bay was dominated by hypoxia. Oxygen concentration was almost lowest in central flat bottom of head bay. Total sulfide observed at low concentration, peaked in central flat bottom of bay with maximum of 0.4 mg/L. Highest turbidity was 15 FPU.

On September 16, (**Figure 3.4**) anoxia occupied majorly flat bottom while hypoxia was minor. Total sulfide reached highest value of 0.15 mg/L in off-Urayasu. Highest turbidity was 6 FPU.

In summary, results of field surveys reveal that anoxia would appear widely across flat bottom areas. More specifically, anoxia focused on central flat bottom enclosed navigation channel. Kawasaki flat bottom generally appeared hypoxia while anoxia just occur rarely with small scope. All field surveys results of total sulfide determined that amount of total sulfide emitted from flat bottom at low level. Lastly, it can be seen clearly that distribution areas of total sulfide in sediment layer associated closely to distribution of anoxic areas to release total sulfide.

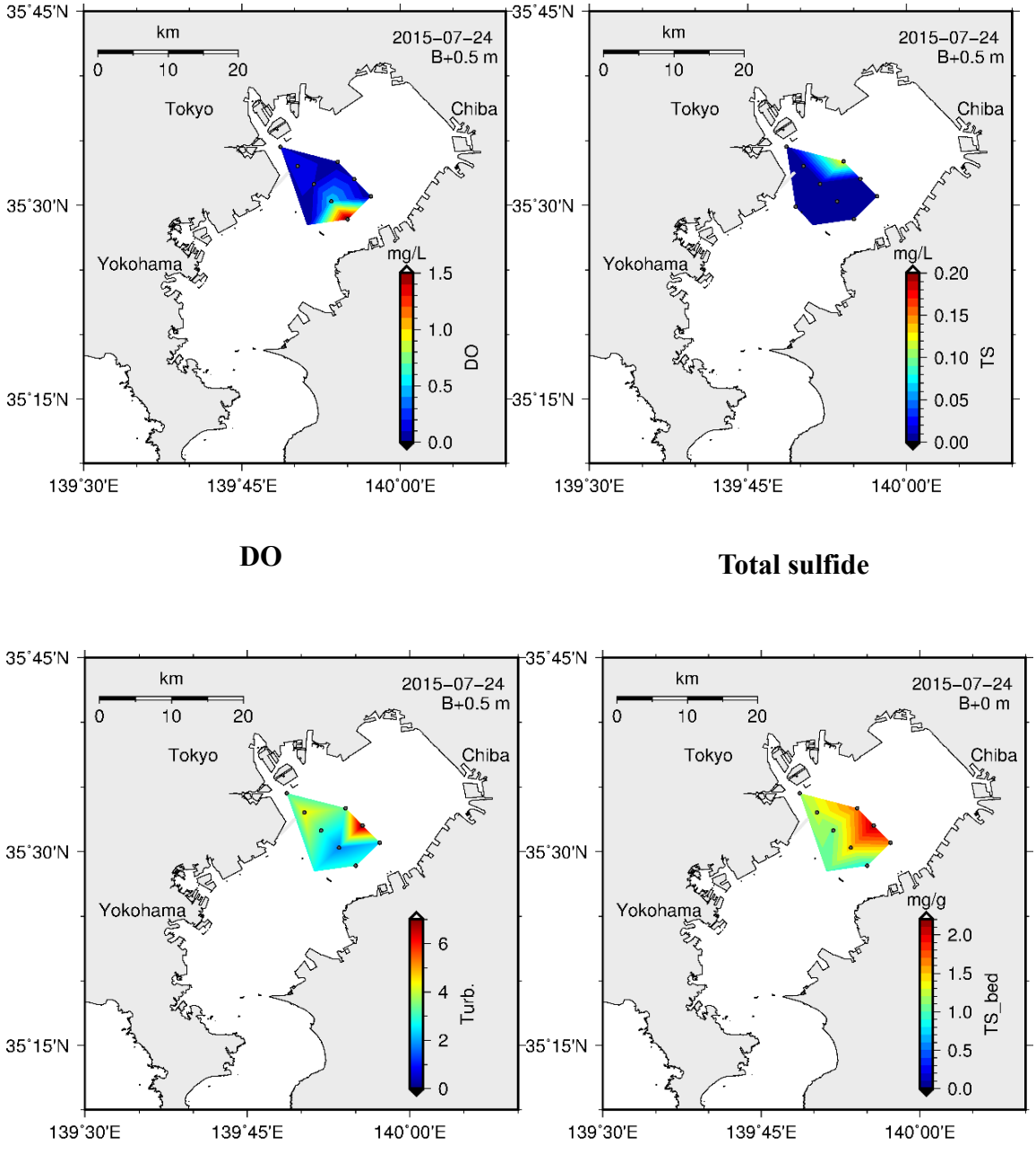

Figure 3.1. Field survey results of water quality in flat bottom on July 24, 2015

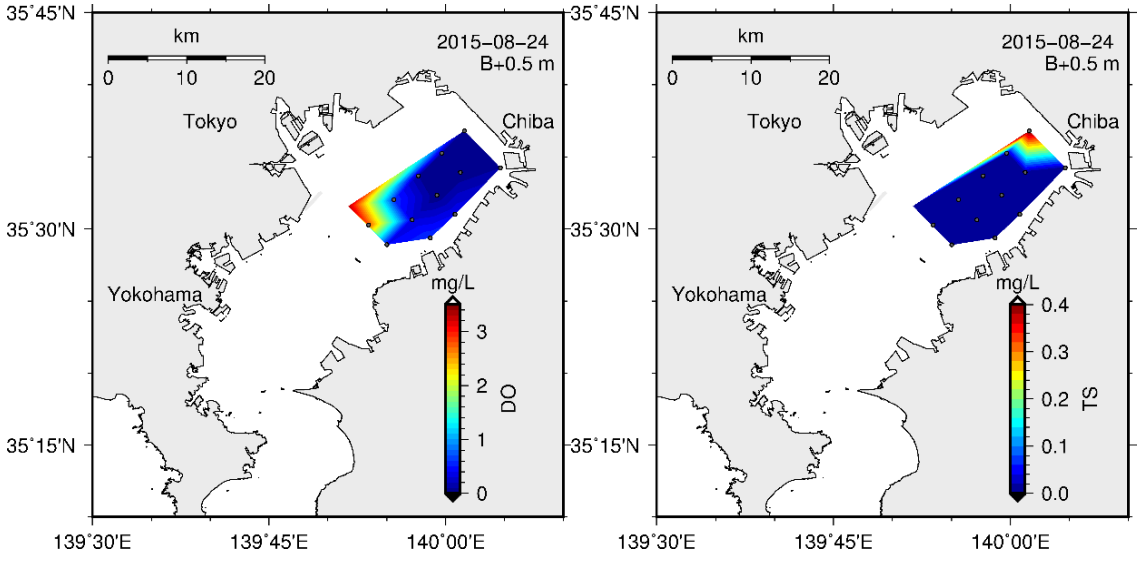

DO **Total sulfide**

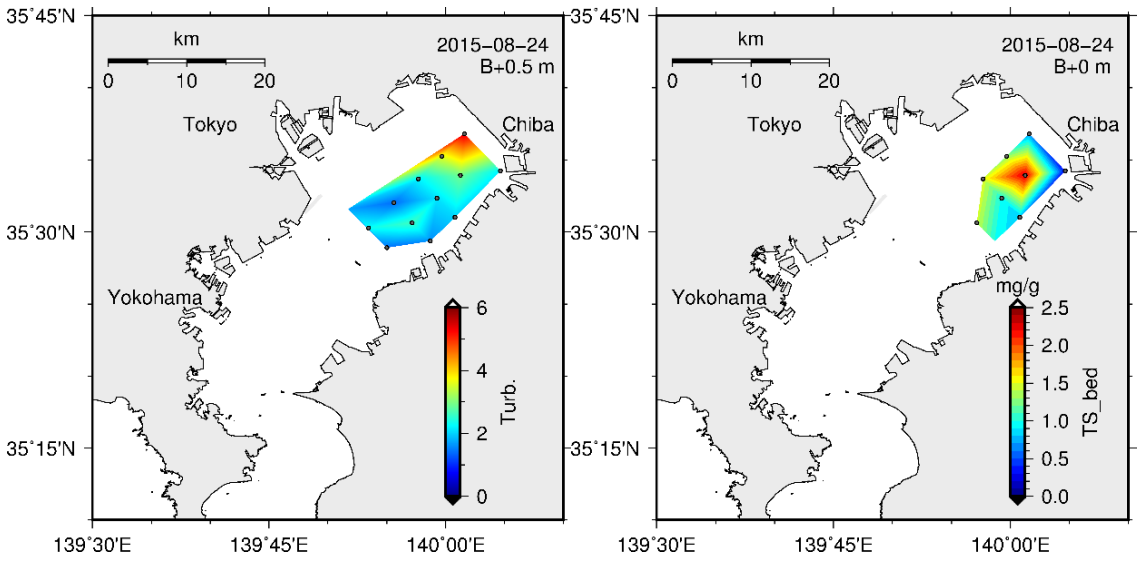

Turbidity **Total sulfide in bed sediment**

Figure 3.2. Field survey results of water quality in flat bottom on August 24, 2015

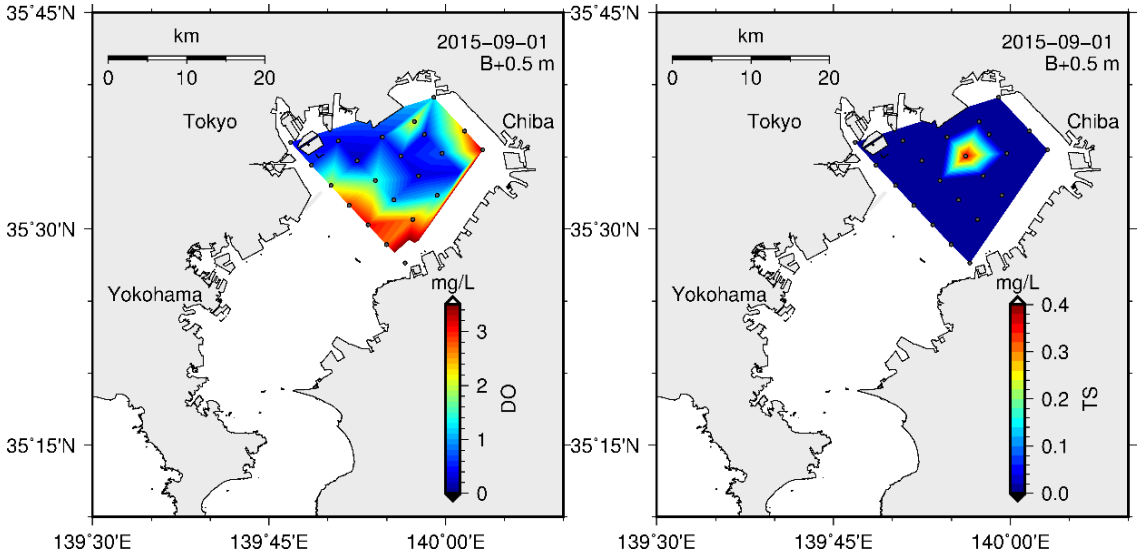

DO **Total sulfide**

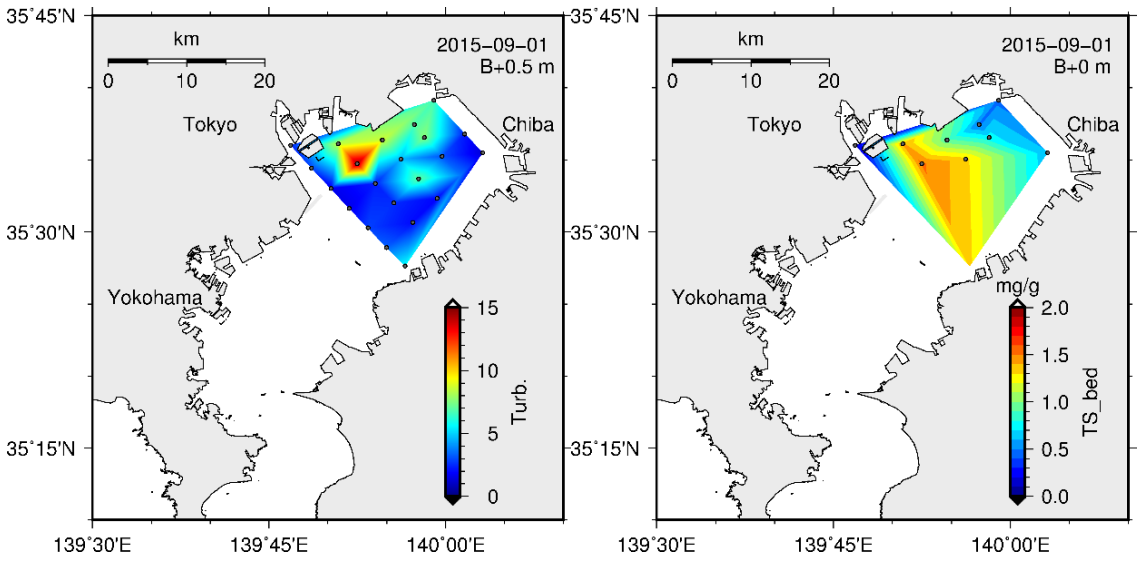

Turbidity **Total sulfide in bed sediment**

Figure 3.3. Field survey results of water quality in flat bottom on September 1, 2015

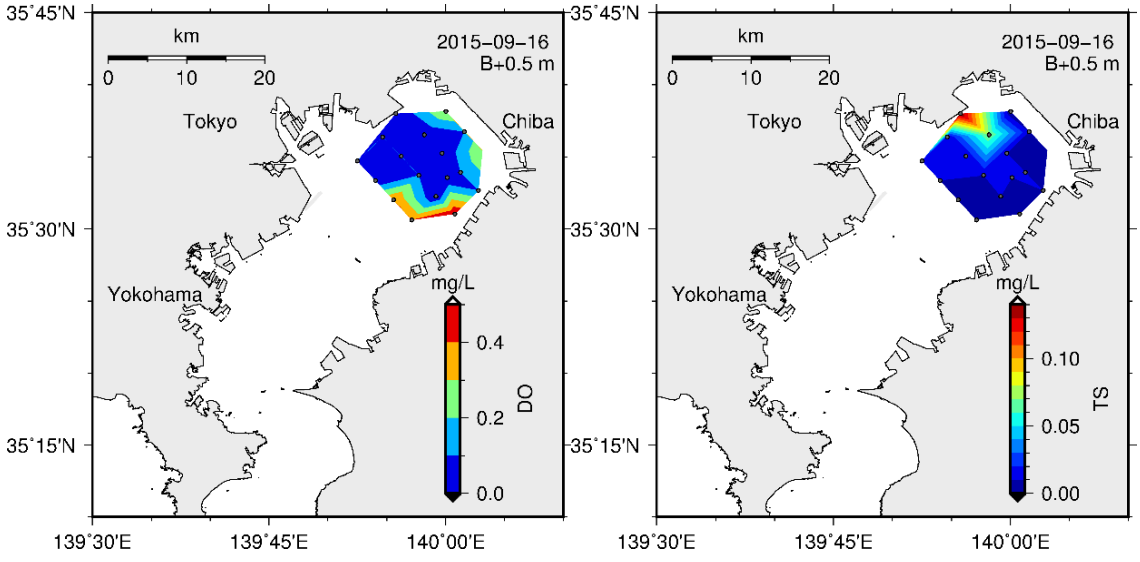

DO **Total sulfide**

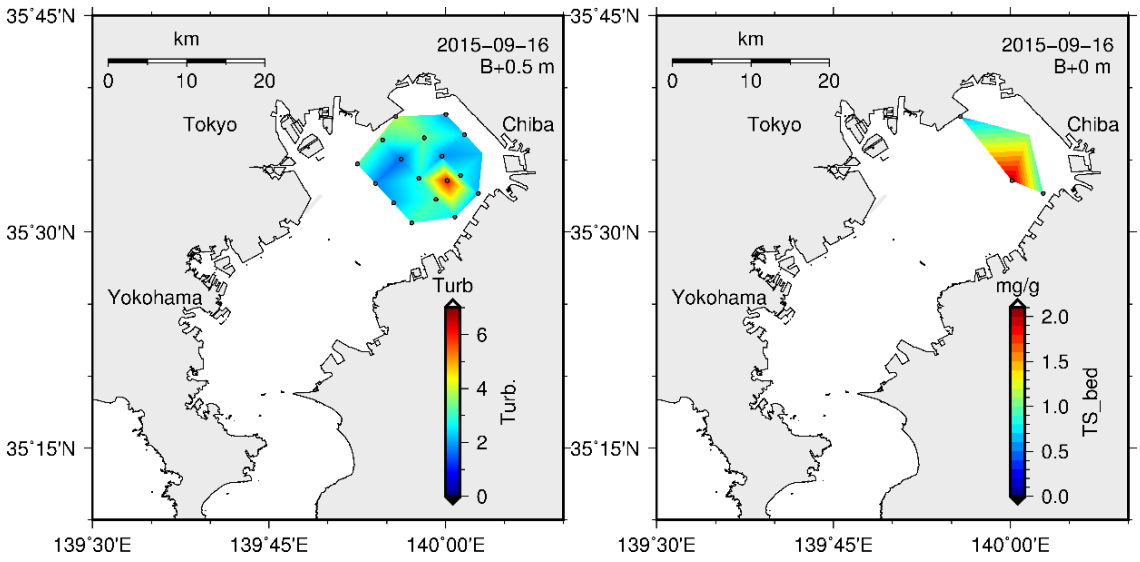

Turbidity **Total sulfide in bed sediment**

Figure 3.4. Field survey results of water quality in flat bottom on September 16, 2015

3.1.3. Water quality in dredged pits

Figure 3.6 indicates vertical profiles of water quality in off-Makuhari dredged pit whereas **Figure 3.7** signifies off-Urayasu's outcomes. First, there is a depletion of oxygen concentration from surface to bottom in these dredged pits. In particular, all field investigations expose that anoxia mostly appeared at bottom in both dredged pits whereas hypoxia just is identified on surface in off-Makuhari dredged pit. More specifically, anoxic water layer tended to expand from the bottom to near surface layer on blue tide days. For instance in off-Makuhari dredged pit, oxic layer seemed to exist up to 10 meters thickness beneath surface collated to 5 meters thickness of anoxic layer on July 24. Otherwise, anoxia raised vertically with 15 meters thickness on August 24 and caused hypoxia on surface. Field surveys results also demonstrate that difference of oxygen concentration between surface and bottom across these areas. On September 1 even surface dissolved oxygen concentration is 20 mg/L, lack of dissolved oxygen at the bottom. During investigation, hypoxia was not recognized on surface in off-Urayasu

On the contrary, there is almost a gradual increase of total sulfide concentration from surface to bottom in dredged pits. Observed results also illustrates the gap of total sulfide released in bottom in off-Urayasu and off-Makuhari. In off-Makuhari dredged pit, total sulfide concentration increased rapidly on August 24 and September 1 at nearly 60 mg/L at the bottom before declining on the following days. While measured result of total sulfide was low on the first investigation trip (July 24). By contrast, in off-Urayasu dredged pit total sulfide was only significant on July 24 with total sulfide dose of 7 mg/L at bottom meanwhile total sulfide was low on the following days even if on blue tide day (on August 24). Due to off-Makuhari is deeper than off-Urayasu, anoxia thus developed more seriously in off-Makuhari leading to more release of hydrogen sulfide especially on August 24 and

September 1.

In another comparison, it is easy to see that hydrogen sulfide concentration in dredged pits is much higher than in flat bottom especially when blue tide occurs. For example, on blue tide day (August 24) the highest hydrogen concentration in flat bottom is 0.4 mg/L (**Figure 3.2**) compared to nearly 60 mg/L at bottom layer (**Figure 3.6**) in off-Makuhari dredged pit.

An interesting point is that turbidity usually reached the highest value at the interface between anoxic layer and oxic layer in a water column in both dredged pits. At interchanging point between two layers, oxygen atoms from oxic layer are provided for oxidizing hydrogen sulfide to form sulfur particulates. For instance, turbidity peaked nearly 6 FPU at depth of 11 meter where anoxia enlarged since the bottom on September 1 in off-Makuhari dredged pit. It is also inevitable to realize that turbidity is higher on blue tide day (August 24) than three other days. There is a difference of surface turbidity in off-Makuhari dredged pit between August 24 and September 1 though total sulfide released similarly at bottom (surface turbidity is 11 FPU on August 24 compared to 2.5 FPU on September 1). **Table 3.1** above revealed that northeast wind blew on day August 24 therefore upwelling appeared then. This phenomenon will diffuse sulfur from lower layer to upper layer and induced high turbidity on surface. On the other hand, dominant wind direction on September 1 is southeast that upwelling would not emerge. Surface turbidities on August 24 and September 16 are lower than on August 24 due to low sulfur formed from oxidation of hydrogen sulfide even if northeast wind is on September 16.

Nevertheless, there is not a reasonable quantitative relationship between turbidity and total sulfide (**Figure 3.5**). For example on day August 24 in off-Makuhari dredged pit, total

hydrogen sulfide and turbidity are both high. However, turbidity is high while total sulfide is low on day September 1 in off-Urayasu dredged pit. Depending on probability of the encounter between hydrogen sulfide and oxygen to produce elemental sulfur resulting in high turbidity or low turbidity then.

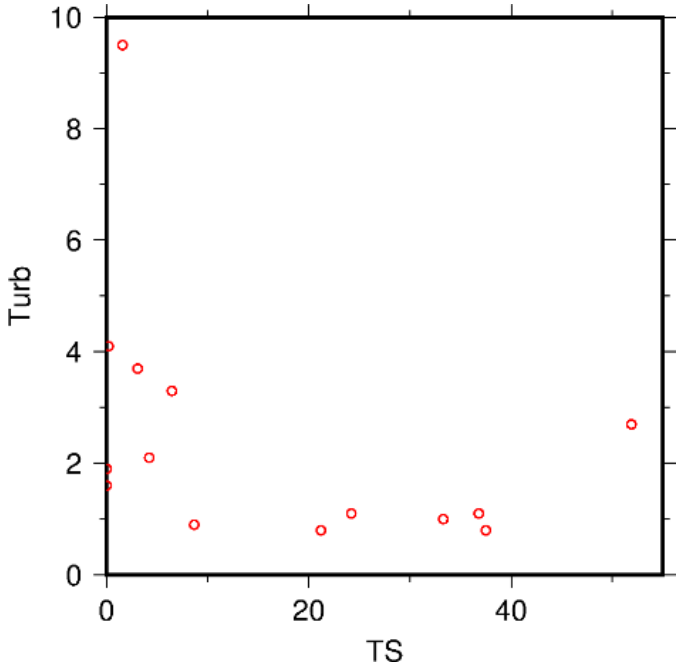

Figure 3.5. Relationship between turbidity and total sulfide

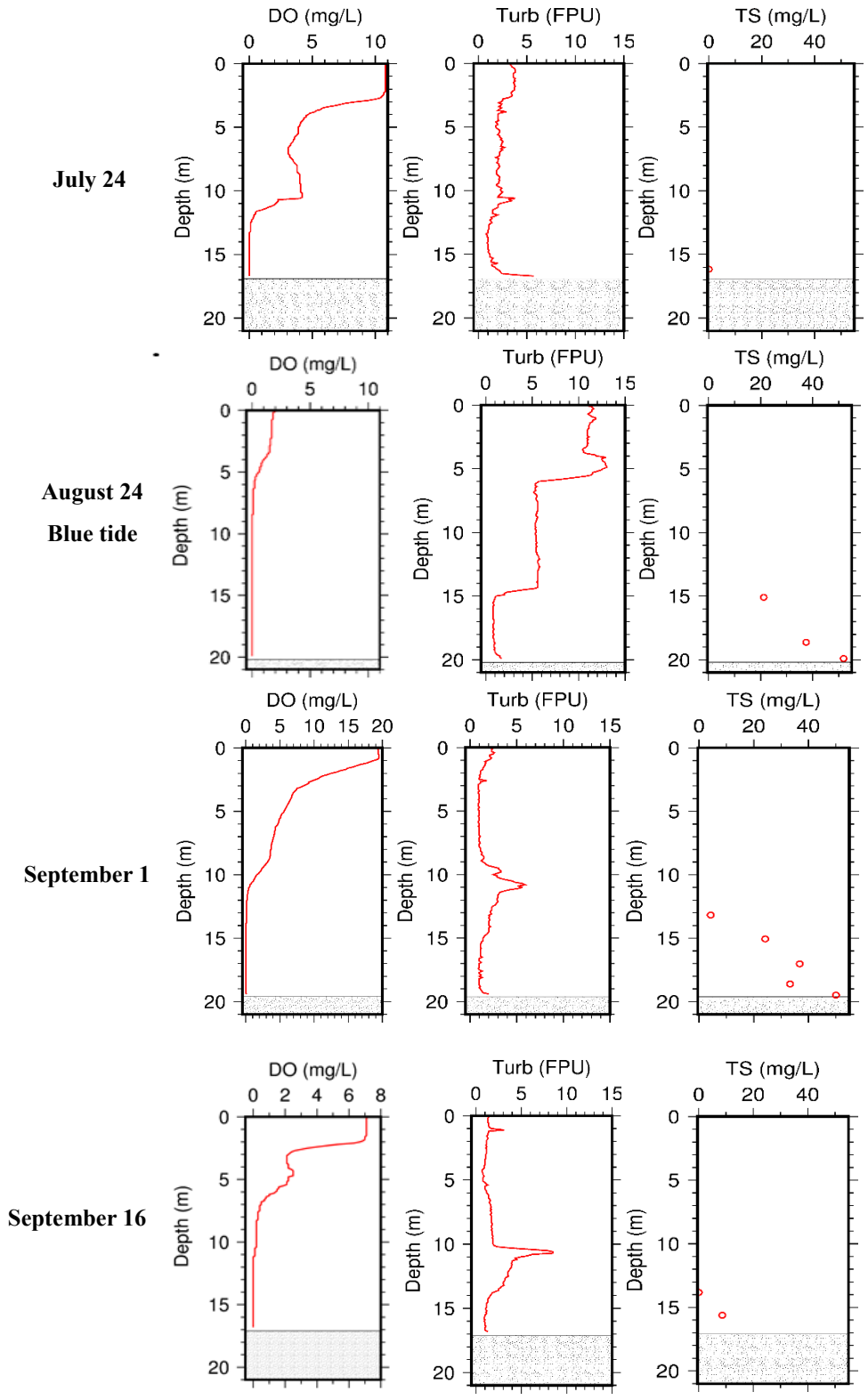

Figure 3.6. Field surveys results of water quality in off-Makuhari dredged pit

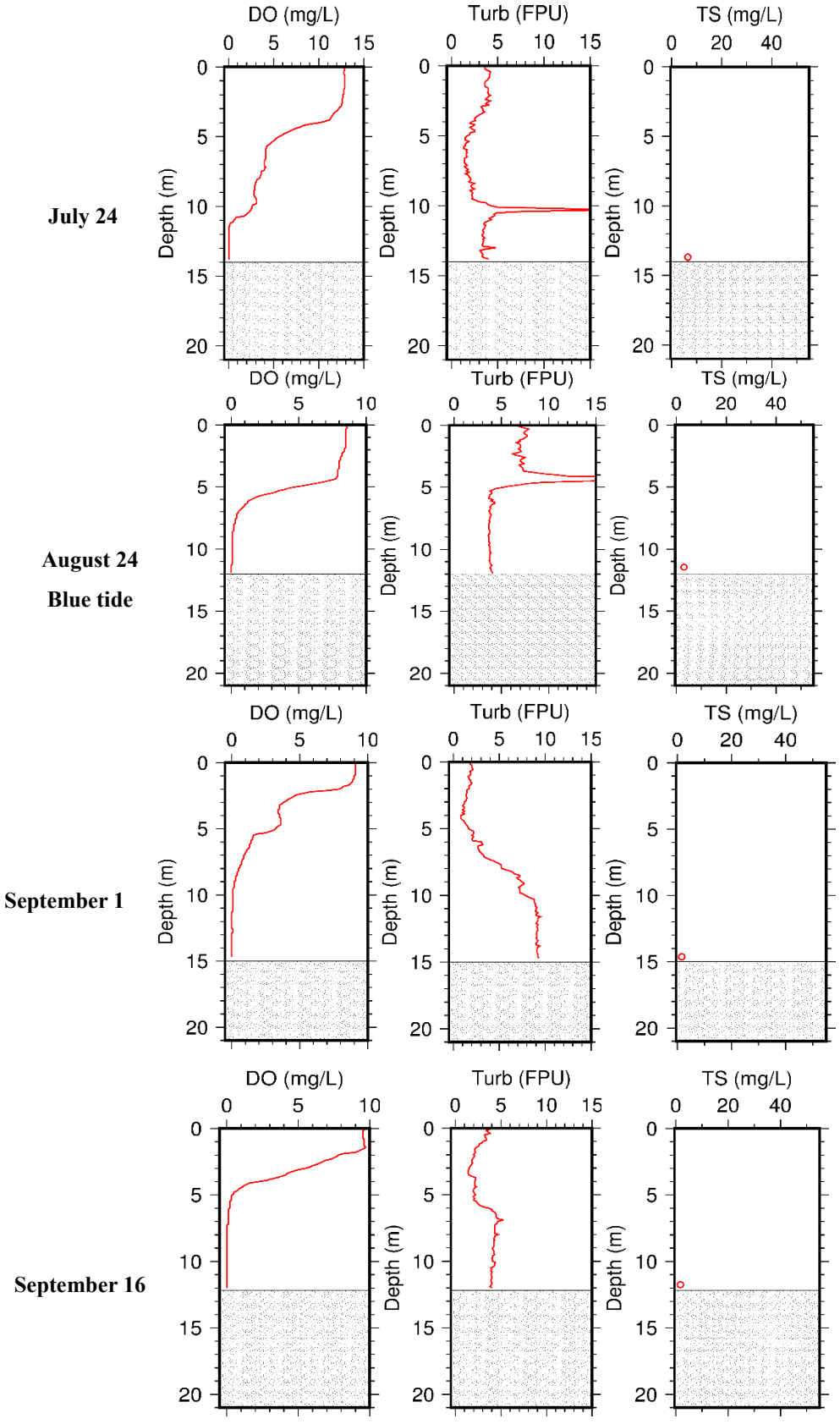

Figure 3.7. Field surveys results of water quality in off-Urayasu dredged pit

3.2. Results of MIKE 3 model

3.2.1. Dissolved oxygen

A system of stations were constructed by government in Tokyo bay to monitor water quality as shown in **Figure 2.24**. Locations of these stations related to study areas. Kawasaki artificial island station represents surrounding Kawasaki flat bottom, Chiba Light Beacon's site is in navigation channel, Chiba Port inspecting for off-Makuhari dredged pit and off-Urayasu station measuring water quality in off-Urayasu dredged pit. Data of dissolved oxygen at four stations have been collected for validation of model simulation from year 2014 to 2015.

To check up reproducibility of model, dissolved oxygen from listed stations above were possessed. Results of observed and simulated variation of dissolved oxygen are shown by list of figures below. Model proved that it can well reproduce seasonal variation of dissolved oxygen at different water layers even though discrepancies appeared. Generally, result of DO at bottom is much better than result's surface. Correlation factor of DO is the best at Chiba Light Beacon station with 0.819 at bottom layer. Dissolved oxygen on surface is strongly affected by complex processes such photosynthesis by phytoplankton or reaeration that sometimes measured data exceeded 20 mg/L. The reason for underestimation of dissolved oxygen on surface is a results of underestimation of phytoplankton on surface.

It is the common point of dissolved oxygen at these stations that DO on surface is higher than DO at bottom. Dissolved oxygen on surface fluctuates strongly at high value while bottom DO tended to reduce to in summer. There are some specific characteristics at each point, namely:

At Kawasaki station (depth of 29 meter), correlation coefficients at surface and bottom

are 0.403 and 0.744 respectively. Surface DO alter strongly and maximum measured value is 16.4 mg/L. On the surface, measured data shown that anoxia didn't appear while hypoxia rarely occurred (just happened in May). At bottom, anoxia also seldom appeared but hypoxia occurred from April to October, especially in August.

At Chiba Light Beacon (depth of 19 meter). This station locates on road of navigation channel to Chiba port. On the surface, DO change with high magnitude in summer, maximum of DO was up to 22.6 mg/L. Anoxia didn't appear on the surface whereas hypoxia occur rarely (just happened in September). At bottom, anoxia would emerge from May to September while hypoxia altered from March to November. Even anoxia happened during July and August in 2014.

At Chiba Port station (depth of 8.4 meter), DO on the surface transformed highly with maximum of measured DO of 23.6 mg/L. Anoxia appeared on the surface (in June) while hypoxia occurred frequently on surface (from May to September). At bottom, anoxia might come from May to September and hypoxia is from April to November. Depth of this station is shallow that bottom DO could reach to 14.6 mg/L. However, here is also near off-Makuhari dredged pit that anoxia occurred regularly at bottom in summer.

At Uraysu station (depth of 5.1 meter), maximum of measured DO on the surface is 21.5 mg/L. On surface, anoxia can be encountered on the surface from June to September while hypoxia is detected from April to November. At bottom, anoxia also appeared from June to November whereas hypoxia is from April to November.

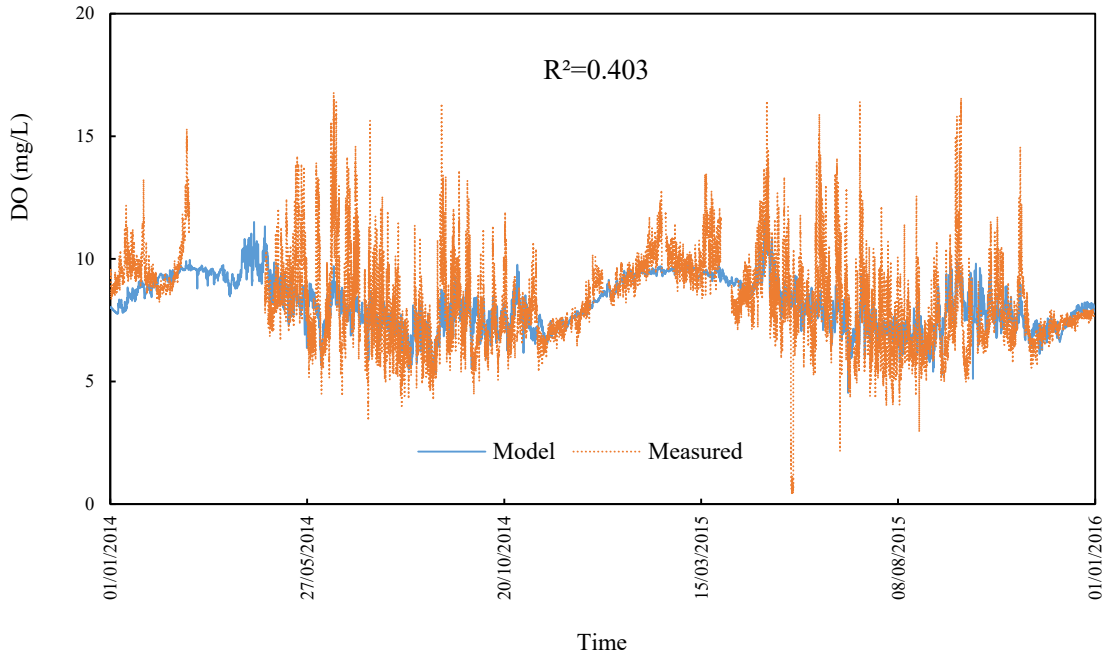

Figure 3.8. Surface DO comparison between model and measured at Kawasaki station

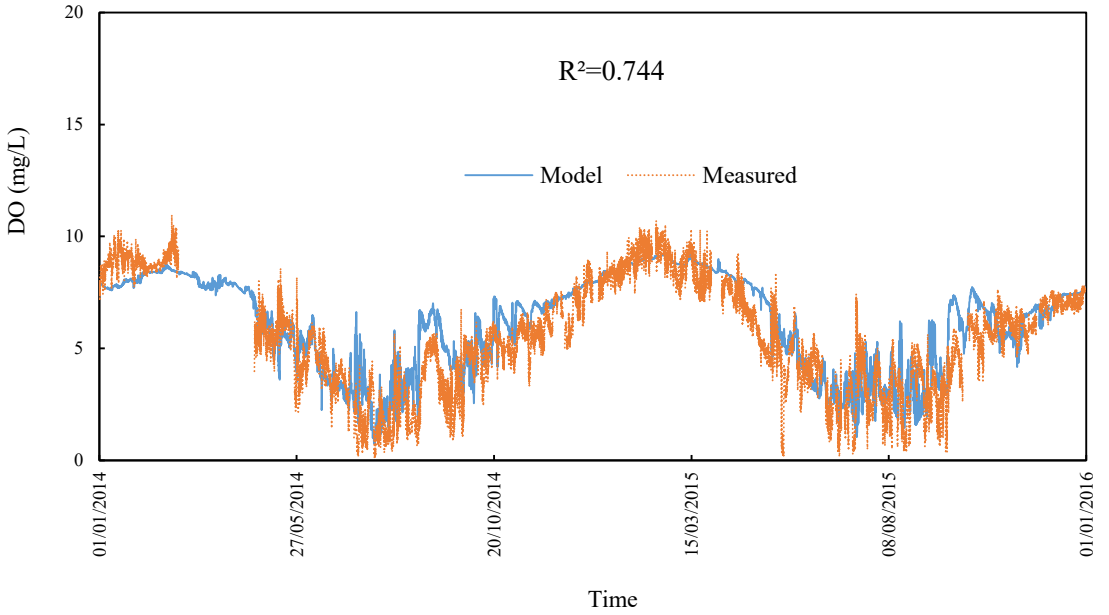

Figure 3.9. Bottom DO comparison between model and measured at Kawasaki station

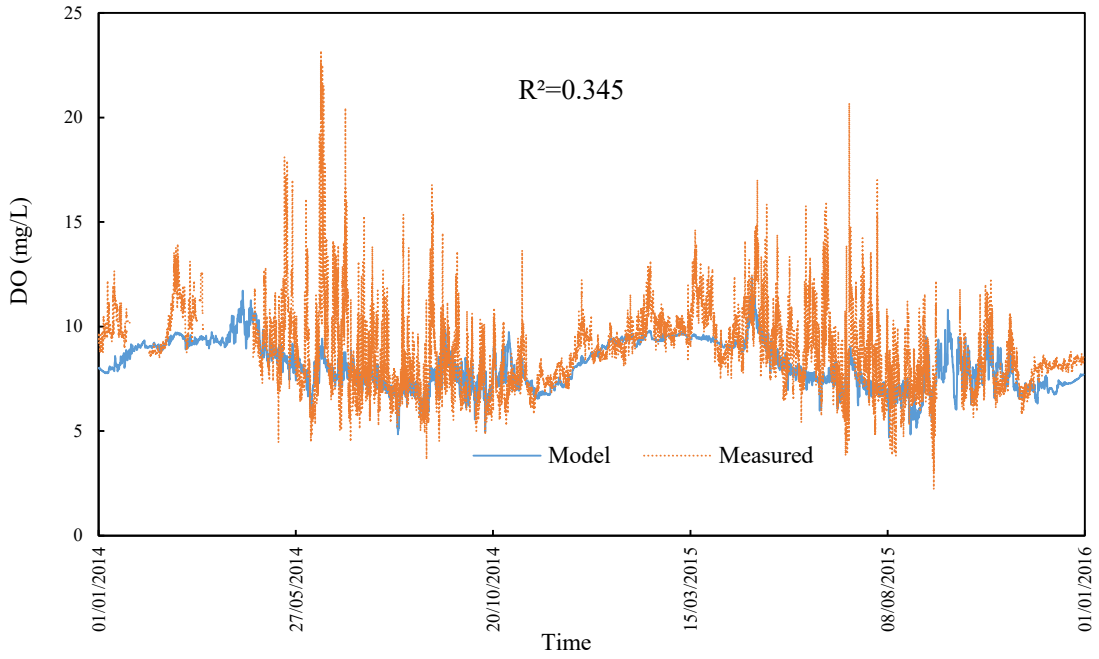

Figure 3.10. Surface DO comparison between model and measured at Chiba Light Beacon station

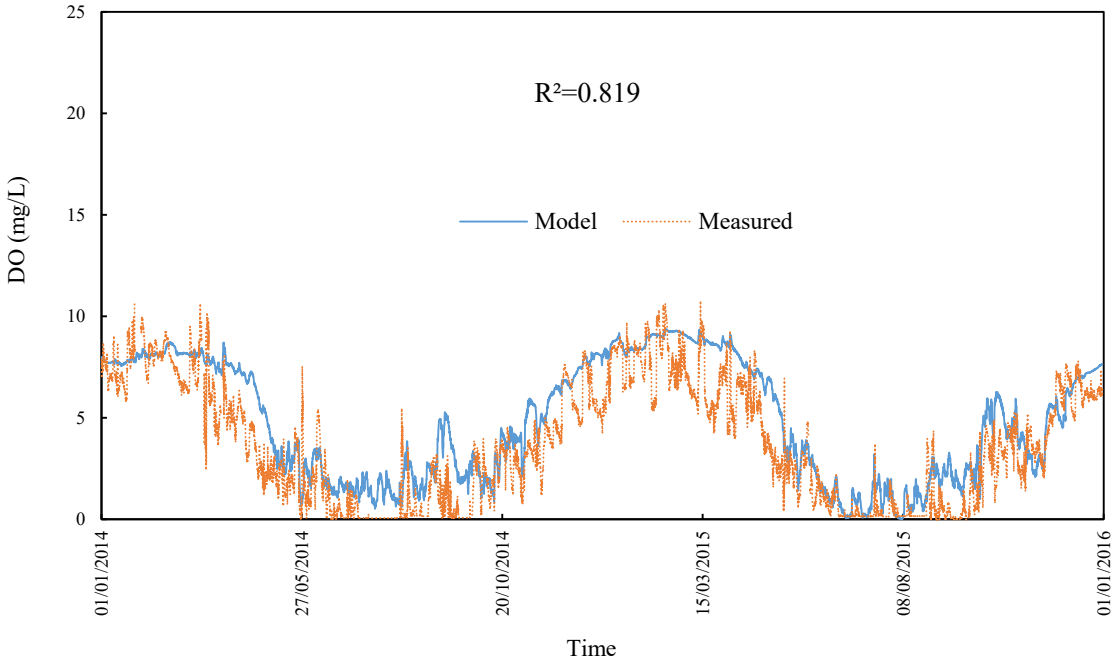

Figure 3.11. Bottom DO comparison between model and measured at Chiba Light Beacon station

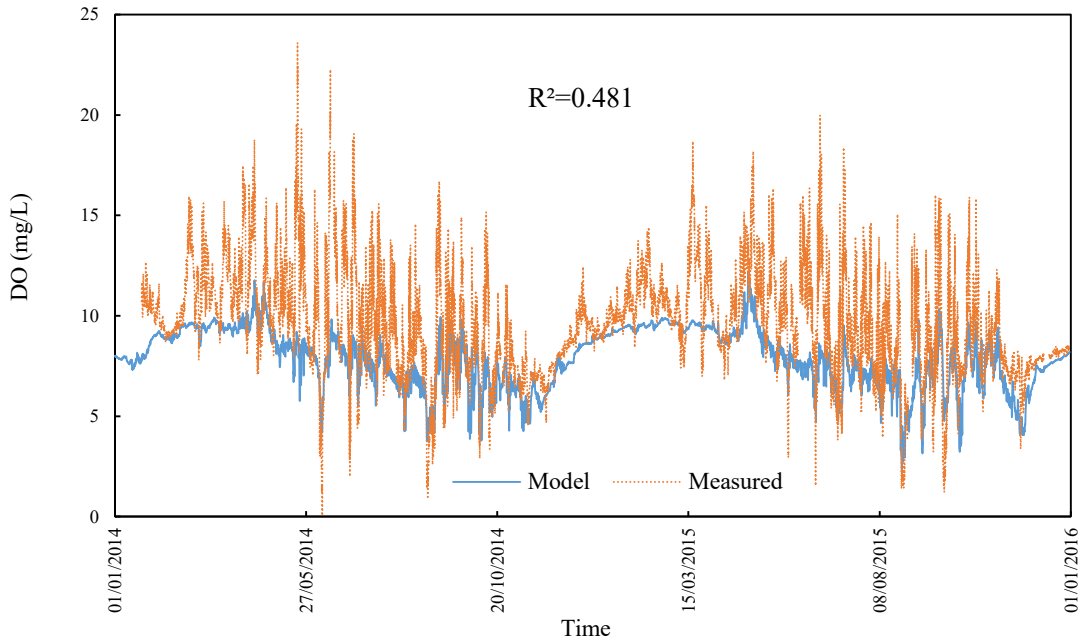

Figure 3.12. Surface DO comparison between model and measured at Chiba Port station

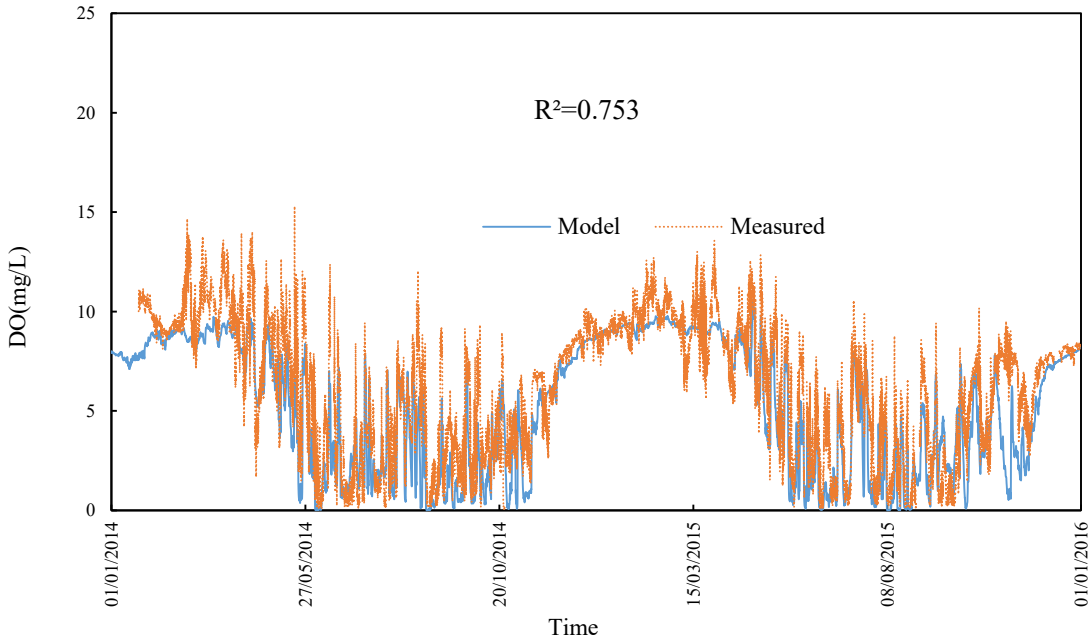

Figure 3.13. Bottom DO comparison between model and measured at Chiba Port station

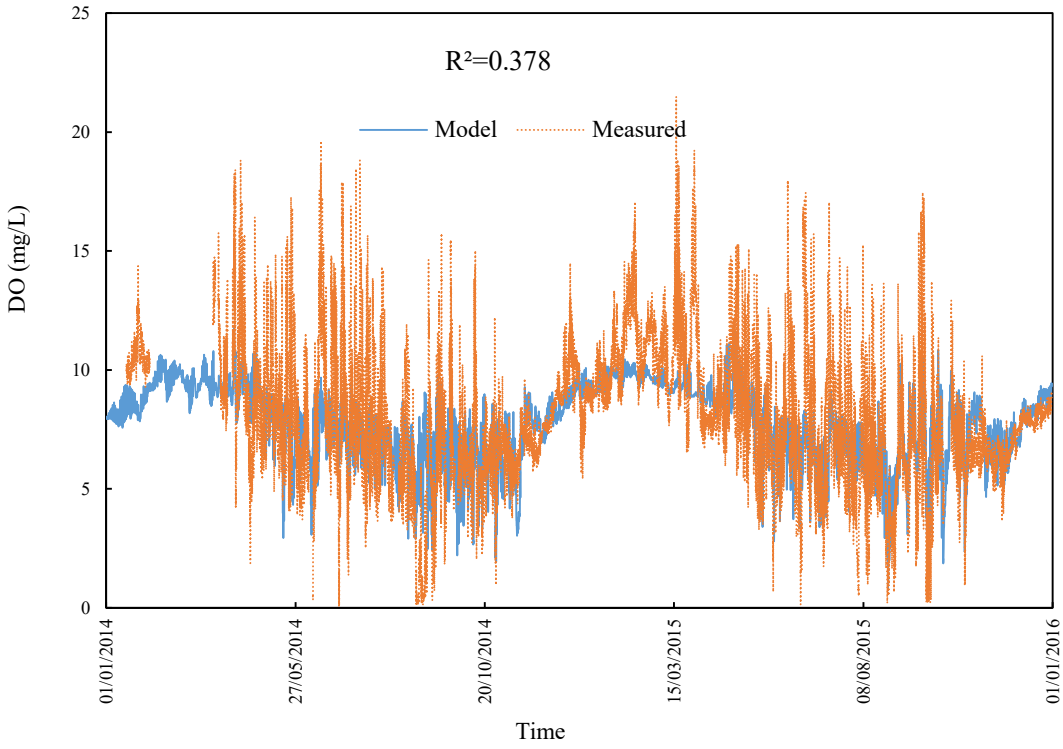

Figure 3.14. Surface DO comparison between model and measured at Urayasu station

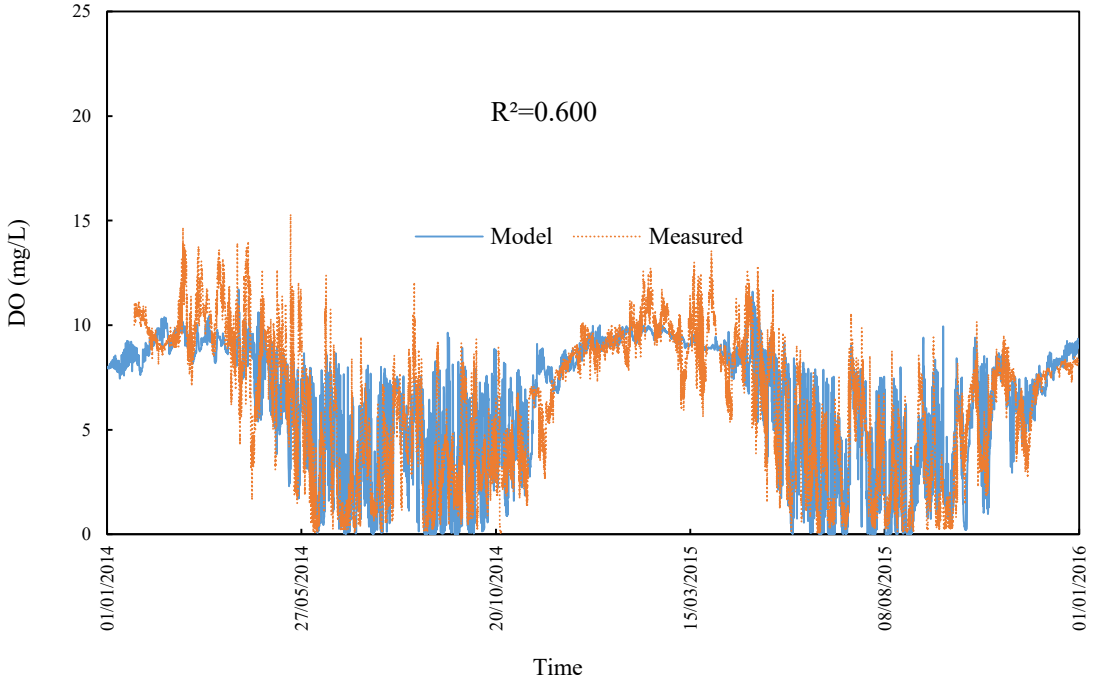

Figure 3.15. Bottom DO comparison between model and measured at Urayasu station

From results of reproduction of MIKE 3 model, hypoxia could appear on surface from May to October whereas anoxia mostly occur on surface from August to October. Especially, late August is the period of anoxia emerged seriously. It is noticeable that hypoxia and anoxia on the surface only occupied the head bay. Initially, hypoxia and anoxia usually presented in top-right of head bay afterward broadening to top-left of head bay. Anoxic surface areas mainly invaded top-right and, top-left and off-Makuhari. For instance, **figure 3.16** and **figure 3.17** illustrate anoxia and hypoxia in head bay by result of reproduction for year 2014 and 2015. Both of longest periods occurred in late August of each year and existed in 6 and 7 days respectively. Due to different meteorological conditions that resulting difference of longest period of hypoxia and anoxia appearance in 2014 and 2015 and scope of this phenomenon. Namely, serious hypoxia and anoxia in year 2014 appeared sooner than year 2015 however they expanded in a larger scale in year 2015.

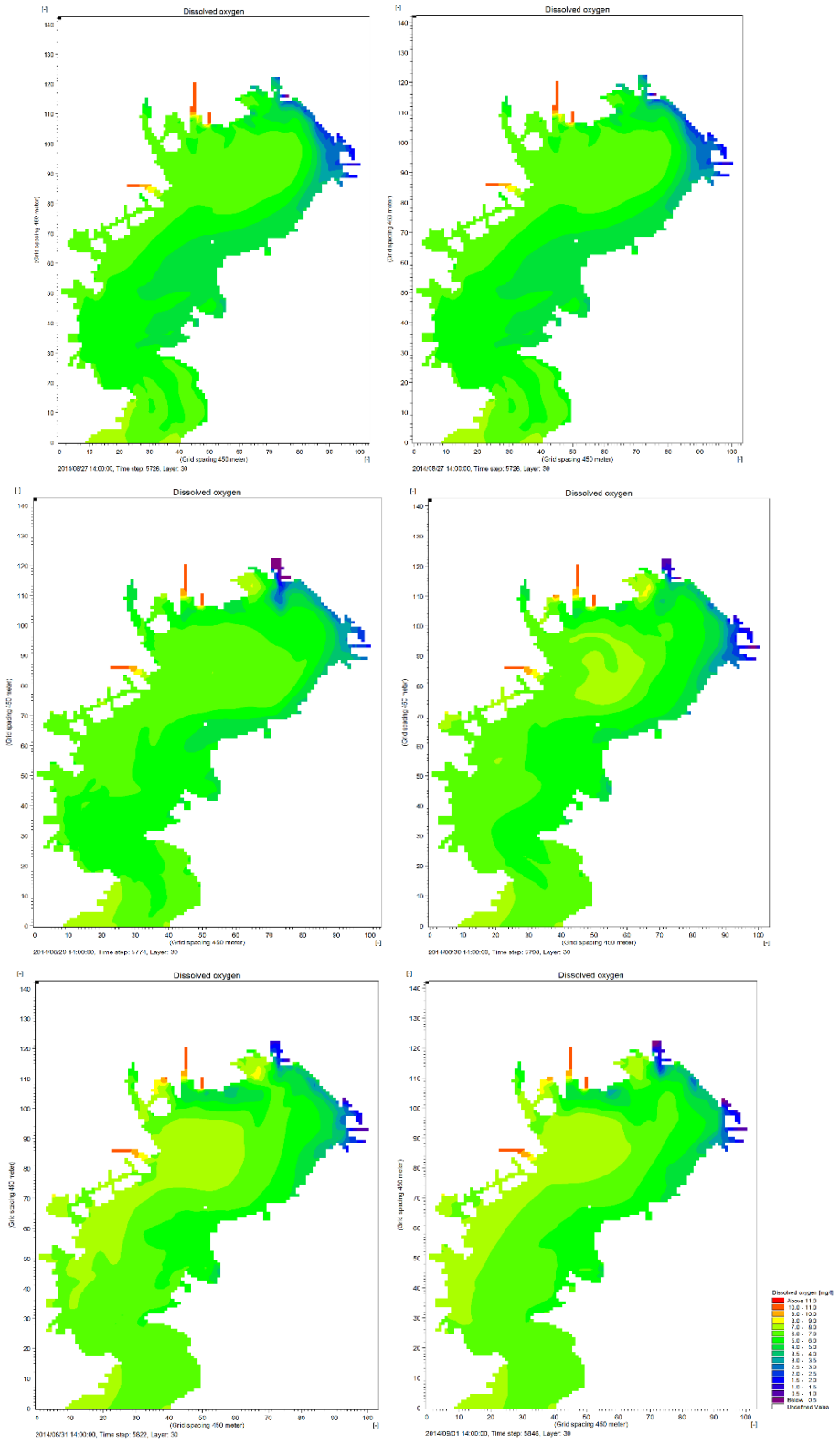

Figure 3.16. Anoxia at surface reproduced by MIKE 3 in Tokyo bay in 2014

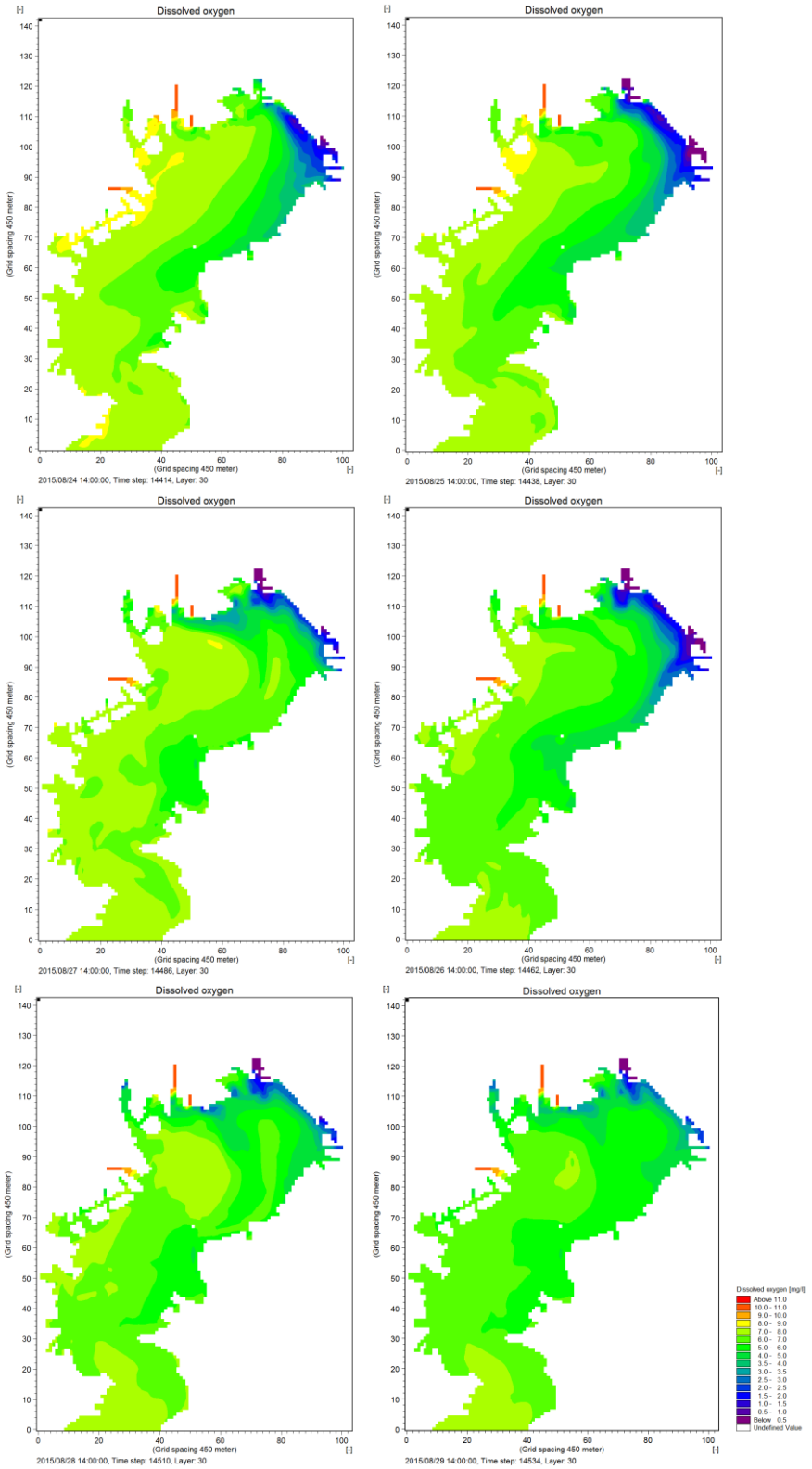

Figure 3.17. Anoxia at surface reproduced by MIKE 3 in Tokyo bay in 2015

A cross section of dissolved oxygen through two dredged pits areas are extracted from result of reproduction (**Figure 3.18**). It shows the existence of anoxia in two these dredged pits. Dissolved oxygen of flat bottom in the middle of two dredged pit usually is affected strongly by two dredged pits. When anoxia became more serious, DO in flat bottom would be infected by anoxia. On surface layer of off-Makuhari dredged pit might encounter anoxia whereas hypoxia existed. Reproducibility of model is also shown by **Figure 3.19** and **Figure 3.20**. Results of DO vertical profiles between field observation and simulation are similar in two dredged pits generally.

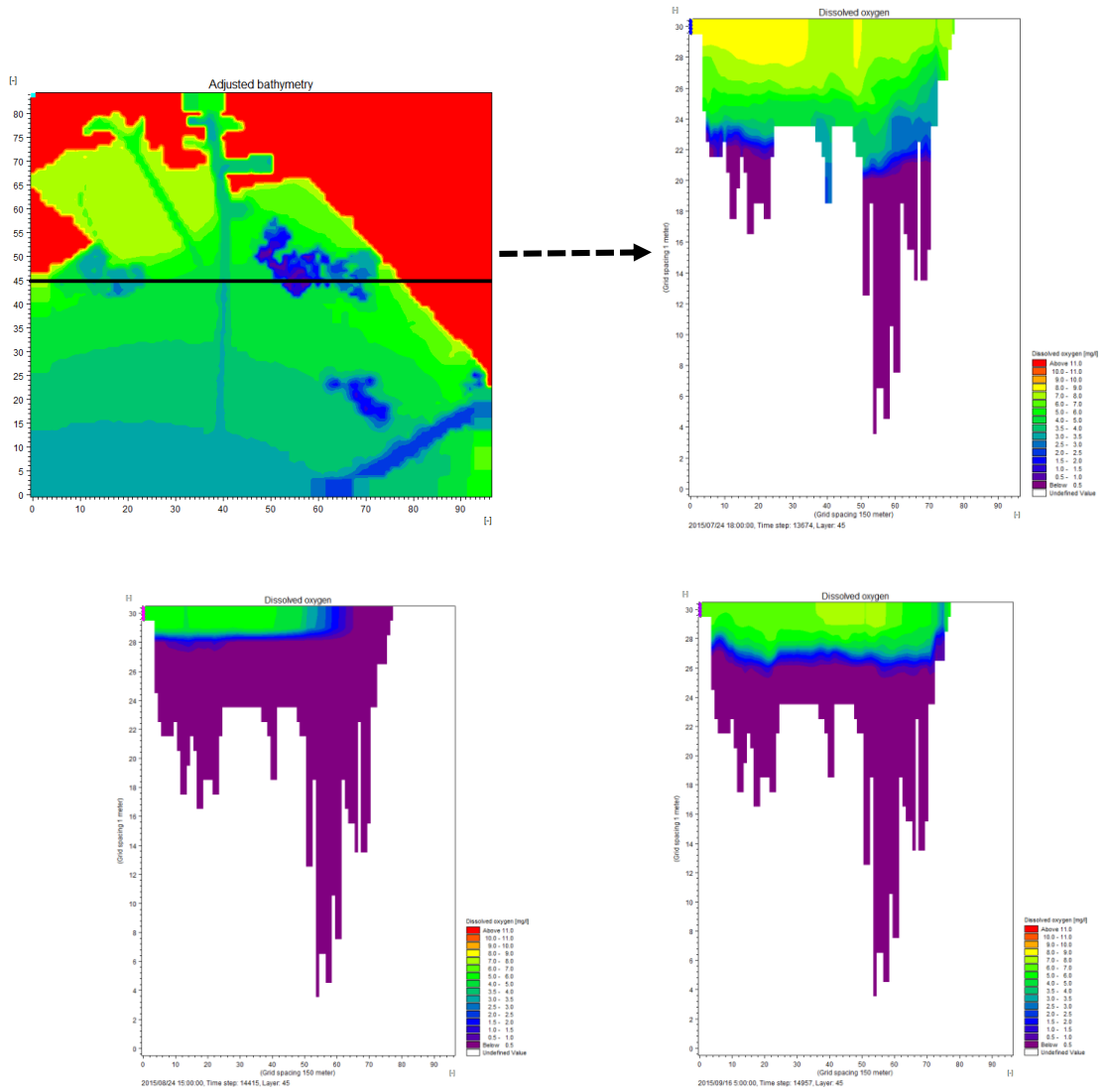

Figure 3.18. DO vertical profile of cross section

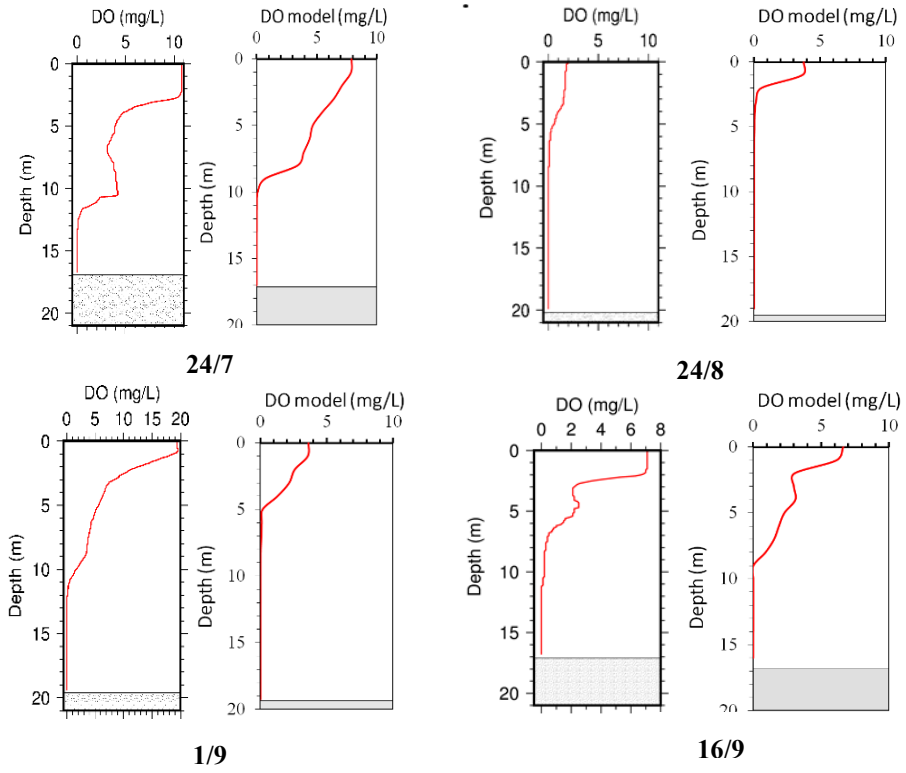

Figure 3.19. DO vertical profile between field surveys and model in off-Makuhari dredged pit

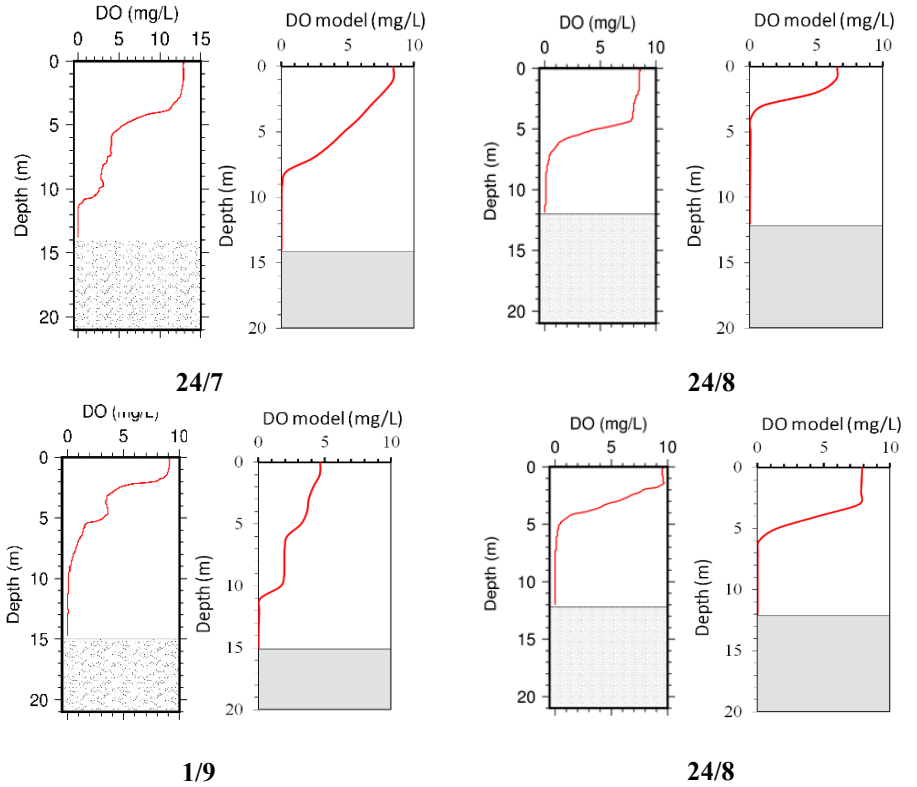

Figure 3.20. DO vertical profile between field surveys and model in off-Urayasu pit

3.2.2. Total sulfide

Reproduction of total sulfide is suitable with field survey results although there is still disparity on some days. Computed results in off-Makuhari exceed in off-Urayasu. It can been clearly via cross section of total sulfides through two dredged pits (**Figure 3.21**). Results of total sulfides in off-Urayasu are more justifiable than in off-Makuhari. In off-Urayasu just on 24/7 model result of total sulfides at bottom is 11mg/L compared to 8 mg/L of observation while others are appropriate. In off-Makuhari, on 24/8 and 1/9 model simulated well total sulfide released at bottom while results is overestimated on 24/7 and 16/9. Results of model on 24/7 in off-Makuhari shows that total sulfides was still released due to anoxia appear on this day with both model and measurement (**Figure 3.19**) meanwhile field survey revealed it is negligible.

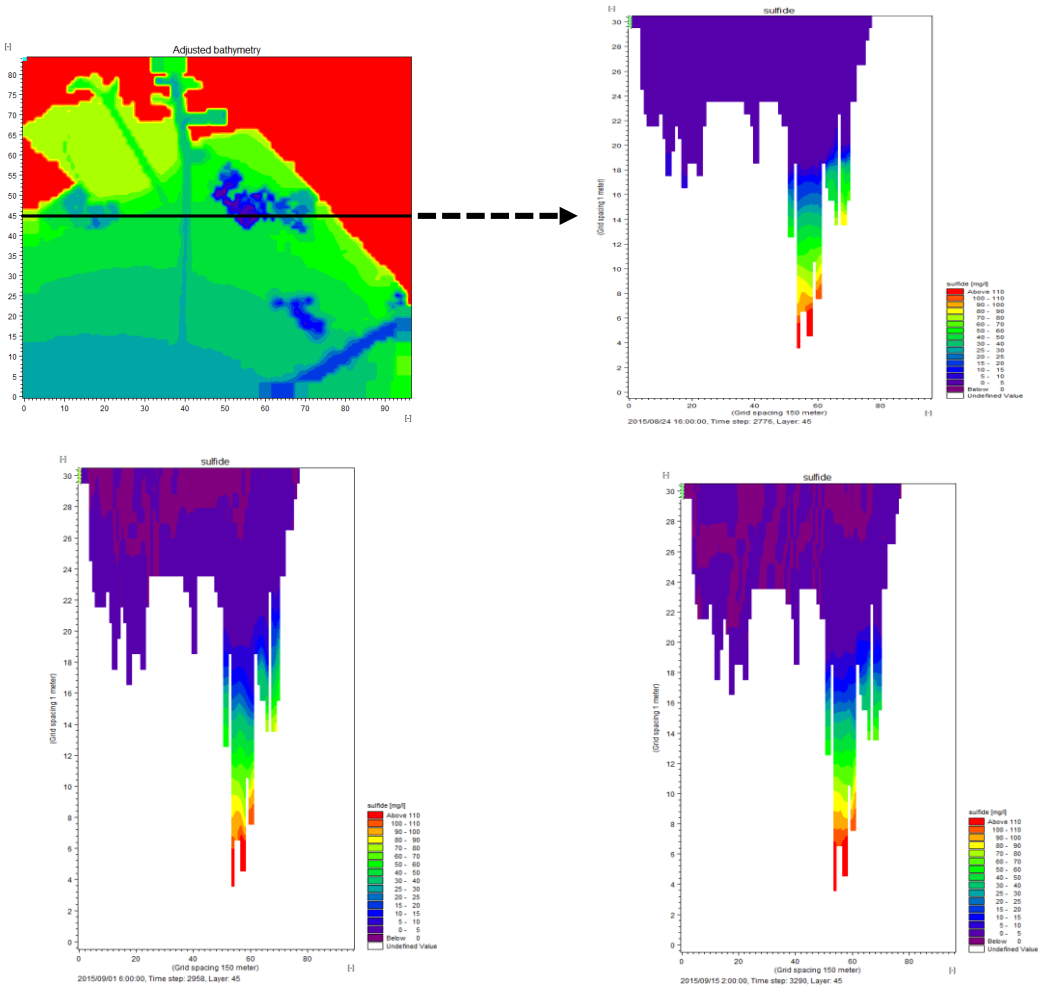

Figure 3.21. Cross section of total sulfide across two dredged pits

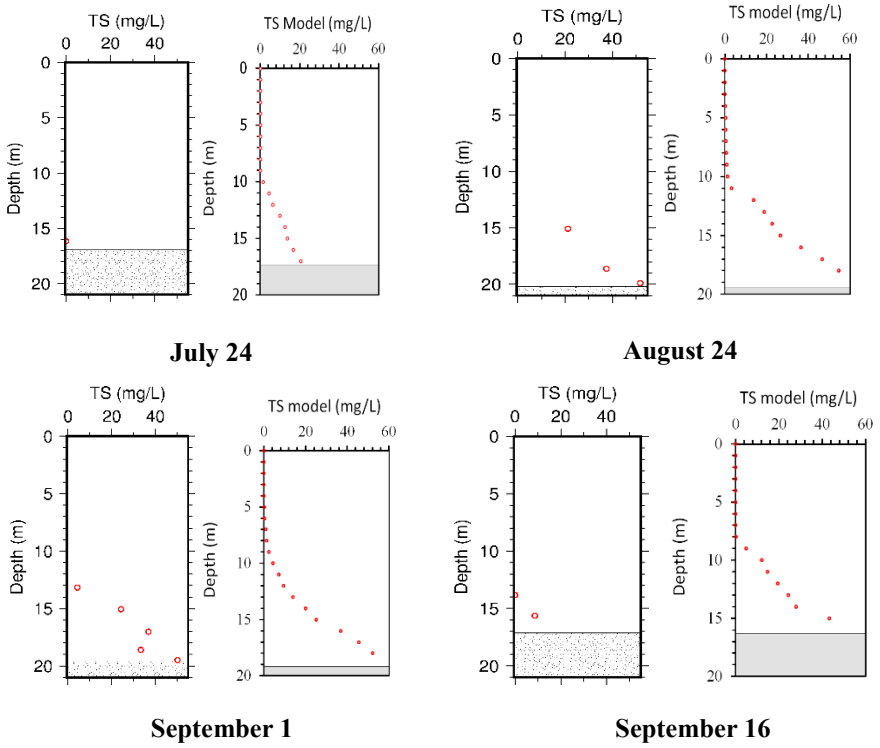

Figure 3.22. Total sulfides between field surveys and model in off-Makuhari dredged pit

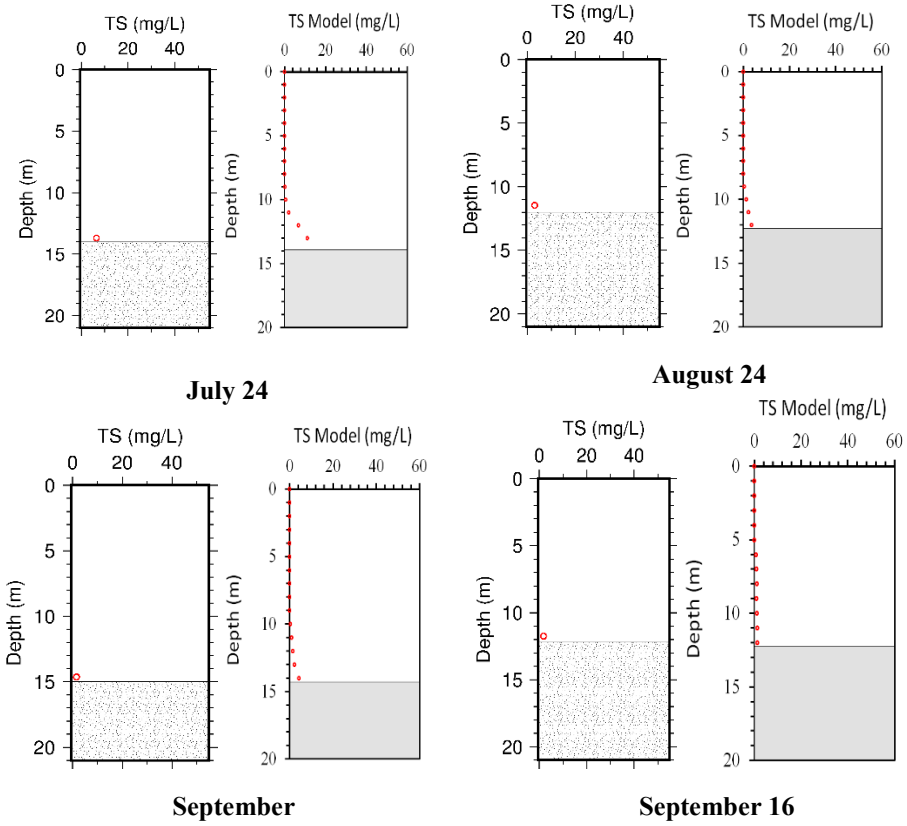

Figure 3.23. Total sulfides between field surveys and model in off-Urayasu dredged pit

3.2.3. Sulfur

As mention in previous section, sulfur is product from oxidation of hydrogen sulfide. Result of computed sulfur in shown as **Figure 3.24** and **Figure 3.25** in off-Makuhari dredge pit and Urayasu dredged pit respectively. Result of sulfur reveal that maximum of sulfur in a water column is at the interface between anoxic layer and oxic layer. For instance, on 1/9 in off-Makuhari sulfur peaked at 5 meter beneath surface similarly to depth of anoxia. Vertical distribution of sulfur on this day is similar to result of turbidity from field survey. Result of sulfur on 24/8 in off-Makuhari dredpit is lower than 24/7 due to result of DO shown computed anoxia was dominated on 24/8 therefore sulfur was low.

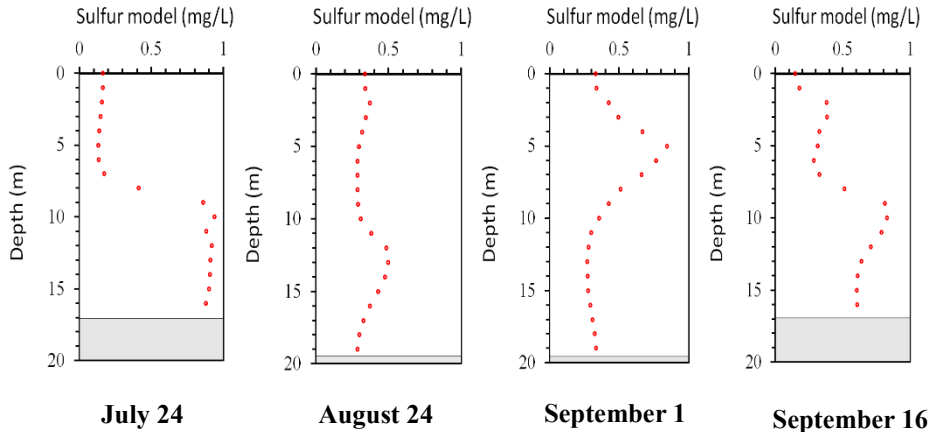

Figure 3.24. Sulfur in off-Makuhari dredged pit

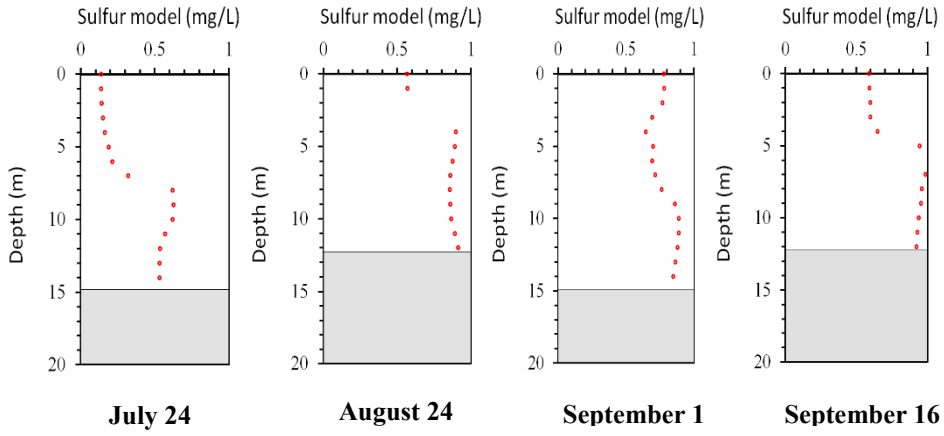

Figure 3.25. Sulfur in off-Urayasu dredged pit

CHAPTER 4: DISCUSSIONS

4.1. Characteristics of spatial-temporal variation in water quality

From results of dissolved oxygen in previous chapter, it can be seen that hypoxia and anoxia on surface just began to evolve in the top-right of head bay before spreading to left direction of head bay. Hypoxic bottom water was identified from April to late November. After August the presence of hypoxia tends to mitigate. These characteristics above are similar to properties of hypoxic water in previous studies. Because so many researches focused on hypoxia (DO < 3 mg/L) but rarely pointed out more characteristics of anoxia in which dissolved oxygen concentration is also equal zero. In particular, results of thesis also shown that hypoxia usually occurs sooner and vanishes later while anoxia appears later and disappears sooner. Specifically, anoxic bottom water normally may increase from May to early November. Dredged pits or navigation channel would appear first. On surface, anoxia just frequently presents from June to September. July and August generally are months when anoxia occurs seriously. From September onward, almost no anoxia is detected. For spatial variation, anoxia can be exposed entire flat bottom from Kawasaki artificial island to head bay coastline although anoxic water has been found in dredged trenches before. Especially, flat bottom in the middle between off-Maakuhari and off-Urayasu often is affected by anoxic bottom water in two dredged pits. Results of field surveys indicates that anoxic water appear frequently in both dredged pits even northeast blow resulting the expansion of anoxic water in a water column.

Although anoxia appeared in flat bottom though total sulfide released was very small. Off-Makuhari dredged pit and off-Urayasu dredged pit are significant sources for generating

total sulfides while off-Makuhari dredged pit is the most predominant. Emission of total sulfide increase intensity when anoxia develops. During blooming of anoxia, total sulfide emitted in off-Makuhari is much higher than other areas.

4.2. Sensitivity of model reproducibility

Reproducibility of model are dominant by some aspects. Model is tuned firstly and evaluated through sensitiveness of critical parameters. Finally, validation will be performed in comparisons with measured data.

4.2.1. Sensitivity analysis on river discharge magnification coefficient

Water temperature and salinity are important factors in order to improve the reproduction of water stratification and phytoplankton development. Especially, surface salinity shown strong fluctuation during flood season. If model uses original measured river discharge, the result of model will be not accurate. Hence to achieve suitable trends between model and measurement of salinity and temperature, tuning of river discharge is required. Because there are only observed data of two rivers, thus tuning procedure have been carried out with this quantity. Magnification factor is different with each river and each period. For example, magnification factor equals 2.5 during flood season whereas 1 was used in dry season for Edogawa river. With Tamagawa river are 2 and 1.1 during flood season and dry season respectively. Results after magnifying are shown in Figure 4.1 and Figure 4.2.

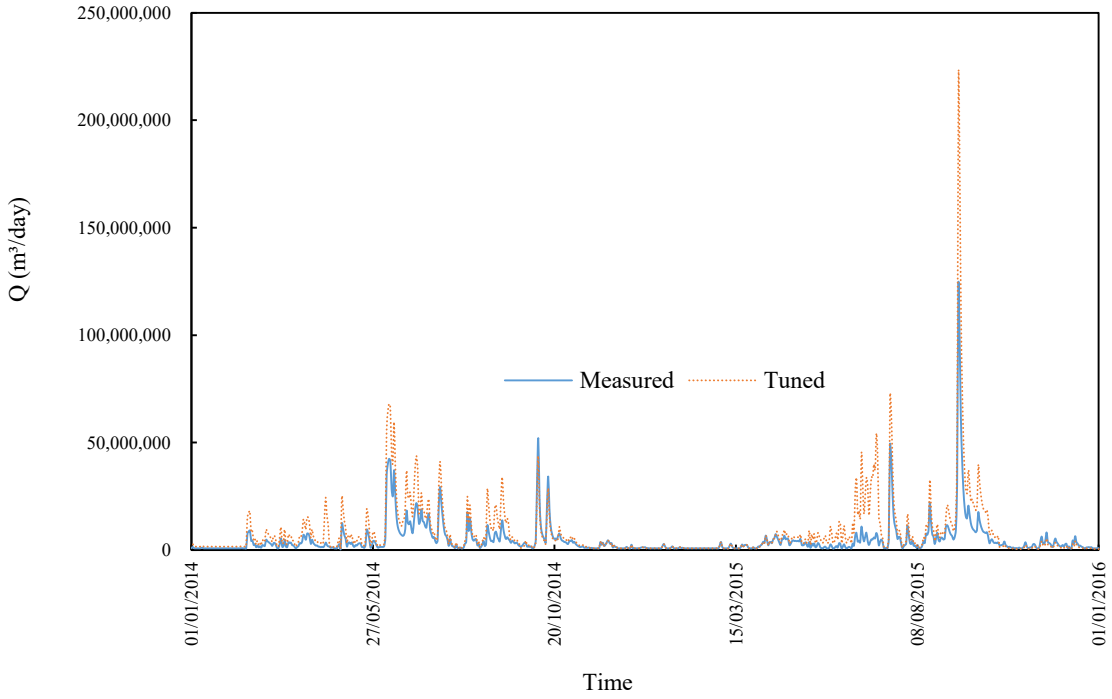

Figure 4.1. Comparison of measured and tuned discharge of Edogawa river

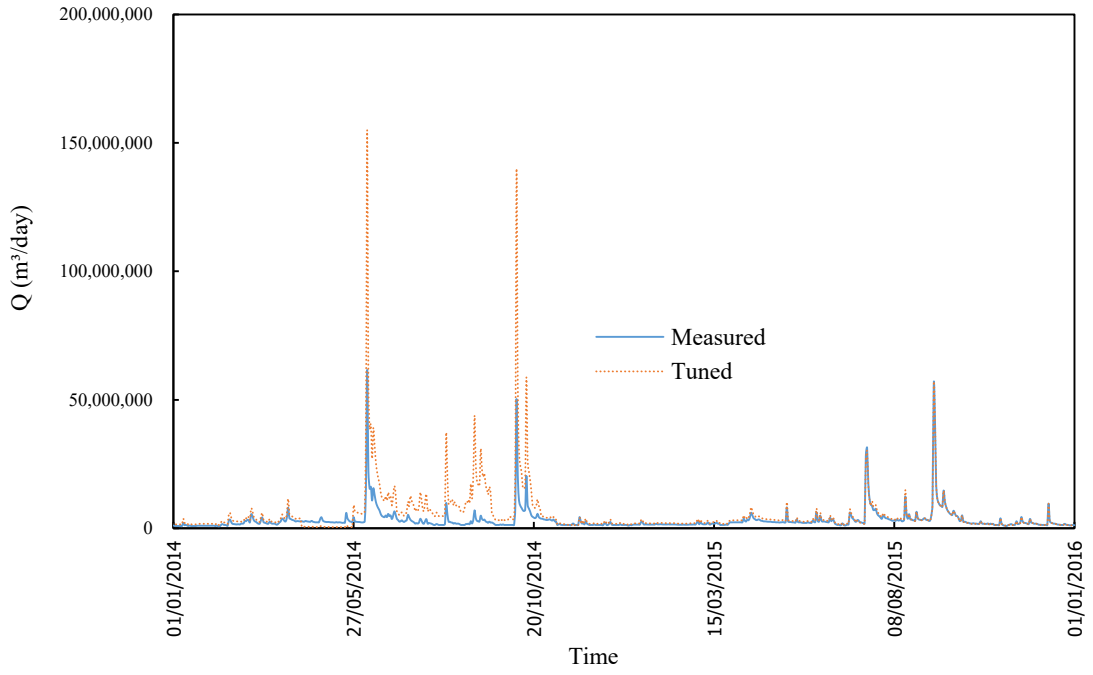

Figure 4.2. Comparison of measured and tuned discharge of Tamagawa river

4.2.2. Sensitivity analysis on phytoplankton settling velocity

Phytoplankton is a vital component in the Eco Lab module. Phytoplankton is not the source to synthesize oxygen but also transform to new sediment in water when they die. Development of phytoplankton depends on nutrient provided by river and sediment, light and settling velocity. Nutrient supply related to river discharge which has been tuned before. Light is obtained from measured data. Because of focusing on anoxic water and release of total sulfides, settling speed thus is a sensitive factor affected to accuracy of the model. If settling speed is set high, this leads to increase of sediment accumulation on the bed and consumes more oxygen at bottom. Anoxic water therefore will appear more frequently than reality and total sulfide also would be released more. In simulation, settling velocity is fixed a constant value of 0.02 m/day. **Figure 4.3** is an example of bottom DO at Kawasaki station to evaluate sensitivity of settling velocity of phytoplankton with different values.

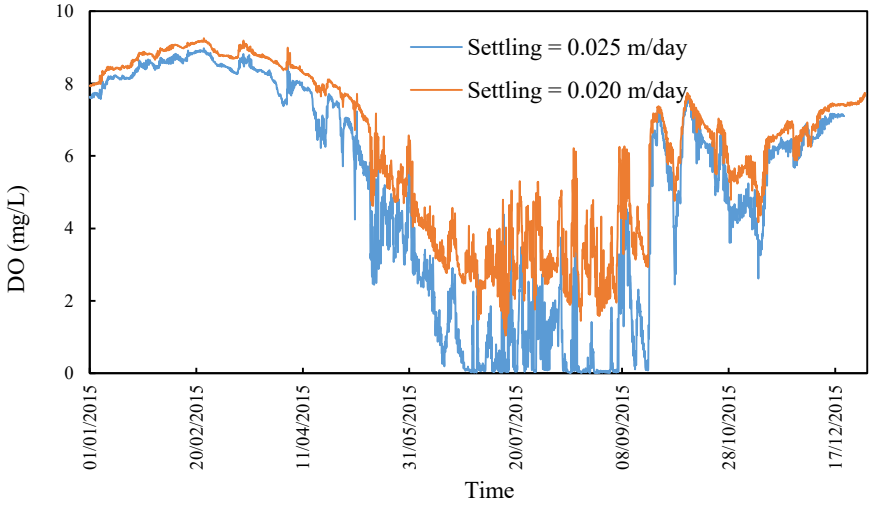

Figure 4.3. Comparison of DO bottom for sensitivity of phytoplankton settling at Kawasaki station

4.2.3. Sensitivity analysis on total sulfide

Satisfaction of dissolved oxygen reproducibility is required before reproducing total sulfide. Two factors is identified that affecting to reproducibility of total sulfides are *fsul* (ratio sulfide/carbon) and *sed_bg* (sediment background concentration). Although they are constants and stable during simulation but they can vary spatially. If model apply uniform value for both factors, model results of total sulfides reflect well in flat bottom and off-Urayasu dredged pit but in off-Makuhari dredged pit outcome could not reach value of total sulfides as field observation revealed. Therefore, there need be a magnification for off-Makuhari dredged pit. Model set fsul = 2.8 and sed_bg = 0.8 g/m² for whole domain. Particularly, to lift reproducibility of total sulfide in off-Makuhari *fsul* is fix at 8 (in sulfide family ratio of H_2S, SO_3, SO_4 to carbon can alter from 2.7 to 8) while sediment background concentration *sed_bg* is valued at 2.0 mg/ m².

4.3. Estimation of total sulfides

As stated above, field surveys observed total sulfide concentration both entire flat bottom and dredged pits. These results are base for reproduction of total sulfides. Result of reproducibility for total sulfide are shown in chapter 3. To examine contribution of total sulfides between flat bottom and dredged pits, time series of total sulfides are extracted from model. Although released total sulfide concentration in flat bottom is much lower than dredged pits, however entire area of flat bottom is much larger than dredged pits. **Figure 4.4** below compares total sulfides released in flat bottom and dredged pits. The graph shows fluctuation in flat bottom while total sulfides in dredged pit accumulates from May before declining from late September. Because anoxic bottom water appears in dredged pit more frequently than in flat bottom resulting fluctuation and accumulation of total sulfides in flat bottom and dredged pits respectively. It can be seen that total sulfide begins to bloom from

May when anoxic water develops and flat bottom might emit total sulfides more than in dredged pit.

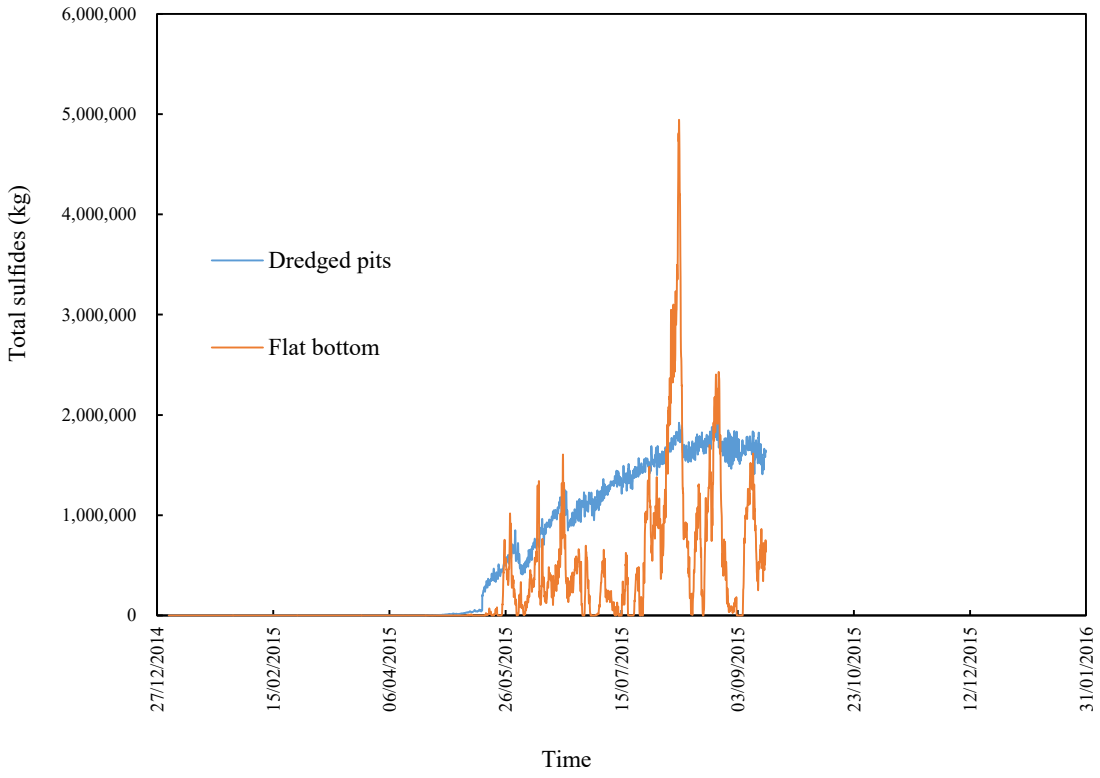

Figure 4.4. Estimation of total sulfide in dredged pit and flat bottom

4.4. Effects on blue tide

Blue tide might occur when high total sulfide concentration combined with appearance of northeast wind. For example, in year 2015 blue tide could be observed on 24/8. Considering from **Figure 4.4** above, total sulfide on that day is generally equal between flat bottom and dredged pit. The following days, flat bottom governed slightly than dredged pits. Before day 24/8, even total sulfide released from flat bottom and dredged pit was at high but northeast didn't exist.

CHAPTER 5: CONCLUSIONS AND RECOMMENDATIONS

5.1. Conclusions

In this research have elucidated results of variations in anoxic waters and sulfide in Tokyo Bay. Field observation and monitoring station showed that anoxic waters have been found in dredged pits, navigation channel and entire flat bottom in Tokyo Bay. Anoxia appears later and disappears sooner while hypoxia usually occurs sooner and vanishes later. Anoxic bottom waters normally emerge from May to early November. Dredged pits or navigation channel would be significant anoxic water sources. From June to September anoxia on surface may develop frequently. Anoxia generally occurs seriously in July and August. From September onward, almost no anoxia is detected. Considering spatial variation of anoxia that can be exposed entire flat bottom from Kawasaki artificial island to head bay coastline beside anoxic waters have been found in dredged trenches before. Results of field surveys also indicates that anoxic water appear frequently in both dredged pits even northeast blow resulting the expansion of anoxic water in a water column.

Field observation results of total sulfide didn't show difference concentration of released sulfide between flat bottom and dredged pits but also in each dredged pit. All results of sulfide concentration in four investigations across entire flat bottom were low. By contrast, field observation demonstrated almost a gradual increase of total sulfide concentration from surface to bottom in dredged pits. Observed results also illustrates the gap of total sulfide released in bottom in off-Urayasu dredged pit and off-Makuhari dredged pit. In off-Makuhari dredged pit, total sulfide concentration increased rapidly on 24/8 and 1/9 at nearly 60 mg/L at the bottom before declining on the following days. While measured result of total sulfide was low on the first investigation trip (24/7). Due to off-Makuhari is deeper than off-Urayasu,

anoxia thus developed more seriously in off-Makuhari leading to more release of hydrogen sulfide especially on blue day.

In addition, numerical simulation showed good reproducibility in variations of anoxic waters and sulfide. Model has also reflected the development of stratification of temperature and salinity of water column in summer that enhanced development of hypoxia an anoxia. A large contribution of flat bottom on blue tide beside significant release of sulfide in dredged pit were examined. To succeed in reproduction of these processes, it needs a magnification for largest dredged pit (off-Makuhari dredged pit) in Tokyo Bay.

5.2. Recommendations

There need be some measures to reduce hypoxia and anoxia phenomenon in Tokyo Bay. Phytoplankton bloom is controlled by natural factor (light intensity) and artificial factor (nutrient input), decline in nutrient loads hence is required to perform. Several evidence proved that reduction of nutrient supply has showed effectiveness in reducing appearance of hypoxia in aquatic system across the world (Diaz and Breitburg, 2009). Tokyo Bay may be a special case, even though secondary treatment of drainage has been carried out before discharging into the bay, improvement of hypoxia doesn't seem to decrease. This indicates that reduction of nutrient loads is not a sufficient measure to reform the current environmental problems in Tokyo Bay. Moreover, reclamations for shore in the past have unintentionally left a system of dredged pits in Tokyo Bay where waters normally become stagnant during summers. These dredged pits is exposing the negative roles itself, particularly causing environment in Tokyo Bay more serious when upwelling depleted oxygen occurs. Filling up these dredged pits would be an effective solution to reduce spatial expansion of hypoxia and anoxia in Tokyo Bay. Although anoxic waters have also been

encountered in navigation channels, but restoration of topography in navigation channel as initial may conflict to economic activities. By reproducing water quality in Tokyo Bay in 2015 with and without proposal of filling up dredged pit and using the same parameters and external forcing, result of DO (**Fig. 5.1**) shows a considerable difference when dredged trench is filled up. Hypoxia and anoxia appeared on the surface in the head of the bay on 24/8/2015 when these dredged pit still exists. Hypoxia on surface seem to disappear after filling up these pits. However, there still need to demonstrate more positive effect of proposal in the future.

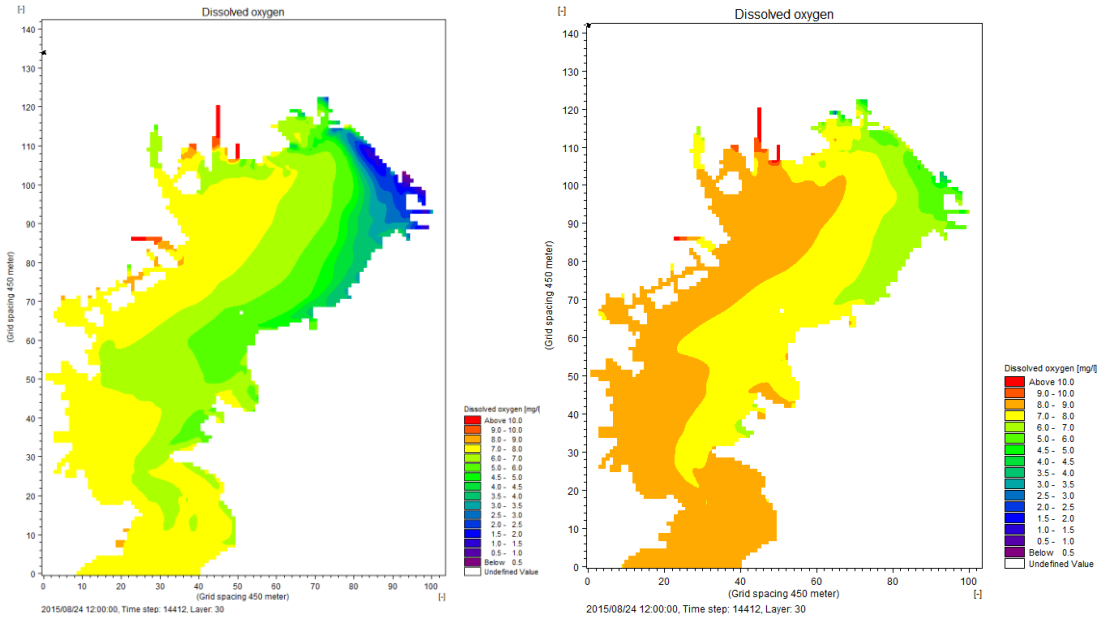

Before After

Figure 5.1. Result of reproduction of DO surface on 24/8/2015 before and after filling up dredged pits

References

DHI, 2014. ECO Lab 1D, 2D and 3D Water Quality and Ecological Modelling User Guide.

DHI, 2014. ECO Lab, Short Scientific Description.

DHI, 2014. MIKE 3 FLOW MODEL manual, Advection/Dispersion Module User Guide.

DHI, 2014. MIKE 3 FLOW MODEL manual, ECO Lab Module User Guide.

DHI, 2014. MIKE 3 FLOW MODEL manual, Hydrodynamic Module Scientific Documentation.

DHI, 2014. MIKE 3 FLOW MODEL manual, Hydrodynamic Module User Guide.

DHI, 2014. Water Quality WQ Templates ECO Lab Scientific Description.

Diaz, R.J., Breitburg, D.L., 2009. The hypoxic environment. In: Richards, J.G., Farrell, A.P., Brauner, C.J. (Eds.), Hypoxia. Elsevier, London, 1–23.

Fujiwara, T. and Yamada, Y., 2002. Inflow of oceanic water into Tokyo Bay and generation of a subsurface hypoxic water mass. Journal of Geophysical Research, Vol. 107, 13-22.

Han, M., Furuya, K. and Nemoto, T., 1992. Species-specific productivity of *Skeletonema costatum* (Bacillariophyceae) in the inner part of Tokyo Bay. Marine Ecology Progress Series, Vol. 79, 267-273.

Ichioka, S., Sasaki, J., Yoshimoto, Y., Matsuzaka, S., Ariji, R. and Morohoshi, K., 2008. Development of an efficient method for estimation of total sulfide in a dredged trench of Tokyo Bay. Proceedings of civil engineering in the ocean, Vol. 24, 669-674. (in Japanese, with English abstract).

Ichioka, S., Sasaki, J., Yoshimoto, Y., Shimosako, K. and Kimura, S., 2009. Analysis of sulfide dynamics including outbreak of blue tide in navigation channels and dredged trench of Tokyo Bay. Journal of Japan Society of Civil Engineers, Series B2, Vol. B2-65, 1041-

1045. (in Japanese, with English abstract).

Ishii, M. and Ohata, S., 2010. Variations in water quality and hypoxic water mass in Tokyo Bay. The Oceanographic Society of Japan, Vol. 48, 37-44. (in Japanese, with English abstract).

Japan Meteorological Agency. Meteorological Data Acquisition System (AMeDAS). http://www.jma.go.jp/jma/index.html

Japan Oceanographic Data Center. RDMDB Data Providing System. http://near-goos1.jodc.go.jp/index_j.html

Junzaburo, M., 1993. Environmental fluid pollution. (in Japanese).
松梨 順三郎, 1993. 環境流体汚染

Kakino, J., Matsumura, S., Sato, Y. and Kase, N., 1987. Relationship between *Aoshio*, blue-green turbid Water, and wind-driven current. Nippon Suisan Gakkaishi, Vol. 53, 1475-1481. (in Japanese, with English abstract).

Kodama, K., Horiguchi, T., Kume, G., Nagayama, S., Shimizu, T., Shiraishi, H., Morita, M. and Shimizu, M., 2006. Effects of hypoxia on early life history of the stomatopod *Oratosquilla oratoria* in a coastal sea. Marine Ecology Progress Series, Vol. 324, 197-206.

Kuramoto, T. and Nakata, K., 1991. Numerical simulation of the formation and movement of an oxygen deficient water mass in Tokyo Bay. The Oceanographic Society of Japan, Vol. 28, 140-151. (in Japanese, with English abstract).

Matsuyama, M., Touma, K. and Ohwaki, A., 1990. Numerical experiment of upwelling in Tokyo Bay – In relation to "Aoshio" (the upwelled anoxic blue-green turbid water). The Oceanographic Society of Japan, Vol. 28, 63-74. (in Japanese, with English abstract).

Mistry of Land, Infrastructure, Transport and Tourism. http://www1.river.go.jp/

Nakane, T., Nakaka, K., Bouman, H. and Platt, T., 2008. Environmental control of short-term variation in the plankton community of inner Tokyo Bay, Japan. Estuarine, Coastal and

Shelf Science, Vol. 78, 796–810.
Otubo, K., Harashima, A., Yasuoka, Y. and Muraoka, K., 1991. Field survey and hydraulic study of “Aoshio” in Tokyo Bay. Marine Pollution Bulletin, Vol. 23, 51-55.

Pennock, J.R., 1985. Chlorophyll distributions in the Delaware Estuary: regulation by light limitation. Estuarine, Coastal and Shelf Science, Vol. 21, 711–725.

Sato, C., Nakayama, K., Furukawa, K., 2012. Contributions of wind and river effects on DO concentration in Tokyo Bay. Estuarine, Coastal and Shelf Science, Vol. 109, 91-97.

Sato, F., Sasaki, J., Sano, H. and O, H., 2015. Spatial and temporal characteristics and numerical reproduction of anoxic water at the head of Tokyo Bay. Journal of Japan Society of Civil Engineers, Series B2 (Coastal Engineering), Vol.71, No.2, 1267-1272. (in Japanese, with English abstract).

Sasaki, J., Kanayama, S., Nakase, K. and Kino, S., 2009. Effective application of a mechanical circulator for reducing hypoxia in an estuarine trench. Coastal Engineering Journal, Vol. 51, 309-339.

Sasaki, J., Kawamoto, S., Yoshimoto, Y., Ishii, M. and Kakino, J., 2007. Evaluation of the effect of anoxic water in dredged trenches on blue tides in Tokyo Bay. Journal of Japan Society of Civil Engineers, Series B2 (Coastal Engineering), Vol. 54, 1041-1045. (in Japanese, with English abstract).

Sasaki, A., Sanuki, H. and Isobe, M., 1998. Reproduction for calculation of eutrophication phenomenon in Tokyo Bay. Coastal Engineering Proceedings, Vol. 45, p1036-1040. (in Japanese).

Tokyo Bay Environmental Information Center.
http://www.tbeic.go.jp/MonitoringPost/index.asp

Wolanski, E., 2006. The environment in Asia Pacific Harbors. Springer, Netherland, 497.

Yoshimoto, Y., Sasaki, J., Shimosako, K. and Kimura, S., 2009. Numerical Study on effective measures using water duct for reducing anoxia in a dredged trench in coastal waters. Journal of Japan Society of Civil Engineers, Series B2, Vol. B2-65, 1176-1180. (in Japanese,

with English abstract).

Zhu, Z. and Yu, J., 2014. Estimating the occurrence of wind-driven coastal upwelling associated with “Aoshio” on the northeast shore of Tokyo Bay, Japan: An analytical model. The Scientific Journal, Vol. 2014, Article ID 769823, 11 pages.

Zhu, Z. and Isobe, M., 2012. Criteria for the occurrence of wind-driven coastal upwelling associated with “Aoshio” on the southeast shore of Tokyo Bay. The Oceanographic Society of Japan and Springer, Vol. 68, 561-574.